



# UNIVERSITA' DEGLI STUDI DI PADOVA

Dipartimento Di Biologia

SCUOLA DI DOTTORATO DI RICERCA IN BIOSCIENZE E BIOTECNOLOGIE

INDIRIZZO DI GENETICA E BIOLOGIA MOLECOLARE DELLO SVILUPPO

*CICLO XXVII*

## **Understanding bone alterations in Gaucher disease using the zebrafish animal model: development of a novel pathogenetic paradigm for lysosomal storage disorders**

**Direttore della Scuola:** Ch.mo Prof. Giuseppe Zanotti

**Coordinatore d'indirizzo:** Ch.mo Prof. Rodolfo Costa

**Supervisore:** Ch.mo Dott. Enrico Moro

**Dottoranda:** Ilaria Zancan



*“The only source of knowledge is experience.”*  
*(Albert Einstein)*



## TABLE OF CONTENT

1.	INTRODUCTION	11
1.1	LYSOSOMAL STORAGE DISORDERS	11
1.2	THE GAUCHER DISEASE	13
1.2.1	<i>Gaucher disease genotype is not always associated with a specific phenotype</i>	15
1.2.2	<i>Bone defects in the Gaucher disease</i>	17
1.2.3	<i>Animal models in Gaucher disease research</i>	19
1.3	ZEBRAFISH A NEW POWERFUL ANIMAL MODEL	21
1.3.1	<i>Morpholino gene knockdown</i>	23
1.3.2	<i>Transgenic zebrafish reporter lines</i>	24
1.3.3	<i>Generation of stable zebrafish mutant lines</i>	25
1.4	MOLECULAR DEVELOPMENT OF VERTEBRATE SKELETON	25
1.4.1	<i>Osteoblast commitment during embryonic and postnatal development</i>	27
1.4.2	<i>The molecular signaling pathways involved in the osteoblasts development</i>	29
2.1	RECIPES	37
2.1.1	<i>Whole-Mount in situ Hybridization Solutions</i>	38
2.1.2	<i>Solutions for bacteria transformation and RNA probe synthesis</i>	40
2.2	MORPHOLINO-MEDIATED KNOCKDOWN	40
2.3	GENOTYPING OF MUTANT	41
2.4	ALIZARIN AND ALCIAN STAINING	41
2.5	TRANSMISSION ELECTRON MICROSCOPY	41
2.6	TRANSFORMATION OF E. COLI	41
2.7	PURIFICATION OF PLASMID DNA	42
2.8	ANTI-SENSE PROBE SYNTHESIS	42
2.9	SINGLE-PROBE WHOLE-MOUNT IN SITU HYBRIDIZATION (WISH)	44
2.10	QUANTITATIVE REAL-TIME PCR	47
2.10.1	<i>RNA extraction</i>	47
2.10.2	<i>RT-PCR data analysis</i>	47
2.11	IMMUNOFLUORESCENCE ON TYPE 1 GAUCHER FIBROBLASTS	48
2.12	APOPTOSIS AND PROLIFERATION ASSAYS	49
2.13	WESTERN BLOT	50
2.14	MICROARRAY	50
2.15	RESCUE WITH HUMAN GBA1 OVEREXPRESSION AND CERESYME TREATMENT	50

2.16	IN VIVO REACTIVE OXYGEN SPECIES DETECTION (DCDFA STAINING)	51
2.17	TARTRATE-RESISTANT ACID PHOSPHATASE ASSAY	51
2.18	ZEBRAFISH DISSOCIATION AND FLOW CYTOMETRY ANALYSIS	51
3.	RESULTS	53
3.1	DETERMINATION OF THE EXPRESSION PATTERN OF GBA 1 IN THE ZEBRAFISH FROM EARLY LIFE STAGES	53
3.2	ZEBRAFISH MODELS USED IN THIS PROJECT	54
3.2.1	<i>Knockdown of the zebrafish Gba1 using morpholino oligo</i>	54
3.2.2	<i>Characterization of a zebrafish stable mutant line for Gba1.</i>	55
3.3	GBA1 LOSS OF FUNCTION AFFECT MULTIPLE CELL LINEAGES IN FISH	56
3.3.1	<i>Hematological defects are observed in Gba1 morphants and mutants</i>	56
3.3.2	<i>Liver and spleen size are compromised in both morphant and mutant</i>	58
3.3.3	<i>Gba1 morphants and mutants display severe bone abnormalities</i>	59
3.4	GLOBAL CELLULAR AND MOLECULAR DEFECTS DUE TO GLUCOCEREBROSIDASE DEFICIENCY ARE TRIGGERED DURING EARLY STAGES OF DEVELOPMENT	64
3.5	CANONICAL WNT PATHWAY ACTIVITY IS SPECIFICALLY HAMPERED BY GLUCOCEREBROSIDASE IMPAIRMENT	69
3.6	BONE DEFECTS ARE REVERSIBLY CORRECTED WHEN A HUMAN GBA1 IS OVEREXPRESSED IN MORPHANTS	73
3.7	CANONICAL WNT SIGNALING ACTIVITY IS SIGNIFICANTLY IMPAIRED IN TYPE 1 GAUCHER DISEASE PATIENTS	74
3.8	GBA1 DEFICIENCY INDUCED ALTERATIONS ALSO IN THE BMP SIGNALING PATHWAY	77
4.	DISCUSSION	81
5.	REFERENCES	87
	APPENDIX	95

## RIASSUNTO

Le patologie da accumulo lisosomiale sono malattie metaboliche rare a carattere ereditario determinate da carenze di specifici enzimi o trasportatori lisosomiali, che hanno complessivamente un'incidenza di  $\sim 1/7000$  nuovi nati nella popolazione mondiale. Al giorno d'oggi, almeno 50 disordini genetici sono causati da difetti in enzimi lisosomiali, che determinano l'incompleta degradazione e/o il riciclaggio di molecole a livello intracellulare con conseguente accumulo all'interno del lisosoma dei substrati enzimatici. Nonostante la presenza di proteine lisosomiali in quasi tutti i tessuti ed organi del corpo, l'accumulo del materiale non digerito è generalmente limitato solo a quelle cellule, tessuti od organi nel quale il ricambio del substrato enzimatico è molto elevato. Questa caratteristica determina differenti fenotipi per le varie patologie da accumulo lisosomiale, in quanto diversi organi o cellule possono essere coinvolti.

Tra queste patologie, la malattia di Gaucher è la più frequente con un'incidenza di 1 su 200.000 nati vivi nella popolazione mondiale. La frequenza di questa patologia, aumenta drasticamente a 1 su 850 all'interno della popolazione degli ebrei Ashkenazi (Europa dell'Est). Questa malattia è causata da mutazioni a carico del gene che codifica l'enzima lisosomiale  $\beta$ -glucocerebrosidase (GBA). Tali mutazioni determinano l'incorretto ripiegamento della proteina enzimatica che, di conseguenza, non è in grado di degradare il suo substrato, la glucosilceramide, che si accumula nel lisosoma. Una delle caratteristiche di questa patologia è la presenza delle così dette "cellule di Gaucher", ovvero macrofagi ad elevato contenuto di substrato non degradato, in differenti tessuti. Insieme alla presenza di questi macrofagi alterati, pazienti affetti dalla malattia di Gaucher presentano ingrossamento di fegato e milza (epatosplenomegalia), anemia, trombocitopenia e gravi disfunzioni a carico del sistema scheletrico quali osteonecrosi, riduzione della densità ossea, dolori cronici e frequenti fratture a carico delle ossa lunghe. Si possono distinguere tre sottocategorie di pazienti affetti da GD, generalmente classificati sulla base della presenza e gravità dei difetti a carico del sistema nervoso centrale (SNC). I pazienti affetti da GD di tipo I sono i più frequenti, hanno un'insorgenza della patologia in età tardiva ma non presentano coinvolgimento del SNC. I pazienti affetti da GD di tipo II, invece, manifestano i primi sintomi della malattia fin nei primi anni di vita e spesso i gravi difetti a carico del sistema nervoso possono portare alla morte del paziente. La terza categoria di pazienti, GD tipo III, manifestano i sintomi durante l'età infantile e i difetti neurologici sono meno gravi rispetto a quelli dei pazienti di tipo II. Al giorno d'oggi, questa classificazione basata

sulla presenza di difetti neurologici è poco credibile a causa della presenza di fenotipi diversificati all'interno della stessa sottocategoria di pazienti. Il concetto di uno spettro continuo di fenotipi che variano dal meno grave (GD tipo I) al più severo (GD tipo II e III) è più appropriato per descrivere questa patologia.

La terapia maggiormente utilizzata per il trattamento della sintomatologia di questa malattia è la terapia enzimatica sostitutiva (ERT), che consiste nella somministrazione di un enzima ricombinante in grado di sopperire alla mancanza della  $\beta$ -glucocerebrosidasi. Nonostante sia ben tollerata dalla maggioranza dei pazienti e sia in grado di far regredire l'ingrossamento di fegato e milza, l'anemia e la trombocitopenia, tale terapia ha effetti davvero limitati sui difetti scheletrici e neurologici.

Nel corso degli anni, diversi modelli murini sono stati sviluppati per cercare di comprendere quali siano i meccanismi patogenetici della malattia che inducono questo ampio spettro di fenotipi. Sfortunatamente, la maggior parte di questi modelli animali non sono vitali o non manifestano tutti i difetti della malattia.

Lo scopo del mio progetto di dottorato è stato quello di generare un nuovo modello animale per comprendere i meccanismi patogenetici a monte dei difetti ossei della malattia di Gaucher. A tal fine, mi sono avvalsa dell'uso dello zebrafish per la sua facilità di manipolazione e la trasparenza delle uova che permettono di seguire lo sviluppo embrionale fin dalle prime fasi.

Utilizzando la tecnica del morfolino e avvalendomi di un modello genetico mutante stabile in zebrafish, ho potuto studiare quale fosse l'effetto della mancanza dell'enzima *Gba1* fin dalle prime fasi dello sviluppo embrionale. Questi modelli, inoltre, manifestano insieme ai principali difetti di questa patologia, come l'ingrossamento di milza e fegato e l'anemia, anche i difetti a carico del sistema scheletrico, rendendoli dei buoni modelli per studiare i meccanismi molecolari a monte del fenotipo osseo.

Analizzando i principali marcatori molecolari coinvolti nello sviluppo osseo, come *col10a1*, *runx2b* e *osx*, ho potuto evidenziare che i difetti ossei osservati in questi modelli sono determinati da un difetto nel processo di differenziamento degli osteoblasti.

Inoltre, l'utilizzo di linee transgeniche di zebrafish nelle quali proteine fluorescenti, come la GFP, sono espresse sotto il controllo di promotori specifici per le principali vie di segnale molecolari, mi ha permesso di individuare alterazioni a carico delle vie di segnale Wnt e BMP in conseguenza alla carenza dell'enzima  $\beta$ -glucocerebrosidasi. Con questo lavoro di dottorato, la caratterizzazione di un nuovo modello animale per lo studio della malattia di Gaucher ha permesso di evidenziare che, disfunzioni a



carico di un enzima lisosomiale come la  $\beta$ -glucocerebrosidasi, può determinare alterazioni in segnali molecolari molto importanti per lo sviluppo embrionale, quali il Wnt ed il BMP. Entrambe queste vie molecolari svolgono ruoli importanti nel processo di formazione e mantenimento degli osteoblasti e alterazioni precoci di questi segnali durante l'embriogenesi possono determinare difetti nel processo di differenziamento cellulare da progenitori mesenchimali staminali. I risultati ottenuti durante questo lavoro di dottorato, hanno evidenziato per la prima volta il precoce coinvolgimento di due vie di segnale molecolari, il Wnt e il BMP, nella patogenesi ossea della malattia di Gaucher.



## ABSTRACT

Lysosomal storage disorders (LSDs) are rare inherited metabolic disorders due to a deficiency of specific lysosomal enzymes or transporters. Almost 50 genetic disorders caused by deficiencies of lysosomal and non-lysosomal proteins are known nowadays, collectively with an incidence of  $\sim 1/7000$  newborns in the worldwide population. Dysfunctions of such lysosomal enzymes or transporters can lead to several consequences that include incomplete degradation and/or recycling of intracellular molecules. Despite lysosomal proteins are present in almost all type of cells, the accumulation of undegraded substrates in LSDs affected patients is generally limited to cells, tissues and organs in which substrate turnover is high, leading to a wide spectrum of phenotypes and affected organs for different LSDs.

Among these LSDs, the most common is the Gaucher disease (GD) with an incidence of 1 in 200.000 newborn in the worldwide population, a rate that increases to 1 in 850 in the population of Ashkenazi Jewish (Eastern European). This disorder is due to a deficiency of the lysosomal enzyme  $\beta$ -glucocerebrosidase (GBA) that in pathological conditions is not able to degrade its substrate, glucosylceramide, into glucose and ceramide. A hallmark of the disease is the presence of "Gaucher cells", which are lipid laden-macrophages, in different tissues. Together with this characteristic, GD patients manifest hepatosplenomegaly, anemia, thrombocytopenia and severe bone dysfunction such as osteonecrosis, osteopenia, bone crisis and fracture of long bones. GD patients can be classified in three different clinical subtype, based upon the presence and severity of neurological defects. Type I GD, also referred to as non-neuronopathic form, is the most frequent subtype, the symptoms manifest in adulthood and patients do not present neurological involvement. Type II GD patients, manifest severe neurological defects since early life stages and death occurs in childhood. Type III GD patients manifest less severe neurological defects when compared to type II GD and generally symptoms occur during childhood. This classification of the disease based on the absence or presence and severity of neurological defects is oversimplified. Nowadays, the broad spectrum of phenotypes and the recognition of overlap among these GD subtypes has led to the concept that this disorder is a continuum of phenotypes, ranging from the less severe (GD 1) to the more severe forms (GD2 and GD3). The most effective and well tolerated treatment available for this disorders is the enzyme replacement therapy (ERT), that consists in the administration of a recombinant enzyme able to restore the  $\beta$ -glucocerebrosidase functions. Despite its effectiveness on

## Abstract

hepatosplenomegaly, anemia and thrombocytopenia symptoms, this therapy has a very limited effect on the recovery of the skeletal and neurological defects.

Different GD murine model have been developed through the years to understand the pathogenetic mechanism behind these broad spectrum of phenotype. Despite the availability of all mice models mimicking different Gaucher disease phenotypes, a completely reliable animal model does not exist and the pathogenic alterations occurring during early life stages can not be explored and elucidated yet.

The aim of my PhD project was to investigate the bone pathogenetic mechanisms of Gaucher disease using a new animal model. To address this purpose, I've used a zebrafish model due to its easy manipulation and the transparency of the embryos that allow to follow all the early developmental stages.

Using a morpholino-mediated knockdown approach and a stable genetic mutant line, I could investigate what was the effect of deficiency of the enzyme *Gba1* during early stages of embryonic development. Moreover, the defects observed in these zebrafish models resemble the most common GD phenotypes, like hepatosplenomegaly, anemia and skeletal deformity, making them good models to study the molecular mechanisms of the bone phenotype.

By analyzing the main molecular markers involved in bone development, as *col10a1*, *runx2b* and *osx*, I could point out that bone defects observed in these models are determined by an alteration in the osteoblasts differentiation process.

Also, using zebrafish transgenic lines in which fluorescent proteins such as GFP are expressed under the control of specific promoters for major molecular signaling pathways, allowed me to identify alterations of Wnt and BMP due to deficiency of the enzyme  $\beta$ -glucocerebrosidase.

In this work, characterization of a novel animal model for the study of Gaucher disease, highlighted that dysfunction of the lysosomal enzyme  $\beta$ -glucocerebrosidase can lead to alteration of major molecular signaling involved in the embryonic development, such as Wnt and BMP. Both these pathways have an important role in the formation and maintenance of osteoblasts lineage and early defects in these signal during embryogenesis could lead to defect in the differentiation program of mesenchymal stem cells progenitors.

The results showed in this doctoral thesis, highlight for the first time the early involvement of two pathways, the Wnt and BMP signaling, behind the bone pathogenesis of Gaucher disease.

## 1. INTRODUCTION

### 1.1 LYSOSOMAL STORAGE DISORDERS

Lysosomal storage disorders (LSDs) are inherited metabolic disorders that arise from deficiencies of specific lysosomal enzymes or transporters. Almost 50 genetic disorders caused by deficiencies of lysosomal and non-lysosomal proteins are known nowadays. The dysfunction of lysosomal enzymes or transporters can lead to several consequences that include incomplete degradation and/or recycling of intracellular molecules. . While LSDs individually are rare, collectively they have a very high prevalence in the population, of  $\sim 1/7000$  newborns.(Fuller et al. 2006)

All lysosomal storage disorders are characterized by the presence of undigested substrates in different cell types. In most lysosomal disorders more than one substrate can accumulate and stored material can be rather heterogeneous. Despite lysosomal proteins are present in almost all type of cells, the accumulation of undegraded substrates in LSDs affected patients is generally limited to cells, tissues and organs in which substrate turnover is high, leading to a wide spectrum of phenotypes and affected organs for different LSDs.

The first LSDs case was reported in the 19<sup>th</sup> century by Warren Tay, a British ophthalmologist who described the case of a 12-month-old male infant in whom a cherry macular spot was associated with delayed development. Few years later, Bernard Sachs an American neurologist provided a more comprehensive description of this pathology. Today, this first described case of LSDs is known as the Tay-Sachs disease. (Americo et al. 2015)

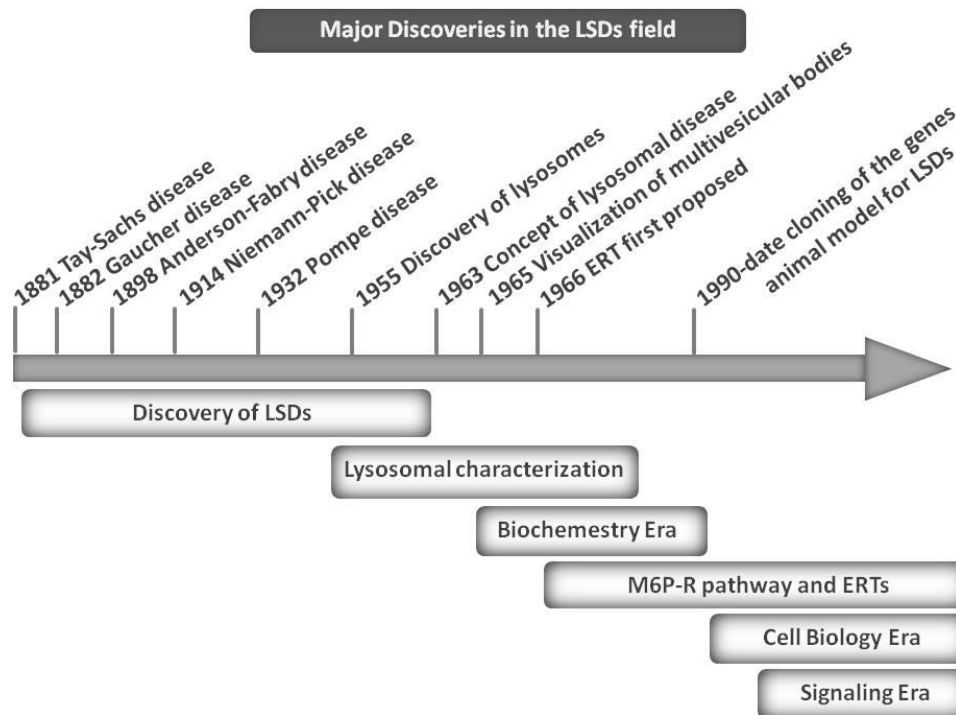
At that time, lysosomes were still unknown, and it was not clear that various diseases share the common feature of lysosomal storage. The first description of the lysosome as organelle with an acidic compartment containing several hydrolases was made by Christian de Duve in 1955, a discovery whereby he was awarded by the Nobel Prize in Medicine in 1974 (De Duve et al. 1955).

Only ten years later, Hers suggested that accumulation of glycogen observed in a patients affected by idiopathic hypertrophy of the heart (Pompe disease) was localized in lysosomes. This discovery permitted to classify the already clinically recognized disorders as lysosomal storage disorders.

The biochemical characterization of lysosomal enzymes during 1970s led to determination of their 3D structure by crystallization and to a mechanistic understanding of the mode of action of these enzymes. Moreover, further studies on Anderson-Fabry disease conducted by Hashimoto and co-workers enabled them to

## Introduction

conclude that there was a disturbance of the lysosomal structure as a consequence of a genetic disease (Klein 2013). Between the 1990s and 2005 most of lysosomal genes involved in LSDs have been sequenced and characterization of mutations has allowed to better understand the etiology of these disorders. Despite increasing knowledge of LSDs pathomechanisms occurring from the disease-causing mutations to the symptoms of the disease are still poorly understood. The big unsolved question is still how the storage material accumulating in the lysosome affect multiple cell populations and organ functions.



**Figure 1:** Time line of discoveries of classic LSDs from the first description of in 1881 to the recent molecular signaling approach. (modified from Klein 2013).

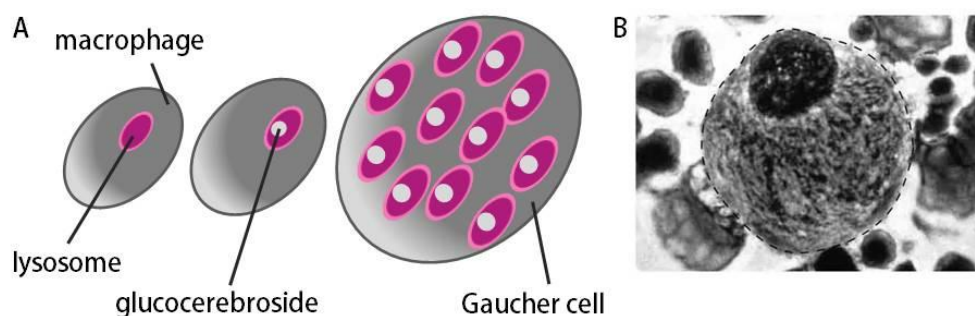
A common characteristic of lysosomal storage disorders is the accumulation of undegraded material begins in infancy and progressively worsen, often affecting various organs including internal organs and the central nervous system. After the discovery that intracellular and secreted lysosomal glycoproteins are targeted to lysosomes by the mannose- 6-phosphate (M6P)-receptor-mediated pathway (Kaplan et al. 1977), a key therapeutic approach has been developed. This treatment is called enzyme replacement therapy (ERT) and consists in the administration of a recombinant enzyme to patients to restore the function of the missing protein. (Shemesh et al. 2013) The effectiveness of this therapy, unfortunately, is very limited for LSDs-associated neurological and bone complications. Few other treatments are available for affected patients: substrate reduction therapies (SRT), aimed at reducing the amount of storage material (Platt & Jeyakumar 2008); small molecules or chaperones, to rescue misfolded or unstable enzymes (Balch et al.

2008); stimulating survival pathways or inhibiting pathways that cause cell death (Lloyd-Evans et al. 2008). Most of these therapies are still under clinical trial investigation and do not rescue all LSDs symptoms.

## 1.2 THE GAUCHER DISEASE

The most common lysosomal storage disorder is the Gaucher disease (GD) with an incidence of 1 in 200.000 live births in the worldwide population. The rate of incidence of this disorder increases to 1 in 850 in the population of Ashkenazi Jewish (Eastern European). This disorder is due to a deficiency of the lysosomal enzyme  $\beta$ -glucocerebrosidase (GBA) that in pathological conditions is not able to degrade its substrate, glucosylceramide, into glucose and ceramide (Sidransky 2004).

This disorder was first defined by Philippe Charles Ernest Gaucher in 1882. He described a 32-year old woman with hepatosplenomegaly. A postmortem examination revealed that cells in the spleen were enlarged. Such cells are now known as “Gaucher cells”, which are lipid laden-macrophages, a hallmark of the disease (fig. 2). Gaucher concluded in his doctoral thesis that the enlarged spleen of his patient was a neoplasm of the spleen. From 1882, different cases of Gaucher disease were reported. In 1927, Oberling and Woringer described an early, infantile acute form of the disease with rapidly progressive neurodegeneration (Gaucher disease type 2). Thirty years later, another type of Gaucher disease was characterized, in an isolated population in Northern Sweden where patients displayed a subacute neuronopathic form (Gaucher disease type 3) (Hruska et al. 2008)

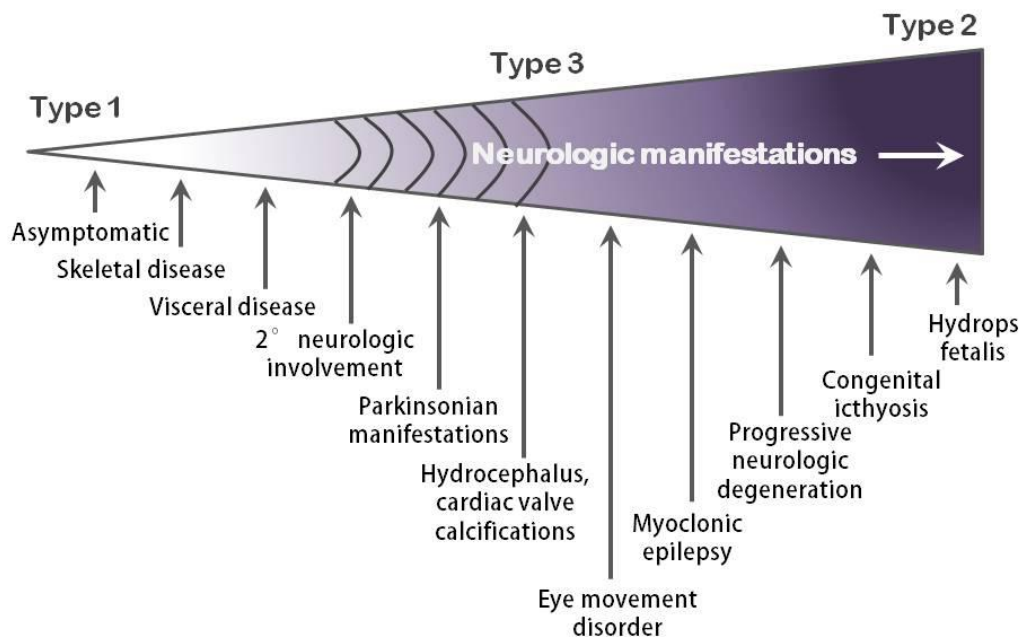


**Figure 2:** The presence of Gaucher cells in different tissue is a hallmark for the diagnosis of GD. (A) A cartoon representation of Gaucher cells. In pathological conditions, the glucocerebroside can't be degraded by  $\beta$ -glucocerebrosidase enzyme and accumulate in lysosomes. This accumulation results in the enlargement of macrophage. (B) An electron microscopy image of a Gaucher cell. (Wennekes et al. 2009)

## Introduction

Through the years, different cases have been reported, and Gaucher disease is now classified into three broad phenotypic categories based on the age of onset, clinical signs, and presence or absence and rate of progression of neurological symptoms. These three clinical subtypes are: infantile Gaucher disease characterized by hepatosplenomegaly and central nervous system involvement within the first year of life (type 2 GD); juvenile Gaucher disease with nervous system involvement in childhood (type 3 GD); and adult or chronic Gaucher disease characterized by splenomegaly, cytopenia, orthopedic complications and lack of neurological symptoms (type 1 GD). This classification of the disease based on the absence or presence and severity of neurological defects is oversimplified. Nowadays, the broad spectrum of phenotypes and the recognition of overlap among these GD subtypes has led to the concept that this disorder is a continuum of phenotypes, ranging from the less severe (GD 1) to the more severe forms (GD2 and GD3)(see fig. 3) (Sidransky 2012).

### A phenotypic continuum spectrum of Gaucher Disease



**Figure 3:** Schematic representation of the phenotypic continuum spectrum of Gaucher patients. Patients with Gaucher disease can have a spectrum of symptoms, ranging from mild to severe neurological defect (modified from Sidransky 2004).

Despite all the knowledge about GBA biochemical structure, enzymatic role, gene structure and mutations, little is known about the pathogenetic mechanisms behind the phenotype observed in Gaucher patients. Accumulation of undegraded material in lysosomes of macrophages has been proposed to activate the interleukin and cytokine cascades thus inducing internal organ defect and neurodegeneration.



However this hypothesis cannot completely explain all the spectrum of phenotypes of GD.

Occasionally, patients with type 1 Gaucher disease manifest later in life characteristics of Parkinsonian syndrome such as bradykinesia, rigidity, myoclonus seizures and resting tremor. Those symptoms are believed to arise from synuclein aggregation within dopaminergic neurons induced by mutations of GBA1. (Choi et al. 2011)

Moreover, patients with Parkinson's disease and associated Lewy body disorders have an increased frequency of GBA1 mutations as compared with control individuals (Sidransky & Lopez 2012). Despite recent findings, showing the link between Gaucher disease mutations and the onset of Parkinson's disease, the mechanisms underlying this association remain elusive.

Gaucher disease is the first lysosomal storage disorder for which enzyme replacement therapy (ERT) was successfully applied in the 1990's (Ceredase®; Genzyme Inc, Cambridge, MA, USA). Since the first ERT clinical trials, alternative therapeutic approaches consist only of palliative treatment such as splenectomy and hip replacement. Nowadays, ERT is the most effective treatment available for this disorders and it is well tolerated with only rare side effects. Currently, more than 5000 patients have been treated with ERTs. Clinical studied revealed that the earlier in life GD patients undergo ERT treatment, the higher is the effectiveness of the therapy. (Mistry et al. 2011)

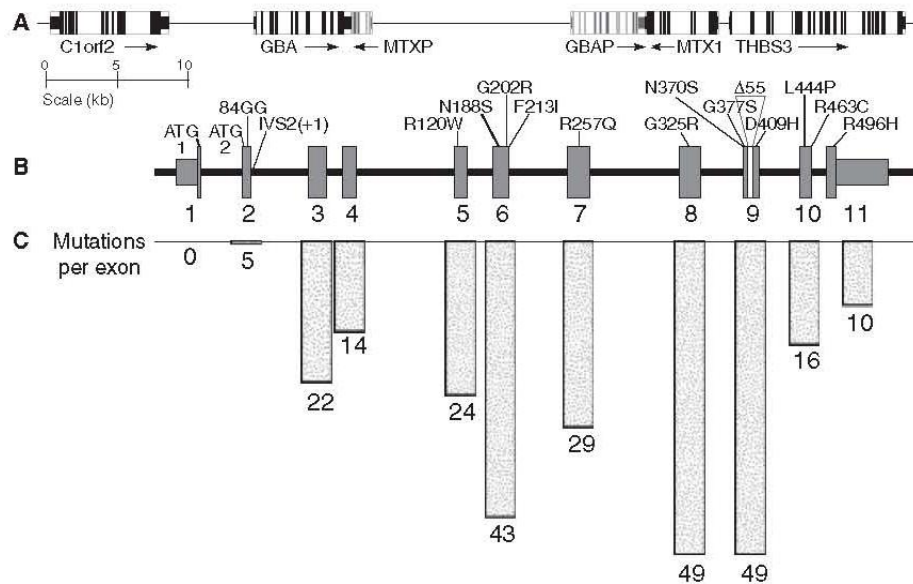
Even if ERT is the most effective therapy available for Gaucher disease, the clinical symptoms are partly ameliorated. In fact, even though ERT is effective for the treatment of GD-associated cytopenia and hepatosplenomegaly, osteopenia and CNS defects are poorly recovered even after long-term therapy.

### *1.2.1 Gaucher disease genotype is not always associated with a specific phenotype*

The lysosomal  $\beta$ -glucocerebrosidase enzyme is encoded by the GBA gene. In humans, this gene is located on chromosome 1q21. It is composed of 11 exons and 10 introns and the length of its genomic sequence is 7.6 kb (fig. 4). In 1989, a highly homologous pseudogene, called GBAP, located 16kb downstream to the GBA gene sequence was discovered. The importance of this pseudogene in the same GBA locus is that recombination events between GBAP and GBA results in several different Gaucher mutations occurring from gene conversion, fusion, or duplication (Hruska et al. 2008). More than 300 mutations have been reported in the glucocerebrosidase gene, with a distribution spanning the whole gene. Among them, missense mutations are the most frequent but also nonsense mutation, small insertion or deletions that

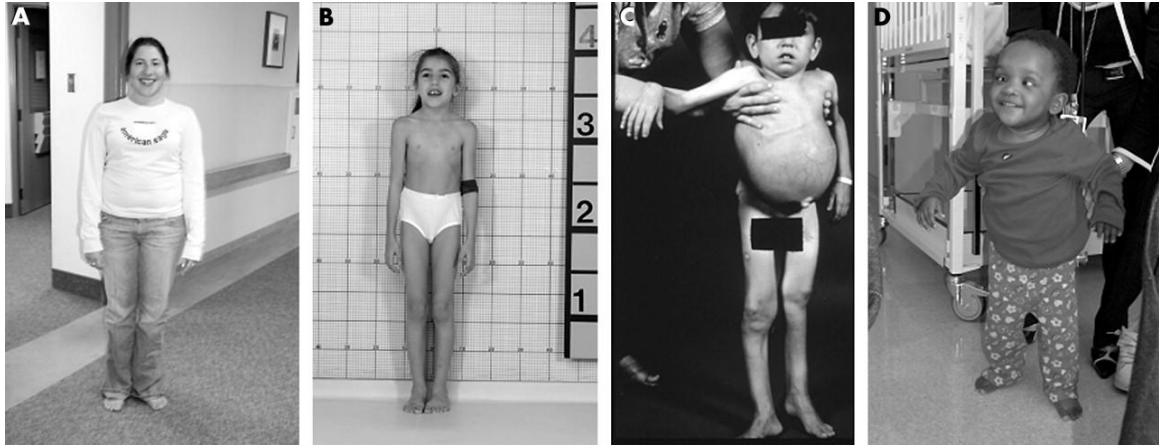
## Introduction

lead to either frameshifts or in-frame alterations and splice junction mutations have been detected. In the general populations, two GBA mutations are the prevalent mutant alleles: the L444P and the N370S. These two mutations are the first described for the GBA gene in the late 1980s and they are associated with the type 3 and type 1 Gaucher disease, respectively.



**Figure 4:** GBA structure and mutation distribution. (A): The 62-kb region surrounding the GBA along chromosome 1q showing the known genes and pseudogenes and their transcription direction. C1orf2, chromosome1open reading frame 2 (cote1); GBA, glucocerebrosidase; MTXP,metaxin1pseudogene; GBAP, glucocerebrosidase pseudogene; MTX1,metaxin1; THBS3, thrombospondin 3.(B) : The exonic structure of GBA, with positions of 15 common mutations. (C): Number of reported substitution, deletion, insertion, and splice-site mutations per exon. (Image from Hruska et al. 2008)

In the last decades, a classification of the patients according to the three GD categories has become very difficult. In fact, patients displaying GD symptoms in infancy or childhood without a neurological involvement, in some cases have been reported as type 1 in the original description of the causative alleles. However, later in life these patients were shown to manifest neurological symptoms leading to their reclassification into type 3 GD patients (Beutler E, Gelbart T 1993).



**Figure 5:** Different patients with Gaucher disease with genotype L444P/L444P. The spectrum of symptoms and disease progression among homozygotes for the same mutations can range from mildly symptomatic young adults to young children with neurological involvement. The following patients description is taken from the archive of *J Med Genet* 2005;42:e37 doi:10.1136/jmg.2004.028019 (A) Patient 16 at age 18. She was diagnosed at age 15 months with organomegaly and horizontal supranuclear palsy. She had skeletal complications before ERT was started at age 7. She is currently a college student and a ballet dancer. (B) Patient 9 at age 8. She presented with organomegaly and failure to thrive at age 9 months, and ERT was begun at age 1 year. Her current findings include interstitial pulmonary infiltrates and mild learning difficulties, but no skeletal involvement. (C) Patient 3 presented at age 1 year with liver fibrosis, severe bone disease, and portal hypertension. At age 10, he underwent a bone marrow transplant and died of sepsis shortly afterward. (D) Patient 29 was diagnosed at age 15 months with organomegaly, ocular apraxia, horizontal supranuclear palsy, and developmental delay. Although ERT was started immediately, at age 26 months she had brain stem involvement with swallowing dysfunction and recurrent stridor. Consents to publish these photographs were provided by the patients and/or parents.

It became evident that the correlation between the genotype and the phenotype of GD patients is not so unequivocal. Frequently, the combination of mutations on both alleles is important to define the phenotype (fig.5). Usually, clinicians define this allele combination with the term “compound heterozygosity”. Indeed, recent studies revealed that individuals with the same genotype can exhibit different disease manifestations, clinical courses and response to therapy (Sidransky 2004), differences that are observed even in sibling and twin GD patients (Amato et al. 2004; Lachmann et al. 2004). Moreover, patients with similar phenotypes may have many different genotypes, even in unique subgroups of patients (Sidransky et al. 1992).

### 1.2.2 Bone defects in the Gaucher disease

One of the clinical symptoms shared by GD subtypes is the presence of bone manifestations. Skeletal complications occur in 70-100% of patients with type 1 or type 3 GD. Despite bone defects do not correlate with the severity of systemic

## Introduction

manifestations, they increase the morbidity and disability associated with Gaucher disease.

The skeletal involvement is multifaceted and can include chronic bone pain, Erlenmeyer flask deformity of the distal femur, severe acute bone crises, bone marrow infiltration, osteopenia, avascular osteonecrosis, pathological fractures of long bones and vertebrae, subchondral joint collapse and growth retardation in children (fig.6) (Guggenbuhl et al. 2008).



**Figure 6:** Representative bone radiography of patients with Gaucher disease (A) Erlenmeyer flask deformity of the distal parts of both femurs (B) Avascular necrosis of the humeral head (C) Vertebral fracture (from Chalès et al. 2004).

Although the pathophysiology of the skeletal involvement is poorly understood, the broad spectrum of bone complications has been explained by the infiltration of Gaucher cells in the bone marrow compartment. The spread of Gaucher cells in the bone marrow probably can lead directly or indirectly to localized bone defects, including osteonecrosis and lytic lesions, but it can explain only part of the symptoms. (Guggenbuhl et al. 2008; Mikosch 2011)

Moreover, the disabling skeletal complications, have been associated with increased bone resorption but the evidence for the involvement of osteoclasts in GD has been recently argued (Mistry et al. 2010).

Alternative mechanisms involved in the pathophysiology of skeletal defects may include a decrease in the number and activity of bone progenitor cells, osteopenia with an increased risk of fractures, deficient fracture healing throughout life, blood vessel alterations with avascular necrosis and acute attacks of pain, and an increased risk of osteoarticular infection. (Guggenbuhl et al. 2008)

As previously mentioned, the capability of ERT to ameliorate the bone defects is very limited and the pathophysiology is still poorly understood. To this purpose, animal

models for the disease represent an important tool to unravel the pathogenic mechanism behind the clinical symptoms.

### 1.2.3 *Animal models in Gaucher disease research*

Throughout the past decades, several groups have attempted to develop a suitable animal model that mimics the complete spectrum of GD phenotypes.

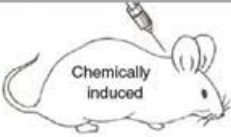
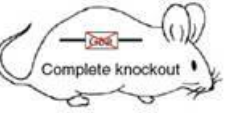
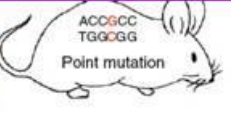
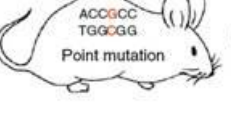
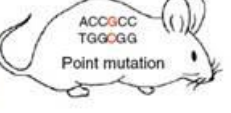
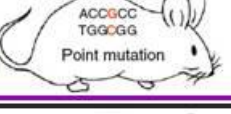
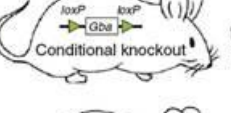
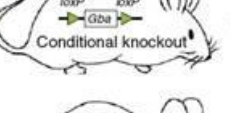

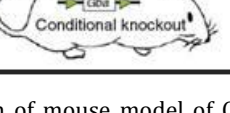
The first mouse model for GD was obtained, in 1975 by Kanfer and colleagues, employing a chemical compound inhibitor of the  $\beta$ -glucocerebrosidase enzyme, the conduritol  $\beta$ -epoxide (CBE) (Kanfer et al. 1975). Daily intraperitoneal injections of CBE for 3 weeks resulted in >90% inhibition of enzymatic activity and accumulation of the substrate in the spleen, liver and brain that could be reversed upon cessation of CBE treatment. Although this chemical GD mouse model recapitulated the visceral and the neurological defects of the pathology, it is not able to resemble the bone defects. Notably, this was not a genetic animal model.

With the advent of genetic engineering in the 1990's, a new approach for the generation of GD animal models was available.

In 1992, Tybulewicz and colleagues produced the first genetic GD mouse model by insertion of a Neo cassette in exons 9 and 10 of the *Gba* gene (Kyriakis J. M. 1992). This mouse was carrying a null mutation which was associated with a strong enzymatic activity decrease compared with wild-type mice. Phenotypic manifestations by this model were very similar to those observed in severe type 2 patients. Accumulation of glucosylceramide was observed in liver, brain, lungs and in the lysosomes of spleen and liver macrophages. Unfortunately, the full knockout mice *Gba*<sup>-/-</sup> die within 24 hours of birth in consequence of permeability barrier defects in the skin (Sidransky et al. 1992; Holleran et al. 1994)

After the generation of this first genetic *Gba*<sup>-/-</sup> mouse model, a number of attempts were made to create alternative mouse models of GD. In the last twenty years, different mouse strains, carrying the most common human GBA mutations (like N370S and L444P), have been generated with the knock-in technology approach (fig.7).

## Introduction

	Mouse	Main features	Use in GD research	Pros	Cons
Chemical mouse model	1975 CBE-induced (Kanfer et al., 1975)	 Chemically induced	Efficacy of gene therapy	Can manipulate dose and time; mimics neurological signs	Non-genetic model
Knockout mice	1992 <i>Gba</i> <sup>-/-</sup> (Tybulewicz et al., 1992)	 Complete knockout	Involvement of GlcCerase in skin formation	Paved the way for creation of more useful mouse models	Die within 24 hours of birth
Knockin mice	1998 RecNcil (L444P/A456P and L444P) (Liu et al., 1998)	 ACCGCC TGGGGG Point mutation	Involvement of GlcCerase in skin formation	Cell culture experiments	Die soon after birth
	2002 <i>Gba</i> <sup>L444P/L444P</sup> ; <i>Ugcg</i> <sup>+/+</sup> (Mizukami et al., 2002)	 ACCGCC TGGGGG Point mutation	Therapeutic evaluation targeting the mutant enzyme	Long lifespan; cell culture experiments	No GlcCer accumulation; no Gaucher cells; does not mimic human phenotype
	2003 V394L, D409H and D409V (Xu et al., 2003)	 ACCGCC TGGGGG Point mutation	Testing therapeutic options	Long lifespan; cell culture experiments	No phenotypic abnormalities; no GlcCer accumulation in the brain
	2003 N370S (Xu et al., 2003)	 ACCGCC TGGGGG Point mutation	-	Cell culture experiments	Die soon after birth
Conditional mice	2006, 2010 <i>Mx1-Cre-loxP</i> (Enquist et al., 2006; Mistry et al., 2010)	 <i>loxP</i> <i>loxP</i> Gba Conditional knockout	Cell and gene therapy; mechanistic basis for osteopenia	Normal life span; model for type 1 GD	The genetic mutation does not mimic a real mutation as seen in patients
	2007 <i>Nestin-flox/flox</i> (Enquist et al., 2007)	 <i>loxP</i> <i>loxP</i> Gba Conditional knockout	Role of microglia in nGD; progression of neuropathological changes	Reminiscent of neuropathological findings in nGD patients	Die within 3 weeks; GlcCer accumulation only in brain
	2007 <i>K14-In1/In1</i> (Enquist et al., 2007)	 <i>loxP</i> <i>loxP</i> Gba Conditional knockout	Efficacy of ICV-delivered GlcCerase	Reminiscent of neuropathological findings in nGD patients	Die within 2 weeks
	2008 <i>Kn-9H</i> mice (Xu et al., 2008)	 <i>loxP</i> <i>loxP</i> Gba Conditional knockout	-	Reminiscent of neuropathological findings in nGD patients	Die within 2 weeks

**Figure 7:** Timeline of the generation of mouse model of Gaucher disease (modified from Farfel-Becker et al. 2011)

All mouse models do not resemble the complete spectrum of phenotype of Gaucher disease. Some of these models are good to study the neurological involvement but do not mimic the visceral defect or the accumulation aspects. On the other hand, models mimicking the visceral defects do not resemble the skeletal and neurological defects. (fig.7)(Farfel-Becker et al. 2011)

In 2010, Mistry and colleagues obtained a nonneuronopathic GD1 conditional mouse model. In this mice the GBA1 gene was conditionally deleted in cells of the

hematopoietic and mesenchymal lineages through an Mx1 promoter. This GBA1 mouse model, display hepatosplenomegaly, hematological defects and skeletal complications, such as osteonecrosis and osteopenia, similar to human GD1 patients. Interestingly in this paper, Mistry demonstrated that the osteopenia found in his mouse model was due to a defect in osteoblastogenesis and it was not accompanied by increased bone resorption due to the activation of the osteoclast population. (Mistry et al. 2010). Despite the availability of all mice models mimicking different Gaucher disease phenotypes, a completely reliable animal model does not exist and the pathogenic alterations occurring during early life stages can not be explored and elucidated yet.

### 1.3 ZEBRAFISH A NEW POWERFUL ANIMAL MODEL

Zebrafish (*Danio rerio*) is a small tropical teleost fish, native of the river Ganges, in the north-east region of India. Since its establishment as a model organism in the 1970s by George Streisinger, this fish became a powerful model organism to study biological processes and vertebrate developmental biology.

Zebrafish is easy to breed and can be kept in laboratory conditions thanks to its small size (about 3-5 cm in length see figure 8). The female can lay more than 200 eggs per each mating event and the fertilization is external allowing an immediate analysis of the progeny at different developmental stages, without the need to dissect and sacrifice pregnant females as required for mammalian models. Developing embryos are transparent for the first 24 hours post fertilization (hpf) and pigmentation can be chemically inhibited so that they can be maintained transparent for many days. Moreover, zebrafish embryos display rapid external development with all the main organs developing within 36 hpf, allowing in vivo observation of embryogenesis and organogenesis since early life stages after fertilization.



**Figure 8:** Representative images of zebrafish embryo at 24 hpf stage (left) and adult male and female (right).



## Introduction

Another advantage of this model, is that adult zebrafish reach sexual maturity within approximately 3-4 months, making this fish a versatile tool for large-scale genetic analysis and mutagenesis screenings (Christiane Nusslein-Volhard 2002; Streisinger et al. 1981).

The rapidity of organogenesis of zebrafish embryo and the features that main organs functions are equivalent to those of other vertebrate, made the zebrafish a usefull animal model in different field of biomedical research in the last decade. Despite it has not been extensively used for analysis of bone development and disease, several studies have highlighted its potential. In zebrafish, the skull bone formation occurs by direct ossification (called dermal bones) as well as using a cartilage template (called cartilage bones) with a mechanism very similar to the tetrapods vertebrate (that will be discussed later in this thesis). Moreover, Li and colleagues in 2009 discovered that the transcriptional hierarchy found in the osteoblast formation in mammals is conserved even in zebrafish and it can be divided into three overlapping stages based on differential gene expression profile: early, intermediate and mature differentiation (Li et al. 2009). During early differentiation, expression of the *runx2a* and *runx2b* transcription factor is detected in both cartilage and bone primordial of cranial region since 36 hpf in zebrafish embryos and diminished by 120 hpf. The intermediate differentiation stage is characterized by expression of *osterix (osx)* in whole bone and partially overlap in time with the *runx2* expression pattern. In the mature stage of differentiation, marked expression of bone matrix genes like *collagen type 1 alpha 2 (col1a2)* and *osteonectin (osn)* is detected in regions that undergo ossification. Usually, their expression is coincident with *osx* or follows shortly later, and perdures around skeletal element even after *osx*, *runx2a* and *runx2b* are not detectable. Together with these bone-related genes, other transcription factors may have a role in osteoblastogenesis in zebrafish. Expression of *collagen type X alpha 1 (col10a1)*, is generally associated with hypertrophic chondrocyte in tetrapods but recent findings suggest a role during both intermediate and mature stage of osteoblast differentiation in zebrafish. Indeed, *col10a1* expression was found during formation of cartilage and dermal bone and it is maintained after bone has formed, presumably in mature osteoblasts. The bone maturation processes and the bone homeostasis in mammals are maintained through the action of several signaling pathways. Among them, WNT signaling and BMP pathway play key roles in these mechanisms. Evidence that the same signaling pathways are involved in zebrafish osteoblastogenesis comes from study of *pcf7* and *cvl2* expression pattern, a known mediator of the Wnt signaling and BMP pathway, respectively (Rentzsch et al. 2006). These two pathways mediator are expressed both in intermediate and mature stages of osteoblasts differentiations in zebrafish



around developing dermal bones and bone primordium with a pattern similar to the osteogenic genes like *osx*, *runx2* and *col10a1*. (Li et al. 2009) Altogether, these finding reveals a shared conserved mechanism of bone development and differentiation between zebrafish and other vertebrates.

A helpful support to elucidate the mechanisms of vertebrate bone formation comes from different powerful tools developed to allow manipulation of zebrafish embryos, like microinjection and cell transplantations. Particularly, DNA, mRNAs and antisense oligo morpholinos are commonly injected in freshly fertilized eggs to overexpress target mRNAs or perform gene silencing by means of morpholino (MO) oligos.

### 1.3.1 Morpholino gene knockdown

The use of morpholino oligos (MOs) is the most commonly and validated antisense technology that permits the investigation of functional gene loss. MOs enable to identify the role of signaling pathways and specific proteins in development or in drug response studies. By the injection of MOs, a graded severity of phenotypes is typically generated, but the complete loss-of-function cannot be obtained. Despite this limitation, the concentration of injected MOs can be modulated to obtain a non-lethal knockdown of the targeted protein leading to the observation of the effects on embryonic development. This aspect of microinjection may be seen as a distinct advantage when compared to the generation of full knockout mice which can be potentially embryonic lethal, like the GBA knockout mice generated by Tybulewicz in 1992 (Fecht 1992).

Morpholinos are synthetic molecules, typically 25 bases in length, that bind to the target complementary sequence of RNA by nucleic acid base-pairing. This binding, creates a steric block and inhibits the translation or splicing of the target gene (Corey & Abrams 2001). Their name derives from the MO structure of the constituent units, each containing one of the four nitrogenous bases (A, C, G or T) linked to a six atoms morpholine ring instead of a ribose or deoxyribose molecule. The morpholino rings are linked through phosphorodiamidate instead of phosphates groups. Different type of MOs can be designed, according to the target protein. A MO complementary to a region between 5'-CAP and the first 25 nucleotides after the translation initiation codon (AUG), generates a sterical block preventing the recognition of the ribosome and the translation of the protein (AUG-MOs). Alternatively, a MO that interfere with the maturation processes of the pre-mRNA in the nucleus (splice-blocking MO) can be obtained. The sequence of these MOs are complementary to splice acceptor (intron-exon boundary) or donor (exon-

## *Introduction*

intron boundary) sites in the unspliced RNA and compete with the splicing apparatus for the binding sites. The results of MOs binding to target premature mRNA lead to loss of an exon or to intron retention (Sazani et al. 2001).

Although MOs are very sequence-specific, nonspecific binding to a similar pre-mRNA sequence of other genes can occur. To understand whether the MOs-induced phenotype observed in the morphant (embryo injected with the MOs) is specific, rigorous controls are performed. For example, the injection of a mismatch MO (a modified oligonucleotide which differs for 4-5 bases from the specific MO) that is unable to bind to the target sequence is commonly carried out. Moreover, rescue experiments performed with the co-injection of the MOs and an mRNA encoding for the target protein derived from another organism should, at least partially, recover the normal phenotype of morphants.

The morpholino technology is currently considered the best readily and accessible gene knockdown approach in zebrafish.

### *1.3.2 Transgenic zebrafish reporter lines*

Microinjection is also used to insert transgenic constructs that express reporter genes, as the green fluorescent protein (GFP), under the control of tissue-specific promoters. The creation of stable transgenic lines allows to follow the differentiation of specific organs or tissues and elucidate the genetic pathways responsible for their development (Christiane Nusslein-Volhard 2002). The knowledge of molecular and biochemical processes regulating cell differentiation, proliferation and fate determination is important to understand tissue homeostasis and embryonic development in normal and pathological conditions.

The discovery of the important role that different signaling pathways play during embryonic and postnatal development comes from the study of the bone morphogenetic proteins (BMPs), wingless-related integration site (Wnt), fibroblast growth factor (FGF) and sonic Hedgehog (Shh).

In the last decades, different cell-signaling specific reporter zebrafish lines have been generated (Moro et al. 2013). In these lines, the expression of fluorescent protein like GFP and mCherry, is under the control of specific responsive elements for the most important cell signaling pathways.

The big advantage of the use of zebrafish comes from the combinations of MOs microinjection of targeted specific mRNAs into different transgenic reporter lines. This approach allows to elucidate if a target gene knockdown may positively or negatively affect specific signaling pathways.

The limitations of the MOs-based knockdown approach, have been overcome by the generation of different specific mutant lines.

### 1.3.3 Generation of stable zebrafish mutant lines

The zebrafish genome is closely related to the human one and approximately 70% of human genes have orthologues in zebrafish (Howe et al. 2013). Among these genes, many are present as paralogs because Teleosts underwent genome duplication (Volff 2005). Different approaches have been developed by the generation of zebrafish mutant lines. Forward genetic studies, have been conducted using irradiation, murine leukemia virus (MLV) and chemical mutagens such as the DNA alkylating agent N-ethyl-N-nitrosourea (ENU)(Solnica-Krezel et al. 1994; Driever et al. 1996; Haffter et al. 1996). By these methods, a large number of mutants have been isolated and mutated genes have then been identified by positional cloning.

However, forward genetic screenings are intrinsically limited in their effectiveness to isolate mutations of every single gene due to functional redundancy between different genes and the need to have measurable phenotypes. Moreover, the genome duplication event that occurred during zebrafish evolution make the generation of fish mutants more complicated.

Due to this limitation, a new “reverse genetic” approach has been introduced in zebrafish gene manipulation. According to this approach, once a gene of interest has been identified, loss of function analysis and phenotypic characterization are performed. Several alternative reverse genetic approach have been developed to produce site-specific genome modifications, like mutagenesis screening based on retrovirus or transposons, TILLING (Targeting Induced Local Lesions IN Genome) strategies and, more recently, zinc finger nuclease (ZFN), transcription activator-like effector nuclease (TALEN) and the CRISPR-Cas9 approach (Doyon et al. 2008; Hwang et al. 2013; Huang et al. 2012).

These mutant lines generated throughout the years, have been demonstrated to serve as models for human diseases as well as to investigate the main mechanisms of development. All these mutant lines can be found at the website of the Sanger Institute: <http://www.sanger.ac.uk/resources/zebrafish/genomeproject.html>

## 1.4 MOLECULAR DEVELOPMENT OF VERTEBRATE SKELETON

In all vertebrates, the mature skeleton is maintained by the balanced activity of the bone-forming osteoblasts and the bone-resorbing osteoclasts. The osteoblasts are part of a group of cells, typically referred to as “osteoblast lineage” cells, build the

## *Introduction*

skeleton, by providing mechanical support, muscle attachment and reservoir of calcium and phosphorus. Beyond these traditional roles, recent findings highlighted new different functions of these cells. In fact, some of these osteoblast lineage cells contribute to the bone marrow microenvironment, which is essential for haematopoietic stem cells homeostasis (Calvi et al. 2003), and furthermore, studies conducted on mice revealed a role of these cells in the regulation of glucose metabolism (Ferron et al. 2010; Fulzele et al. 2010).

Defects in the equilibrium between bone-forming osteoblasts cells and bone-resorption cells are frequently associated with human bone disorders, such as osteoporosis or osteopetrosis (Helfrich et al. 2007).

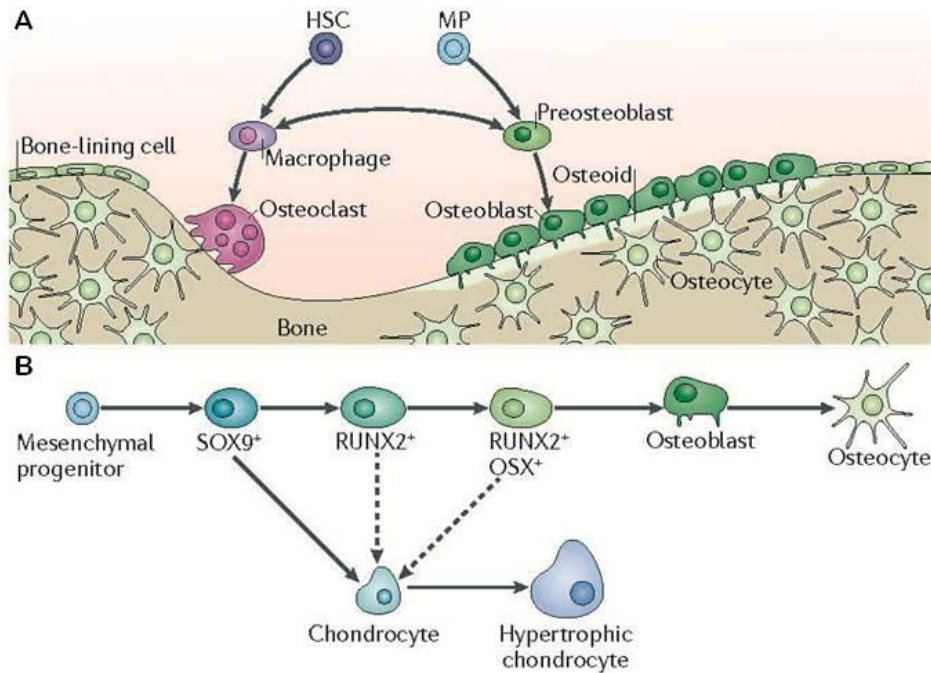
Several type of cells are included in the osteoblast lineage cells like mesenchymal progenitors, preosteoblasts, osteoblasts (also called mature osteoblasts), bone-lining cells and osteocytes. Cytologically, osteoblasts are characterized by abundant mitochondria, basophilic cytoplasm and a large Golgi apparatus, functionally related to the production of a large amount of extracellular matrix proteins, including osteocalcin, alkaline phosphatase and type I collagen (Long 2011).

The osteoblasts maturation process is generally divided into three stages mesenchymal progenitors, preosteoblasts and osteoblasts. The transition from one stage to the other is finely regulated by specific transcription factors expressed by osteoblasts lineage cells (fig.9).

The molecular markers for the mesenchymal progenitor are matter of debate, but generally the expression of SOX9, the transcription factor of the sex-determining region Y, is associated with mesenchymal progenitors that give rise to osteoblasts. In fact, SOX9 is not expressed by mature osteoblasts (Akiyama et al. 2002).

Preosteoblasts comprise an heterogeneous pool of cells ranging from progenitors to mature osteoblasts and are usually considered expressing the transcription factor RUNX2 or, later in differentiation, both RUNX2 and osterix (OSX, also known sp7) (Nakashima et al. 2002). However, the precise cellular identity of each different-cellular stage during osteoblasts maturation process is not well understood.

Only osteoblasts covered by bone matrix become osteocytes and usually these cells represent the 95% of the mature bone tissue. Osteocytes create a complex network with osteoblasts, and the lining cells of the bone surface. Moreover, recent studies revealed their important role in regulation of bone remodeling in response to mechanical and hormonal signals. This tight regulation seems to be propagated, at least in part, by sclerostin, which is encoded by the SOST gene and produced predominantly by osteocytes (van Bezooijen et al. 2004).



**Figure 9:** (A) Osteoblast and osteoclast lineage cells. Osteoblasts derive from a mesenchymal cell precursor (MP) while osteoclasts derive from hematopoietic stem cell differentiation (HSC). The balance between osteoblast activity (bone formation) and osteoclast activity (bone resorption) maintains the homeostasis of bone tissue. (B) Schematic representation of the transcription factors expressed by different osteoblast lineage cells during ossification processes. (from Long 2011).

#### 1.4.1 Osteoblast commitment during embryonic and postnatal development

The vertebrate skeleton is composed of different kinds of bones: long bones like the thighbone and humerus, flat bones like craniofacial bones and short bones like ribs. Osteoblasts composing these different bones derive from distinct embryonic germ layers. Craniofacial bones are generally derived from neuroectoderm, particularly by the commitment of neural crest cells, a mesenchymal cell type typical of the vertebrates. Instead, osteoblasts of the axial and appendicular skeleton are derived from paraxial mesoderm (somites) and the lateral plate mesoderm, respectively (Olsen et al. 2000). Bones of the vertebrate skeleton are generated through two distinct processes involved in the differentiation of osteoblasts from an embryonic mesenchymal cell progenitor: intramembranous or endochondral ossification (fig. 10). Osteoblasts originated by both these differentiation processes are characterized by the expression of RUNX2, a Runt domain-containing transcription factor, that is usually expressed in early differentiated osteoblasts (fig. 9).

During intramembranous ossification, mesenchymal progenitors condense and directly differentiate into osteoblasts. This process is usually limited to certain parts of the skull, as well as to part of the clavicle in mammals (Long 2011).

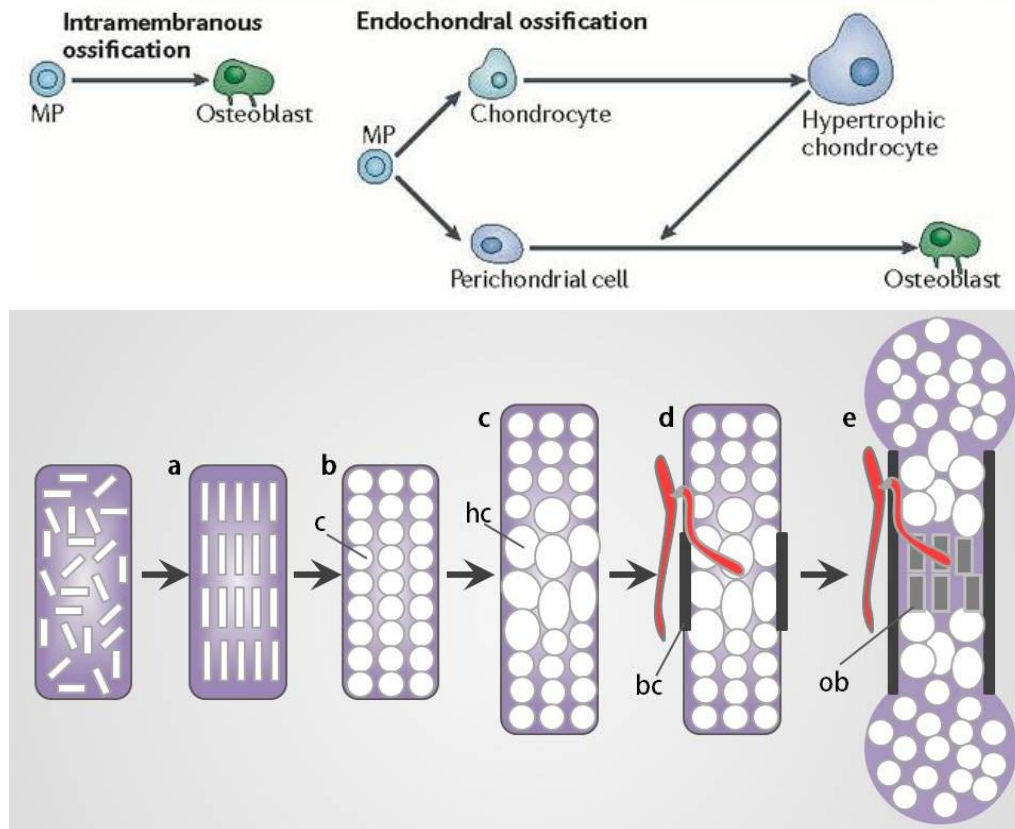
## *Introduction*

In the endochondral ossification process, mesenchymal cell progenitors condense to form chondrocytes (cartilage cells) and perichondrial cells, that compose the cartilage primordium. Chondrocytes in the primordium undergo to a fast proliferation process and later, exit the cell cycle and increase their cell size (hypertrophic chondrocytes). The increase of chondrocyte size is an important step because triggers the initial osteoblasts differentiation from perichondrial cells.

Immediately after this initial step in osteoblastogenesis, blood vessels invade the hypertrophic cartilage to form a primitive marrow cavity and induce osteoblast differentiation within the cavity. Blood vessels invasion of the hypertrophic cartilage probably allows to recruit osteoclast-like resorptive cells (which belong to the blood cell lineage and are generally called chondroclasts) that degrade the cartilage matrix to produce the bone marrow cavity (fig.10). Moreover, blood vessels permit the preosteoblasts to enter the nascent bone marrow, where they differentiate into mature osteoblasts. At the end of both intramembranous and endochondral ossification, terminally differentiated osteoblasts are identifiable by the expression of osterix (OSX), a transcription factor containing three C2H2-type zinc-fingers that function downstream of RUNX2 during osteoblast differentiation (fig.9). New osteoblasts continue to form after birth but the origin of osteoblast progenitors in post-natal life is not well understood.

Different transcription factors expressed by osteoblast lineage cells during ossification processes are regulated by a range of developmental signals that have important roles in the cell fate determination.

In the next subchapter, I'll introduce the major signaling pathways known to be involved in the osteoblastogenesis process. Furthermore, for the comprehension of the results of this thesis, I will focus my description on two different pathways, the Wnt and BMP signaling pathways.



**Figure 10:** Representation of intramembranous and endochondral ossification processes (upper panel) highlighting the differences among these two mechanisms (Long 2011). In the lower panel, a schematization of the different steps that occur on endochondral ossification from mesenchymal cells condensation to vascularization of neo-formed bone. c: chondrocyte; hc: hypertrophic chondrocyte; bc: bone collar; ob: osteoblast. (modified from Kronenberg 2003).

#### 1.4.2 The molecular signaling pathways involved in the osteoblasts development

As discussed above, the osteoblasts maturation processes is characterized by several steps that give rise to different cell types, like hypertrophic chondrocytes, preosteoblasts and mature osteoblasts. All these cell types derive from the differentiation of a mesenchymal stem cell precursor.

The differentiation program is tightly regulated by different cell signaling pathways since early life stages during embryonic development and the crosstalk and balance between them is important in bone homeostasis and maintenance.

Among the signaling pathways, Hedgehog signaling (Hh) is involved during early steps of osteoblasts differentiation. Indian Hedgehog (Ihh) is specifically expressed by the pre-hypertrophic and early hypertrophic chondrocyte within the endochondral cartilage primordium during endochondral ossification. Several studies revealed that in the absence of IHH signaling, the perichondrial progenitors failed to express RUNX2 which is indispensable for osteoblast differentiation (Long et al. 2004; Tu et al. 2012). Despite its pivotal role in endochondral ossification, Hh

## *Introduction*

signaling does not seem to be involved in intramembranous osteoblasts differentiation and the differential requirement of this pathway in these two processes is not well understood.

Another pathway involved in osteoblasts differentiation is the Notch signaling. Notch signaling generally mediates the communication between neighbouring cells by direct cell-cell contact. In osteoblasts differentiation, Notch signaling normally inhibits osteoblast formation from mesenchymal progenitor cells acting upstream of OSX activation. Different human genetic disorders have been associated with defects in Notch signaling. Due to its negative role in osteoblast differentiation, downregulation of this pathway is frequently associated with ectopic ossification in humans whereas gain-of-function mutations are responsible for Hadju-Cheney syndrome, a disorder of severe and progressive bone loss (Simpson et al. 2011).

A pathway that is responsible for a broad range of congenital skeletal disorders in humans is the FGF signaling. FGF signaling comprises a large family of proteins that account for 22 members in humans and mice. It plays several biological functions in vertebrates (Itoh & Ornitz 2008) and, specifically during the osteoblasts differentiation process, FGF can act at both embryonic and postnatal stages. This pathway seems to be involved in regulating preosteoblast proliferation, osteoblast differentiation and activity of mature osteoblasts through the action of different receptors (Montero et al. 2000; Liu et al. 2007; Jacob et al. 2006).

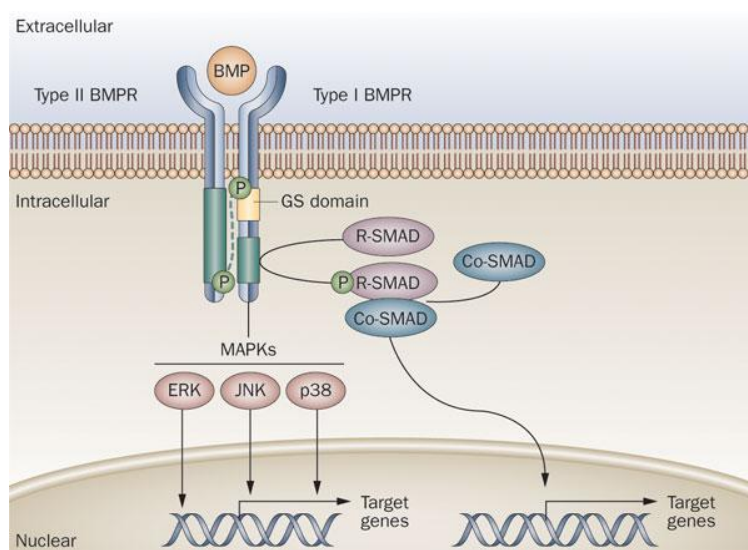
Despite its multifaceted roles in osteoblast differentiation, the precise stages at which FGFs regulate each differentiation process and the intracellular cascades responsible for each function, remain unclear.

Bone morphogenetic proteins (BMPs) were discovered in 1965 as potent inducers of ectopic bone formation when implanted subcutaneously. BMPs are members of the transforming growth factor- $\beta$  (TGF- $\beta$ ) gene superfamily and the signal is transduced through transmembrane receptor complexes composed of heterotetramers of BMP type I and type II serine/threonine kinase receptors (Feng & Derynck 2005). Upon ligand binding to the receptor, a phosphorylation cascade is propagated through activation of SMADs (SMAD1, SMAD 5 or SMAD8) in the cytoplasm. Phosphorylated SMADs form a complex with their common partner, SMAD4 that translocate into the nucleus and regulate gene expression. There are three type I receptors and three type II receptors and approximately 30 ligands are identified in the BMPs pathways.

BMPs signaling is involved in both bone formation and bone resorption by affecting multiple cell types such as mesenchymal cells, chondrocytes, osteoblasts, osteoclasts and endothelial cells. Genetic studies have highlighted the role of BMP2 and BMP4 in promoting osteoblast differentiation from mesenchymal cell precursors. Loss-of-



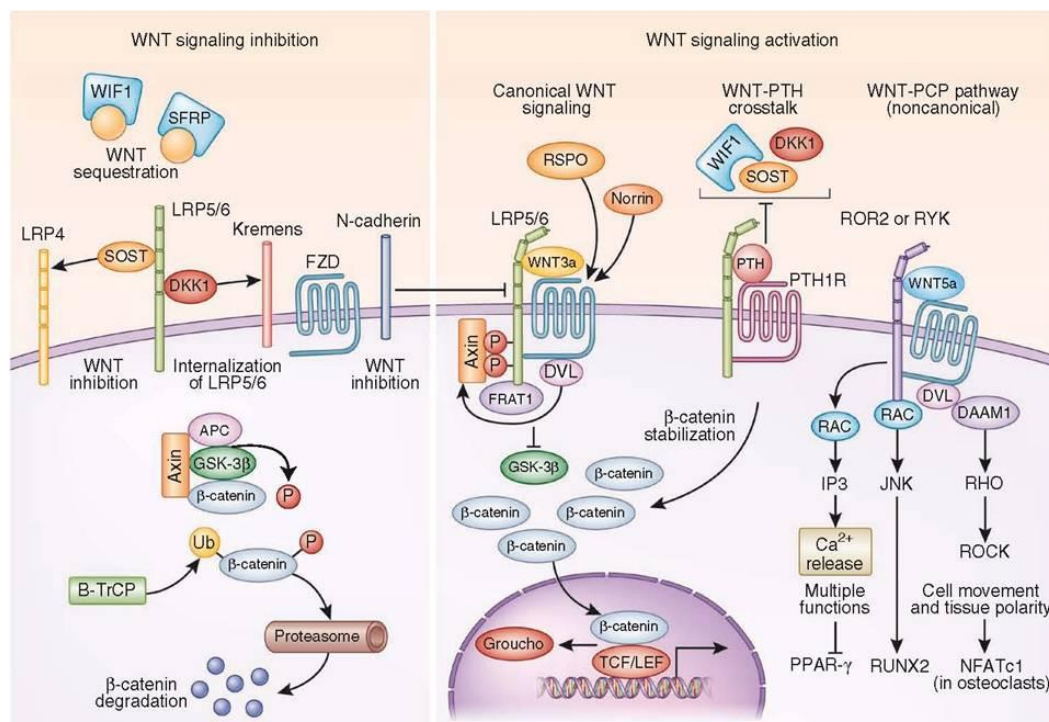
function experiments showed that differentiation into mature osteoblasts requires a critical threshold level of BMP2 and BMP4 signaling, while overexpression of BMP4 in osteoblasts results in increased osteoclastogenesis and reduced bone mass (Bandyopadhyay et al. 2006). Moreover, deletion of BMP receptor 1A (BMPR1A) in preosteoblasts and osteoblasts, resulted in increased bone mass. These findings indicated that despite BMPR1A knockdown usually reduces bone formation, it also inhibits bone resorption resulting in increased bone mass (Mishina et al. 2004). Both BMP2 and BMPR1A are expressed in osteoclasts, suggesting a possible direct effect of BMPs signaling on bone resorption. Several studies depicted an important role of endocytosis during TGF- $\beta$  signal activation. Phosphorylation at serine residues of the membrane receptors after ligand-binding lead to internalization of this complex into endosomes. Once into endosomes, binding of the receptors complex to SMAD anchor for receptor activation (SARA) can take place. These protein complex recognizes the activated receptor and recruits SMAD1 or SMAD2 transcription factors to signaling endosomes to promote its phosphorylation. Then phosphorylated SMADs are released into cytoplasm, bind the cofactor SMAD4, enter the nucleus and promote gene transcription (fig.11) (Hayes et al. 2002). Involvement of endocytosis has emerged to be crucial for activation and propagation of BMPs signaling. Recent findings show that inhibition of dynamin-dependent endocytosis reduces the levels of phosphorylated SMAD1/5/8 formation, affecting their translocation into the nucleus. Moreover, inhibition of endocytosis during initial phase of BMP-2 activation in mesenchymal cell precursors resulted in down regulation of mature osteoblast markers although expression levels of early osteoblast markers such as Runx2 and Osx were increased (Hartung et al. 2006; Heining et al. 2011).



**Figure 11:** Schematic representation of the BMP signaling pathway (from Shore & Kaplan 2010).

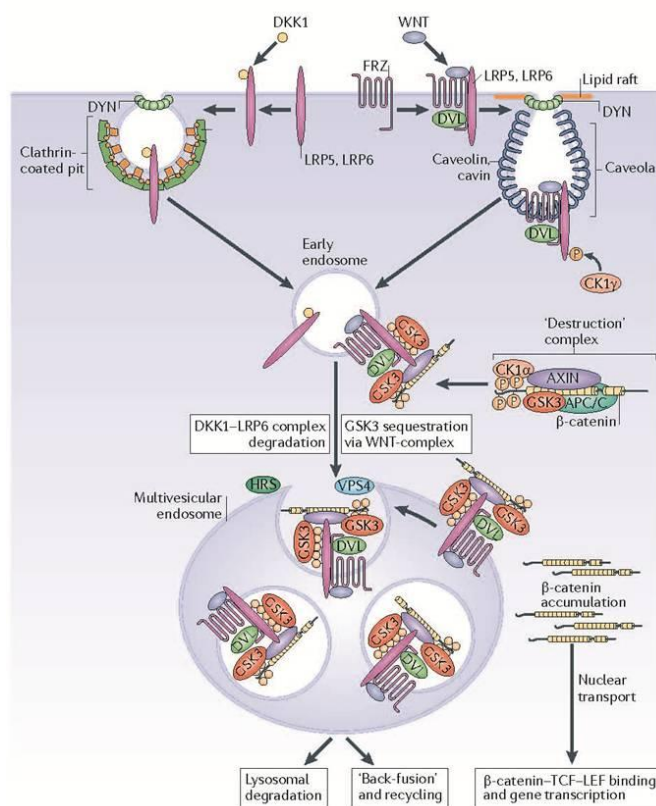
## Introduction

Another cell signaling pathway that has several different roles in osteoblastogenesis is the WNT signaling, that is emerged being a pathway important not only in developmental processes but also in postnatal health and disease conditions (Baron & Kneissel 2013). The transduction of this pathway can be propagated through the activation of numerous intracellular signaling cascades that are either dependent (canonical) or independent (non-canonical) on  $\beta$ -catenin (Huelsenken & Birchmeier 2001; Veeman et al. 2003). Both these mechanisms of action of Wnt signaling can affect the osteoblastogenesis and the bone homeostasis, but the canonical pathway has emerged as the predominant component of WNT signaling affecting bone cells. The canonical WNT signaling is established by the binding of WNT ligands to the dual receptor complex comprising of frizzled (FZD) and either the low density lipoprotein receptor-related protein 5 (LRP5) or LRP6. The binding to the receptor inhibits the degradation of the  $\beta$ -catenin by proteasome, promoting the inactivation of the multiprotein “destruction complex”, composed by glycogen synthase kinase 3 (GSK 3), AXIN, adenomatous polyposis (APC) and casein kinase 1 (CK1). Stabilized  $\beta$ -catenin can accumulate in the cytoplasm and translocate into the nucleus, where it associates with lymphoid enhancer-binding factor 1 (LEF1), T cell factor 1 (TCF1), TCF3 and TCF4 to control target gene transcription (fig.12).



**Figure 12:** Illustration of the Wnt signaling cascades. In the absence of Wnt ligands, the  $\beta$ -catenin is sequestered by the “destruction complex” composed by Axin, adenomatous polyposis (APC), glycogen synthase kinase 3 (GSK-3 $\beta$ ) and casein kinase 1 (CK1) and is degraded. When Wnt signaling is activated, the “destruction complex” is inhibited and the  $\beta$ -catenin can translocate into the nucleus and activate the transcription of target genes. (image from Baron & Kneissel 2013).

The signal cascade generated upon binding of WNT ligands to the membrane receptor, is finely regulated. Recently, it has been demonstrated that GSK 3 and other components of the WNT pathway implicated in the signal transduction, such as LRP6, Frizzled, AXIN, DVL and  $\beta$ -catenin, are internalized into intraluminal vesicles (ILVs) and are targeted to endosomes and multivesicular bodies (MVBs) (fig.13). Once in MVBs, this WNT receptor complexes may progress into lysosomes for degradation or fuse back to endosomal membranes, recycling GSK3 to the cytoplasm when the WNT signal is terminated. (Dobrowolski & De Robertis 2011) This mechanism highlights a possible active role of the MVBs lysosomal precursor in the regulation of the WNT signal transduction and maintenance.

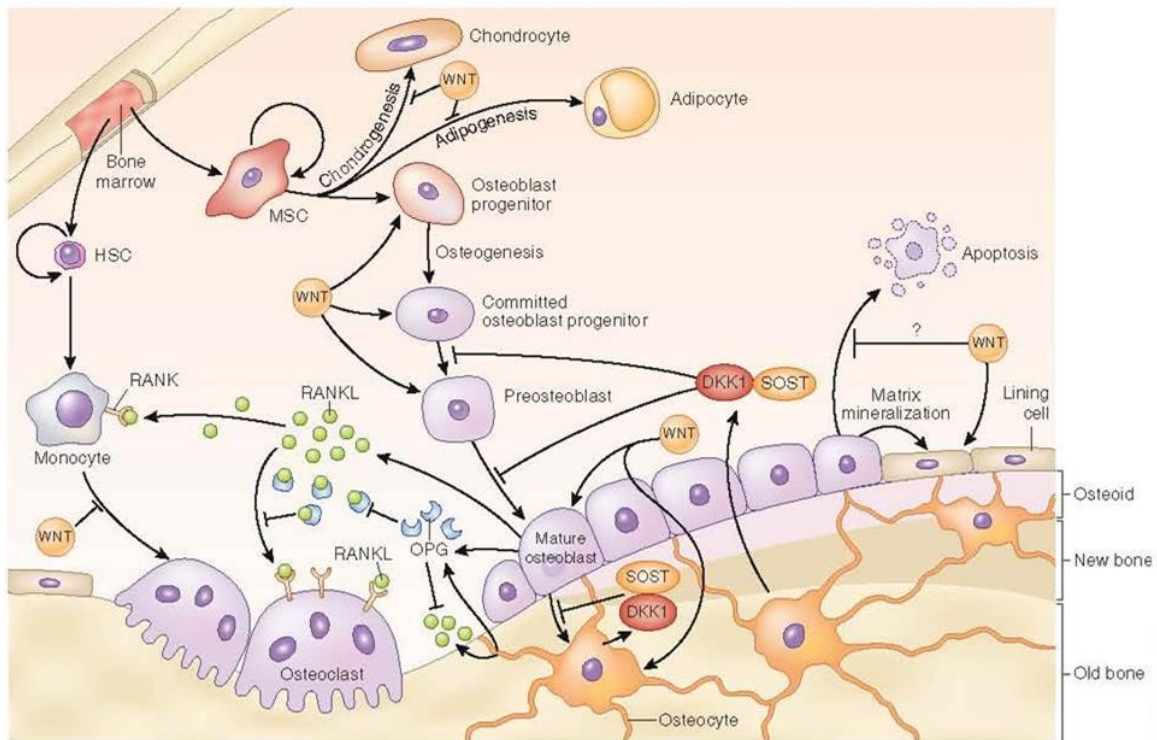


**Figure 13:** Schematic representation of regulatory mechanism of the Wnt signaling cascades mediated by MVBs. In presence of Wnt ligands, the destruction complex, that includes GSK 3, is sequestered into early endosomes. This lead to the accumulation of  $\beta$ -catenin in the cytoplasm and subsequent translocation into the nucleus and activation of the target genes. (image from Dobrowolski & De Robertis 2011)

The canonical WNT signaling can affect the entire osteoblastic lineage by regulating the equilibrium between osteoblasts and osteoclasts (fig.14) and genetic mutation affecting several members of this pathway results in severe skeletal malformations in human and mice. Loss-of-function mutations in the gene encoding the LRP5 co-receptor are associated with low bone mass in osteoporosis-pseudoglioma syndrome (Gong et al. 2001) while gain-of-function mutations in LRP5 make the co-receptor insensitive to extracellular WNT inhibitors, like Dikkopf-related 1 (DKK1), and are associated with high bone mass in otherwise healthy patients (Little et al. 2002). Moreover, Van Buchem disease and high bone mass in sclerostosis are

## Introduction

frequently associated with mutations in the SOST gene that encodes for the secreted antagonist of the Wnt signaling, sclerostin (Loots et al. 2005). This protein can bind to LRP5 and the related LRP4 and LRP6 receptors and is secreted primarily from osteocytes (Poole et al. 2005). The mechanism of action of sclerostin seems to be related to inhibition of the WNT signaling, but also its role in inhibition of the bone morphogenetic pathway (BMP) has been suggested (Krause et al. 2010).



**Figure 14:** The Wnt signaling can influence the osteoblast differentiation process at different level. Its stimulate the differentiation to osteoblast from mesenchymal stem cells and the maturation of osteocyte. Moreover, Wnt signaling is able to inhibit the osteoclast formation from monocyte precursor. (image from Baron & Kneissel 2013)

Together with the effects on osteoblast, this pathway is important even in modulation of bone resorption (fig.14). Recent findings revealed that WNT  $\beta$ -catenin signaling indirectly represses osteoclast differentiation and bone resorption by increasing secretion of osteoprotegerin (OPG) (Glass et al. 2005; Kramer et al. 2010). Furthermore, osteoblast overexpression of the WNT antagonist Dkk1 reduces WNT signaling in hematopoietic stem cells (HSCs), altering the HSC self-renewal potential and quiescence (Fleming et al. 2008; Schaniel et al. 2011).

Altogether, these finding suggest a role of the WNT signaling not only in osteoblast formation but even in the differentiation of the HSCs and potentially in hematopoiesis.

The precise signaling mechanisms that orchestrate the osteoblastogenesis are still poorly understood. All the molecular pathways described above and the crosstalk between them are essential for the correct bone formation and homeostasis.

Moreover, recent studies have been highlighting important roles of the endocytic pathway for the correct signal transduction and activation of several important signaling cascades, such as Wnt and BMP (Dobrowolski & De Robertis 2011).

In this thesis, a possible pathogenic mechanism behind skeletal defects in a new zebrafish model of Gaucher disease were investigated. Characterization of a GBA1 morpholino-induced knockdown and a stable genetic mutant lines *gba1<sup>sa1621/sa1621</sup>*, showed defects resembling the human pathology, such as hepatosplenomegaly and skeletal alterations. Further investigation using transgenic zebrafish line reporter for the well known signaling pathway involved in bone formation, highlighted a clear alteration of Wnt and BMP signaling in the absence of  $\beta$ -glucocerebrosidase lysosomal enzyme. This approach allowed to investigate the effect of GBA deficiency since early stages of embryonic development suggesting that depletion of this lysosomal enzyme induces alterations in the correct osteoblasts specification program, probably as a consequence of Wnt and BMP signaling dysfunction.





## 2. METHODS

All procedures involving fish husbandry and manipulation were evaluated and accepted by the Local Ethical Committee at the University of Padova. Fibroblasts from type 1 Gaucher patients, supplied by the Biobank (G. Gaslini) have been obtained for analysis and storage with the patients' (and/or a family member's) written informed consent. The consent was sought using a form approved by the local Ethics Committee. The mutant sa1621 fish line was obtained by the Zebrafish International Resource Center at Eugene (OR, USA). The following fish lines were used for the analysis of *gba1* knockdown: *Tg(dusp6:d2GFP)<sup>pt6</sup>* (Molina et al. 2007), *Tg(7xTCFXla.siam;EGFP)<sup>ia4</sup>* (Moro et al. 2012); *Tg(fli1a:EGFP)<sup>y1</sup>* (Lawson & Weinstein 2002), *Tg(sox10:mRFP)<sup>vu234</sup>* (Kirby et al. 2006), *Tg(kdrl:EGFP)<sup>s843</sup>* (Beis et al. 2005), *Tg(Col2a1aBAC:mCherry)<sup>hu5900</sup>* (Hammond & Schulte-Merker 2009); *Tg(Ola.Sp7:NLS-GFP)<sup>zf132</sup>* (Spoorendonk et al. 2008), *TgBAC(col10a1:Citrine)<sup>hu7050</sup>* (Mitchell et al. 2013); *Tg(12xGli-HSV.Ul23:GFP)<sup>ia11</sup>*; *Tg(EPV.TP1-Mmu.Hbb:EGFP)<sup>ia12</sup>*; *Tg(12xSBE:EGFP)<sup>ia16</sup>*; *Tg(BMPRE:EGFP)<sup>ia18</sup>* (Moro et al. 2013), *Lipan* (Korzsh et al. 2008); *Tg(gata1:dsRed)<sup>sd2</sup>* (Traver et al. 2003), *Tg(-6.0itga2b:EGFP)<sup>ia2</sup>* (Lin et al. 2005).

### 2.1 RECIPES

#### FISH WATER 1X:

100 ml SALINE STOCK SOLUTION 50X

50 µl Methylene Blue 1000X

ddH<sub>2</sub>O up to 5 lt.

#### SALINE STOCK SOLUTION 50X:

25 mM NaH<sub>2</sub>PO<sub>4</sub> (3.43 g)

25 mM Na<sub>2</sub>HPO<sub>4</sub> (4.45 g)

75 g INSTANT OCEAN

ddH<sub>2</sub>O up to 5 lt.

#### RINGER'S SOLUTION NORMAL:

116 mM NaCl

2.9 mM KCl

1.8 mM CaCl<sub>2</sub>

5 mM HEPES, pH 7.2.

## Methods

### PTU:

0.003% PTU (1-phenyl-2-thiourea) in lish water.

### TRICAINE:

(3-amino benzoic acid ethyl ester also called ethyl 3-aminobenzoate) comes in a powdered form from Sigma. Make tricaine solution for anesthetizing fish by combining the following in a glass bottle with a screw cap.

#### Stock solution 25X:

400 mg tricaine powder

97.9 ml DD water

~2.1 ml 1 M Tris (pH 9).

Adjust pH to ~7. Store this solution in the fridge. To use tricaine as an anesthetic combine the following in a 50 ml beaker:

2 ml tricaine solution

~48 ml clean lish water

### 2.1.1 Whole-Mount *in situ* Hybridization Solutions

#### HYBRIDIZATION MIX (HM):

60% formamide

4,6  $\mu$ M citric acid pH 6

SSC 5X

0.1% Tween-20

50  $\mu$ g/ml heparin

500  $\mu$ g/ml torula yeast total RNA (tRNA)

dH<sub>2</sub>O up to 100 ml

#### WASHING MIX (HM WASH):

HM without tRNA and heparin

#### PBS 1X:

150 mM NaCl

10 mM Na<sub>2</sub>HPO<sub>4</sub>

ddH<sub>2</sub>O up to volume



PBT 1X:

1X PBS

0.1% Tween-20

PFA:

4% paraformaldehyde in PBS 1X

ANTIBODIES ANTI DIGOXIGENIN/FLUORESCEIN:

Antibodies used for whole mount in situ hybridization are provided by Roche, they are diluted 1:1000 in a PBT 1X/2% sheep serum/200 mg/ml BSA solution and pre-adsorbed using 50 fixed embryos/ml of various developmental stages. After 2 h at RT, the antibody solution is diluted to 1:3000 and filtered. Then  $\text{NaN}_3$  is added for better storage at 4°C.

NBT/BCIP STAINING BUFFER:

100 mM Tris-HCl pH 9.5

50 mM  $\text{MgCl}_2$

100 mM NaCl

0.1% Tween20

ddH<sub>2</sub>O

NBT/BCIP STAINING SOLUTION:

NBT/BCIP (La Roche) 20  $\mu\text{l}/\text{ml}$  in staining buffer.

Alternatively use separate

- 7,5  $\mu\text{l}/\text{ml}$  NBT (Nitro Blue Tetrazolium provided by Sigma) 50 mg/ml (50 mg NBT dissolved in 0.7 ml anhydrous dimethylformamide and 0.3 ml H<sub>2</sub>O). Store in the dark at -20°C.
- 3,5  $\mu\text{l}/\text{ml}$  BCIP (5-Bromo 4-Chloro 3-Indolyl Phosphate, provided by Sigma) 50 mg/ml (50 mg dissolved in 1 ml anhydrous dimethylformamide). Store in the dark at -20°C.

BENZYL BENZOATE-BENZYL ALCOHOL

Benzyl-benzoate:benzyl alcohol 2:1



one-cell stage embryos under a light microscope. Pigmentation was prevented using a 0.003% 1-phenyl-2-thiourea solution in the first 24 h.

### 2.3 GENOTYPING OF MUTANT

Tail clip genotyping was performed on tail clips after 10 mg/ml proteinase K overnight digestion at 55°C. Genomic DNA was purified by phenol-chloroform extraction and ethanol precipitation. Purified DNA was dissolved in DNase-free water. PCR was performed using the set of oligos, GBA forward(for) (5'-GGACCAGCTGCTCAGGACAGT) and GBAreverse(rev) (5'CTGACCCGAAAGGTAGCAAA) at the following conditions: predenaturation 5 min at 94°C, and 35 cycles of 94°C for 1 min, 56°C for 30" and 72°C for 1 min. Amplicons were then treated with EXOSAP (Roche Diagnostics, Monza, Italy) and sequenced on both strands.

### 2.4 ALIZARIN AND ALCIAN STAINING

Skeletal staining was performed as previously described (Walker & Kimmel 2007). In addition Alizarin staining was performed using a modified procedure. Briefly, larvae were fixed 1 h at room temperature in 4% buffered paraformaldehyde, washed in 50% ethanol and dehydrated overnight in 95% ethanol. Staining was carried out in Alizarin solution (0.25%, w/v, in 2% KOH) for 3 h and larvae were then briefly cleared in 2% KOH (w/v) and stored in KOH/glycerol (20 : 80).

### 2.5 TRANSMISSION ELECTRON MICROSCOPY

Fish were fixed in 3% glutaraldehyde in 0.1 M cacodylate sodium buffer and processed as described previously (Parsons et al. 2002). Ultrathin sections were viewed on a Zeiss 902 electron microscope.

### 2.6 TRANSFORMATION OF E. COLI

Bacterial transformation allows to obtain large plasmids copy number. Vectors containing part of the cDNA of interest were introduced in bacterial E. coli cells (One Shot® TOP10 Chemically Competent E. coli provided by Invitrogen™). Vectors confer to the bacterial cells antibiotic resistance as a selectable marker for plasmid-containing cells. Chemically competent E. coli stored at -80°C were placed on ice, a small amount of plasmid DNA (10-50 ng) is added to the bacteria cells that were left on ice for 15 minutes before performing heat shock. A 30-second long heat

## Methods

shock at a temperature of 42°C allow the *E. coli* cells to take up vector DNA. Transformed cells are re-placed on ice for 2 min adding 200 µl of nutrient S.O.C medium (Invitrogen™) and then incubated for about 45 min in a shaker at a temperature of 37°C. This incubation allows antibiotic resistance to be expressed so that cells can be plated on agar containing ampicillin or kanamycin. Plates are incubated over night and plasmid- containing colonies can grow on solid medium. Positive colonies are then selected and singles clones are cultured in Luria-Bertani medium where the suitable antibiotics has been added to improve selection of vector-containing clones. Liquid cultures provide massive bacterial growth in order to obtain a large plasmid copy number after extraction and purification

### 2.7 PURIFICATION OF PLASMID DNA

The extraction and purification of plasmid DNA was performed using commercial kits provided by Qiagen (QIAprep®) based on the alkaline lysis of bacterial cells in order to release plasmid DNA. These kits are equipped with special silica matrix columns that binds plasmid DNA with high affinity in the presence of high salt (Vogelstein and Gillespie, 1979). Then two wash with suitable buffers are performed to remove excess of salts and improve DNA recovery. High-quality plasmid DNA is then eluted from the column with 50–100 µl of nuclease-free water pre-heated at 65-70°C in order to increase elution efficiency.

### 2.8 ANTI-SENSE PROBE SYNTHESIS

An improving possibility to study the expression of genes of interest is to generate an epitope-tagged antisense RNA probe directed against the targeted gene/mRNA. To construct digoxigenin antisense RNA probes the partial cDNA of the gene of interest is cloned in a plasmid vector such it is under the control of a phage promoter. These phage promoters are recognized by the RNA polymerases encoded by phages as T3, T7 or SP6 and they allow large amounts of RNA to be produced in vitro. After extraction and purification, the plasmid is linearized, using a suitable restriction enzyme, at the 5' end of the inserted gene of interest. This step is necessary as polymerases will fall off the end of the linearized plasmid after transcription and the enzyme can start a new transcription, in a process called run off synthesis. The GBA1 antisense probe was derived from an 821 bp cDNA cloned in pCRII-TOPO plasmid (Lifetechnologies, Milan, Italy) using the following set of oligos, GBAfor (5'-TGTCTCTGTCTTCCGGAGCT) and GBArev (5'-ATGTCATGGGCGTAGTCCTC). The plasmid was linearized with HindIII and the probe

was transcribed by T7 polymerase using DIG-dUTPs. Sense control probe was prepared with the same plasmid, linearized with XbaI and transcribed with Sp6. The runx2b probe was generated by amplifying a 523 bp fragment and cloning it in pCRII-TOPO. Antisense- and sense-labeled riboprobes were obtained by T7 and SP6 transcription, respectively. GFP and mCherry antisense riboprobes were generated by KpnI digestion of a Tol2 middle entry vector containing the GFP and mCherry cassette, respectively, and followed by T7 transcription. Together with this riboprobes, also col10a1 and cMyb were synthesized by digestion of pBK-CMV plasmid with EcoRI.

Linearization reaction is performed in a 50  $\mu$ l total volume with approximately 5  $\mu$ g of plasmid to be digested, and using 1,2  $\mu$ l of the suitable restriction enzyme coupled with its buffer and BSA when requested to enhance endonuclease performance:

- ddH<sub>2</sub>O up to 50  $\mu$ l
- plasmid DNA 5  $\mu$ g
- 10X buffer 2  $\mu$ l
- BSA 100x (if needed) 0.5  $\mu$ l
- restriction enzyme 1.2  $\mu$ l

Linearization reaction goes 2 h at 37°C or at a temperature suitable to improve enzyme performance. The linearized plasmid is then purified and precipitated over night at -80°C. The purification of the vector after linearization is carried out using Phase Lock gel tubes (Eppendorf):

- centrifuge column tubes 1 minute max speed to pack the gel at the bottom of the tube;
- add nuclease free water to 100  $\mu$ l to the sample of linearized DNA, and transfer the volume on the top of the gel of Phase Lock column;
- add 50  $\mu$ l phenol and 50  $\mu$ l chloroform;
- centrifuge 5 min max speed;
- the Phase Lock gel separates solvents with saline buffers and enzymes of the linearization reaction from the aqueous phase containing the DNA;
- add 100  $\mu$ l chloroform and centrifuge 5 min max speed;
- collect the aqueous phase containing purified linearized DNA (approx. 100  $\mu$ l) that is on the top of the gel, and transfer it in a new 1,5 ml tube.

Then add to the purified DNA 0,1 volumes (10  $\mu$ l) NaCl and 2,5 volumes of Ethanol absolute, mix well and precipitate at least 2 h or over night at -80°C. After

## Methods

precipitating add 2  $\mu$ l of glycogen to the linearized DNA mixture and centrifuge 15 min max speed;

- remove the supernatant being careful not to touch the pellet;
- wash the pellet 3 times with 200  $\mu$ l 70% ethanol centrifuging 2 min max speed each time and removing supernatant;
- dry the pellet from ethanol residuals and the re-suspend it in 14  $\mu$ l of nuclease-free water.

Then run an electrophoresis on 1,5% agarose gel loading 1  $\mu$ l of purified linearized plasmid DNA in order to control the quality of the digestion.

If the linearization was successfully carried out the antisense RNA probe can be transcribed starting from a phage promoter (T7, T3 or SP6) flanking the 3' end of the inserted gene of interest. Nucleotides added by RNA polymerases are UTP digoxigenin-labelled. Synthesis of mRNA probes were performed in a 20  $\mu$ l reaction volumes at a temperature of 37°C from 2 hours to 6 hours depending on probe length.:

- |  |            |
|--|------------|
| • linearized plasmid DNA                   | 13 $\mu$ l |
| • 10X transcription buffer (Roche)         | 2 $\mu$ l  |
| • DIG- or FLUO-RNA Labeling Mix (Roche)    | 2 $\mu$ l  |
| • RNasin® Ribonuclease Inhibitor (Promega) | 1 $\mu$ l  |
| • (T7, T3 or SP6) RNA Polymerase (Roche)   | 2 $\mu$ l  |

After the transcription, a step is required to digest template plasmid DNA with 2  $\mu$ l of DNase (RNase-Free DNase, Promega) at 37°C for 20 min. This allow to purify a high quality RNA probe. The purification of antisense RNA probes is performed using a commercial kit (MEGAclear™ provided by Ambion®). Once purified, the RNA probe can be stored at -80°C. Then an electrophoresis has been run on 1,5% agarose gel loading 1  $\mu$ l of purified probe in order to control and quantify the transcription. Prior to being loaded on gel, the probe has to be denatured at 65°C for at least 5 min.

### 2.9 SINGLE-PROBE WHOLE-MOUNT IN SITU HYBRIDIZATION (WISH)

In situ hybridization is a method useful in studying the expression of genes of interest. This method is based on the generation of epitope-tagged RNA probes directed against the gene/mRNA of interest. Zebrafish embryos and larvae allow to perform whole-mount in situ hybridization, thus permitting three dimensional analysis on tissues and organs. The most common protocol for in situ hybridization implies fixing zebrafish embryo in 4% paraformaldehyde (PFA) in PBS 1X for 2 h at

room temperature (RT) or overnight at 4°C in 2 ml eppendorf tubes. Embryos are selected at different developmental stages and, if necessary, removed from their chorion using dissection needles. Before late somitogenesis stage embryos have to be dechorionated after fixation, while in later and larval stages it is more suitable to carefully dechorionate embryos alive to avoid they remain curved as if they were fixed inside the chorion. After fixation PFA is removed, embryos are washed in PBS and then transferred in methanol 100% for at least 2 h at -20°C before starting the in situ hybridization protocol. Embryos can be stored in methanol for months but this step is necessary for permeabilization of embryos (Christiane Nusslein-Volhard 2002).

### Day 1

1. Rehydration of samples stored in Methanol 100% at -20°C.

- |                          |           |    |
|--------------------------|-----------|----|
| • 75% MetOH - 25% PBS 1X | 5 min     | RT |
| • 50% MetOH - 50% PBS 1X | 5 min     | RT |
| • 25% MetOH - 75% PBS 1X | 5 min     | RT |
| • 100% PBT               | 4 x 5 min | RT |

2. After PBT washes, digest with proteinase K (10 µg/ml). This step permeabilizes the embryos permitting access of the RNA probe. The digestion time is dependent on the developmental stage. No digestion is needed for embryos at blastula, gastrula and somitogenesis stages (up to the 18 somite stage). For 24 hpf old embryos digest for 5 min and for older embryos (from 36 h to 5 days old embryos) digest for 40-60 min. Proteinase K digestion works at RT and it is stopped by incubation in 4% paraformaldehyde in 1 x PBS.

- Post-fixation of digested embryos with PFA 4% in PBS for 20 min at RT. Also embryos that do not need proteinase K digestion are usually post- fixed to strengthen the samples.
  - Washes with PBT
- |           |    |
|-----------|----|
| 5 x 5 min | RT |
|-----------|----|

3. Pre-hybridization step is performed by incubation in 500-800 µl of Hybridization Mix (HM) for 2 to 5 h in a waterbath set at 60-70°C, depending on the melting temperature of the probe.

4. Hybridization step: remove and discard the pre-hybridization mix. Replace with 200 µl of hybridization mix containing about 100-200 ng of antisense DIG (or FLUO) labelled RNA probe. Hybridize overnight in a waterbath at 60-70°C.

## Methods

### Day 2

Remove the hybridization mix with the RNA probe and recover it: probe-containing solutions can be used several times.

1. Wash briefly with HM for washes (HM without tRNA and heparin) at 65°C
  - 75% HM Wash - 25% SSC 2X                      15 min                      65°C
  - 50% HM Wash - 50% SSC 2X                      15 min                      65°C
  - 25% HM Wash - 75% SSC                      15 min                      65°C
  - 100% SSC 2X                      15 min                      65°C
  - 100% SSC 0,2X                      2 x15 min                      65°C
  - 75% SSC 0,2X - 25%                      10 min                      RT
  - 50% SSC 0,2X - 50% PBT                      10 min                      RT
  - 25% SSC 0,2X - 75% PBT                      10 min                      RT
  - 100% PBT                      10 min                      RT
2. Incubation with blocking buffer of PBT/2% sheep serum/2 mg:ml BSA, at RT for 2 to 4 hours.
3. Incubation in 400 µl of antibody solution diluted at 1/3000 in blocking buffer overnight at +4°C under slow agitation on a horizontal orbital shaker.

### Day 3

Remove the antibody solution diluted at 1/3000 and recover it, antibody solutions diluted can be used up to three times.

1. Wash briefly with PBT at RT, then wash extensively 6 x 15 min at RT under slow agitation on a horizontal orbital shaker. Before starting the staining step, embryos are washed 3 x 5 min in NBT/BCIP staining buffer.
2. Staining step: embryos are transferred from eppendorf tubes into wells of a 24-well plate, the staining buffer is then removed and NBT/BCIP staining solution is added. Embryos are incubated in staining solution at room temperature under slow agitation on a horizontal orbital shaker and protected from day light by a layer of aluminium foil. Staining reaction is regularly monitored under a dissection microscope.
3. The staining reaction is topped by removing the staining solution, washing 3 x 5 min with PBT and then placing back the embryos in the eppendorf tubes in PFA 4%. Stained samples are usually stored in PFA 4% in the dark at 4°C.



Labelled embryos are mounted in 100% glycerol. Embryos at early developmental stages are observed in glycerol on depression slides. Whole mount pictures were taken with a Nikon SMZ 1500 Microscope provided with a digital camera. Embryos starting from 20 somite stage were manually de-yolked using dissection needles and then flat mounted on slides. Slides were provided with small chambers cut into several layers of adhesive tape (1 layer until 24 hpf, 2 layers for 48 hpf and so on), the embryos is placed, in the desirable position, in glycerol into the chamber and then flattened using a coverslip. Flat mount pictures were taken with a Leica DMR Microscope. Digitalized pictures are saved as TIFF files, then adjusted for contrast, brightness and color balance using a Photoshop CS2 software and stored as such or after conversion to the .jpeg format to reduce the files size.

## 2.10 QUANTITATIVE REAL-TIME PCR

### 2.10.1 RNA extraction

Zebrafish morphants embryos and mutant sa1621 at 48 hpf were homogenized in Trizol reagent (Lifetechnologies) and total RNA was isolated using the standard trizol-chloroform-ethanol extraction procedure. RNAs were resuspended in 20  $\mu$ l of water RNase free. RNA samples were checked for integrity by capillary electrophoresis (RNA 6000Nano LabChip, Agilent Technologies, Santa Clara, CA, USA). A total of 2  $\mu$ g of RNA was reverse transcribed into cDNA using a SuperScript III Reverse Transcriptase (Lifetechnologies), according to standard procedures. The cDNA was subsequently subjected to SYBR Green-based real-time PCR using a RotorGene 3000 (Corbett, Concorde, NSW). Primers are listed in Table 1.

### 2.10.2 RT-PCR data analysis

RT-PCR data were analyzed using a manually set threshold and the baseline was set automatically to obtain the threshold cycle ( $C_t$ ) value for each target. GAPDH was used as an endogenous housekeeping control gene for normalization. Relative gene expression among samples was determined using the comparative  $C_t$  method ( $2^{-\Delta\Delta C_t}$ ). Results are expressed as the mean  $\pm$  SEM in relative expression

## Methods

Oligo name	Sequence 5' -> 3'	Genbank Association number
GFP for	ACGTAAACGGCCACAAGTTC	AEVGFPB
GFP rev	AAGTCGTGCTGCTTCATGTG	AEVGFPB
zGAPDH for	GTGGAGTCTACTGGTGTCTTC	ENSDARG0000043457
zGAPDH rev	GTGCAGGAGGCATTGCTTACA	ENSDARG0000043457
zPlod1 for	CTGATGGGTTTCAGACGGTTT	ENSDARG0000059746
zPlod1 rev	TTGGCCTGCTGAAACTTCTT	ENSDARG0000059746
zPON1 for	AAAGGCTCGGCACACTTAGA	ENSDARG0000032496
zPON1 rev	TTCAAGCCAGTGCTCAGAAA	ENSDARG0000032496
zGpx1b for	CTGCGAGACAAGGAGGAAAC	ENSDARG0000006207
zGpx1b rev	TGCAGCTCGTTCATCTGAGT	ENSDARG0000006207
zAxin1 for	GAGAGACAGCCATGGAGAGG	ENSDARG0000026534
zAxin1 rev	TGCTCATAGTGTCCCTGCAC	ENSDARG0000026534
zSmad1 for	CTGTGAAGGATCACGTCGAG	ENSDART0000033566
zSmad1 rev	GCCCAGTCAACACAGTCTCA	ENSDART0000033566
zSmad5 for	CGGCTCAAACAGAAAAGAAG	ENSDART0000054175
zSmad5 rev	TGGAGGGTAGGGTGAGTTTG	ENSDART0000054175
zSmad8 for	GGAGAGCAGTCCGTCTGAAG	ENSDART00000132823
zSmad8 rev	GGATCTGTGAAACCGTCCAC	ENSDART00000132823
zBMP4 for	GTGAGGCGAACTCCTTTGAG	ENSDART0000075150
zBMP4 rev	TTTGTCGAGAGGTGATGCAG	ENSDART0000075150
hDkk1 for	CAGGCGTGCAAATCTGTCT	ENSG00000107984
hDkk1 rev	CCCATCCAAGGTGCTATGAT	ENSG00000107984
hAxin1 for	ACAGGATCCGTAAGCAGCAC	ENSG00000103126
hAxin1 rev	GCTCCTCCAGCTTCTCCTC	ENSG00000103126
hSmad1 for	GCTTACCTGCCTCTGAAGA	ENSG00000170365
hSmad1 rev	ACCATCCACCAACACACTTG	ENSG00000170365
hGPX-1 for	CGGGACTACACCAGATGAA	ENSG00000233276
hGPX-1 rev	CCGGACGTACTTGAGGGAAT	ENSG00000233276
hGAPDH for	CACAATATCACTTTACCAAGAGTTAAAAGC	ENSG00000111640
hGAPDH rev	CGAGCCACATCGCTCAGAC	ENSG00000111640

**Table 1:** listed primer used for real-time PCR.

### 2.11 IMMUNOFLUORESCENCE ON TYPE 1 GAUCHER FIBROBLASTS

Patient history has been described elsewhere (Filocamo et al. 2000). Fibroblasts were maintained in Dulbecco's modified Eagle's medium supplemented with 4.5 g/l glucose, 10% fetal calf serum, 50mg/ml gentamicin and 4mM glutamine. Thirty thousands fibroblasts per well were seeded on polylysine-coated coverslips in a 24-well plate. After 24 h cells were fixed with 4% buffered paraformaldehyde. Blocking was achieved with a 10% (v/v) sheep serum, 1% BSA (w/v), 0.1% Triton X-100 and

0.3 M glycine. After few washes in PBS-Tween (0.1%, v/v), cells were incubated overnight with primary antibody at 4°C and after three washes in PBS-Tween (0.1%, v/v), a 2 h secondary antibody incubation was performed. Coverslips were finally mounted with DAPI (Lifetechnologies) on glass slides and observed under C2 confocal microscope (Nikon, Milan, Italy). The following antibodies were used: antiGSK3 $\beta$  (Sigma, 1 : 100) rabbit anti  $\beta$ -catenin (Abcam, Milan, Italy, 1 : 100), goat anti Vps28 (Abcam, 1 : 100), rabbit anti GBA (Novus Biologicals, Milan, Italy, 1 : 100).

## 2.12 APOPTOSIS AND PROLIFERATION ASSAYS

For apoptosis analysis with a Cleaved caspase 3 antibody (Cell signaling, Milan, Italy, 1 : 100) fish at 2–6 dpf were fixed in 4% PFA in PBS, permeabilized in methanol washes and acetone for 20 min and finally incubated in primary antibody in PBS/DMSO 1% overnight at 4°C. After three washes for 30 min incubation with an alkaline phosphatase-conjugated secondary antibody was performed (Sigma, 1 : 500). Staining was carried out with an NBT/BCIP solution (Roche Diagnostics), according to manufacturer's instructions. Alternatively, fish at the same developmental stages were fixed in 4% PFA overnight, dehydrated in several methanol washes and kept in 100% methanol for 30 min. After rehydration, fish were digested with collagenase (Sigma, 1 mg/ml), and incubated in TdT reaction (Apotag, Chemicon, DBA, Milan, Italy) for 2 h at 37°C. Fluorescein-conjugated antidigoxigenin antibody incubation was performed at 4°C overnight and images were taken with C2 Nikon confocal microscopy. For proliferation assay, the Click-it Edu proliferation assay kit (Lifetechnologies) was considered. Briefly, fish larvae at 2–4 dpf were incubate for 30 min in 10 mM EdU on ice. After several washes with cold embryo medium, a 30 min to 4 h incubation at 28.5°C for EdU incorporation was carried out. After fixation in 4% PFA larvae were treated with 10  $\mu$ M Proteinase K (Sigma) and treated with the reaction cocktail as suggested by the manufacturer's instructions. Images were taken on fixed larvae with a C2 Nikon confocal system (Nikon). Alternatively, fish from the *Tg(Ola.Sp7:NLS-GFP)<sup>zf132</sup>* line were outcrossed with a *Tg(H2b:RFP)* line and heat shocked at 37°C for 1 h at 1 dpf. Images from the opercle were taken at 3–4 dpf with the C2 confocal system and processed by ImageJ analysis. In particular, the number of RFP-labeled opercle cells was assessed by adjusting the thresholded acquired image of each sample above the background of faintly stained cells. Manders coefficient was used to measure the double RFP/GFP co-labeled opercle cells in control and morphant larvae.

## Methods

### 2.13 WESTERN BLOT

Total proteins were extracted from zebrafish morphants and controls at 48 hpf with Tissue extraction lysis buffer II (Invitrogen). Samples of denaturated proteins (10 µg) were separated on Nu-PAGE® Novex® 4–12% Bis-Tris Gels (Invitrogen) and transferred to PVDF membranes. The membranes were subsequently incubated with antibodies: GSK3β (1 : 50000) (Sigma), β-catenin (1 : 1000) (Sigma) and β-actin (1 : 5000) (Santa Cruz, Dallas, TX, USA) at 4°C overnight after incubation in Western blocker solution (Sigma) for 2 h. Meanwhile, 10 µg of type 1 Gaucher fibroblast and control fibroblast protein lysates were examined using western blotting according to procedures described above. The membranes were incubated with: GBA (1 : 1000; Novus Biologicals); β-catenin (1 : 1000; Sigma) and β-actin (1 : 5000; Santa Cruz) antibodies. After the incubation with horseradish peroxidase conjugated secondary antibody (1 : 2000; Sigma) for 1 h at room temperature, visualization was performed with SuperSignal West Pico Chemiluminescent Substrate detection kit (Thermo Scientific, Milan, Italy) followed by exposure to X-ray film (Thermo Scientific). β-Actin served as an endogenous control.

### 2.14 MICROARRAY

Four pools of GBA1 MO and control MO-injected fish were independently collected after 48 h and total RNA was isolated according to standard procedures. RNA quality was assessed by Nanochip Agilent Bioanalyzer and microarray analysis was performed using the 44 × 4 Agilent platform, according to the manufacture's protocol. Raw data were intra- and interarray normalized. Normalized data were then tested with the SAM software (Stanford University, USA) and processed by the David platform (<http://david.abcc.ncifcrf.gov>). t-Test statistical analysis was carried out with Welch correction of  $\alpha = 0.01$ .

### 2.15 RESCUE WITH HUMAN GBA1 OVEREXPRESSION AND CERAZYME TREATMENT

The human glucocerebrosidase cDNA cloned into the commercial vector pCMV6-XL5 (Origene, USA) was used as template for T7-mediated RNA transcription. Isolated RNA was DNAase treated for 2 h and recovered by MEGAclear Spin column purification (Euroclone). Qualitative and quantitative assessment was carried out by agarose gel and Nanodrop Instrument, respectively. Up to 2.5 ng of hGBA1 mRNA per embryo were microinjected with 17.5 pg gba1 morpholino without any evident

toxic side effect. Alternatively, coinjection with the GBA MO was carried out with  $1 \times 10^{-5}$  U of Cerezyme per embryo in Danieau buffer (58 mM NaCl, 0.7 mM KCl, 0.4 mM  $\text{MgSO}_4$ , 0.6 mM  $\text{Ca}(\text{NO}_3)_2$ , 5.0 mM HEPES, pH 7.6.)

#### 2.16 IN VIVO REACTIVE OXYGEN SPECIES DETECTION (DCDFA STAINING)

For ROS analysis, fish were either microinjected or incubated with a 10 mM DCF diacetate (DCDFA, Lifetechnologies) at one-cell stage embryo and visualized by a fluorescent microscope at 520 nm at 24–48 hpf.

#### 2.17 TARTRATE-RESISTANT ACID PHOSPHATASE ASSAY

Fish at 10–14 dpf were processed using an adapted colorimetric TRAP assay (Sigma), according to manufacturer's instruction. Bleaching for larval clearing was achieved by 10% peroxide hydrogen in water for 4 h.

#### 2.18 ZEBRAFISH DISSOCIATION AND FLOW CYTOMETRY ANALYSIS

The protocol for dissociation of zebrafish cells was previously described (Covassin et al. 2006); however, several modifications were introduced. Protease solution was replaced with  $1 \times$  PBS, 0.25% trypsin phenol red free (Gibco, Life Technologies, Milan, Italy), 1 mM EDTA, pH 8.0, 2.2 mg/ml Collagenase P (Sigma) and resuspension medium was replaced with Opti-MEM (Gibco), 1% filtered heat inactivated FBS (Gibco),  $1 \times$  Penicillin–Streptomycin solution (Sigma). Dissociated cells were filtered by a 70  $\mu\text{m}$  nylon membrane and subjected to FACS (BD FACSCanto II system). FSC, SSC and fluorescence (564–606 nm) have been analyzed. Unfluorescent dissociated zebrafish cells at 3 dpf were used as negative control, P1 gate contained all autofluorescent and unfluorescent cells. 106 events were recorded. P2 gate was setup outside the P1 gate, collecting highly fluorescent events (564–606 nm). FITC fluorescence (515–545 nm) was also used as internal negative control. Samples were collected by 35 dissociated fish larvae. Fluorescent control, Gba1 morphants and unfluorescent samples were generated by microinjecting the offspring from the same mating process, between a *Tg(gata1:dsRed)<sup>sd2(+/-)</sup>* fish and a wild-type larva in each replica.



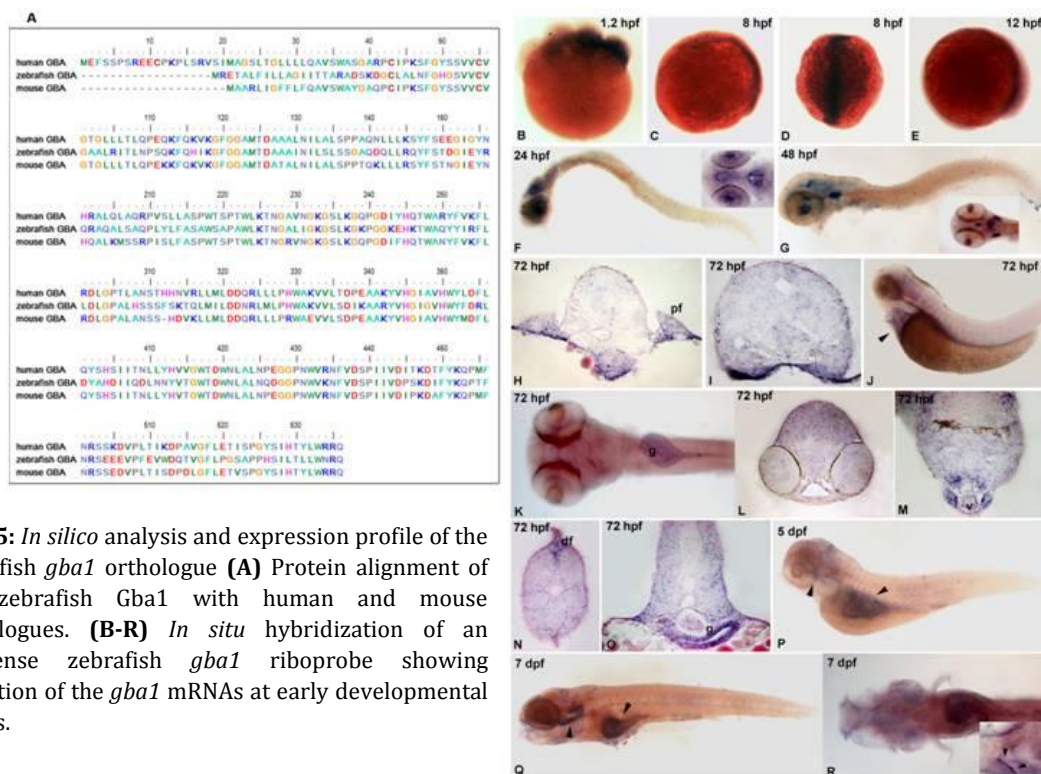
### 3. RESULTS

#### 3.1 DETERMINATION OF THE EXPRESSION PATTERN OF GBA 1 IN THE ZEBRAFISH FROM EARLY LIFE STAGES

The aim of this project is approach to a functional study of the lysosomal  $\beta$ -glucocerebrosidase (Gba1) enzyme using zebrafish as model organism.

The zebrafish *gba1* gene is located on chromosome 16 and is made of 10 exons and the protein is composed of 518 residues.

For understand the level of aminoacidic conservation of the protein analysis of the zebrafish *gba1* orthologue with *in silico* methods was carried out. Protein alignment of the zebrafish Gba1 revealed a 53% of aminoacidic identity and similarity with human and mouse orthologues (fig 15) revealing a high level of conservation between these species. To investigate the spatio-temporal expression of *gba1* mRNA in the zebrafish development, WMISH assays were performed on WT embryos and larvae from 1.2 hpf to 7dpf using digoxigenin-labeled antisense *gba1* mRNA probes. Expression of the *gba1* is detected since the 1-cell stage of zebrafish embryos. Particularly, despite later in development its expression is maintained widespread in the whole organism, a high level of *gba1* is found in some specific tissues like the central nervous system, gut, liver, bones and heart (fig 15). These data are the first results in which the expression pattern of the *gba1* is characterized, pointing out the importance of this enzyme during the early developmental stages.



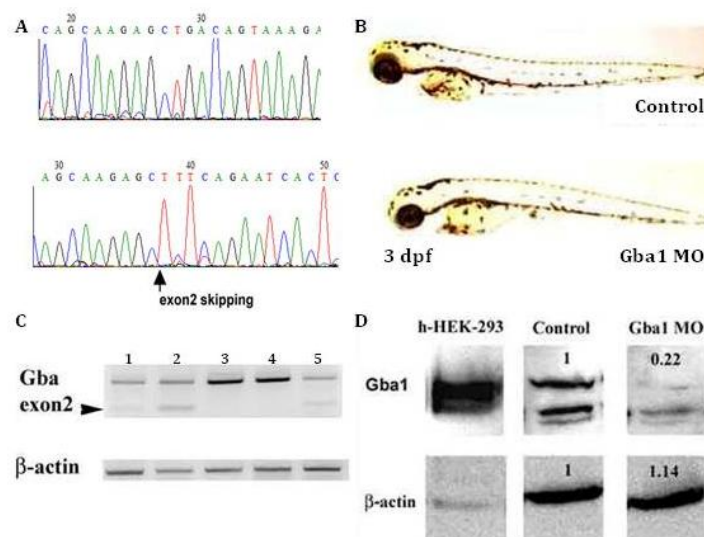
**Fig.15:** *In silico* analysis and expression profile of the zebrafish *gba1* orthologue (A) Protein alignment of the zebrafish Gba1 with human and mouse orthologues. (B-R) *In situ* hybridization of an antisense zebrafish *gba1* riboprobe showing detection of the *gba1* mRNAs at early developmental stages.

## Results

### 3.2 ZEBRAFISH MODELS USED IN THIS PROJECT

#### 3.2.1 Knockdown of the zebrafish *Gba1* using morpholino oligo

To determine the function of *gba1* during zebrafish embryonic development, a morpholino oligo targeted to the splicing donor site of the exon2 sequence of *Gba1* (*Gba1*MO) was designed and microinjection on wild type embryos of different concentrations revealed that at a dose of 1,75 mg/ml a 60% of the exon skipping was produced (fig.16C). To evaluate possible off-target effect of the morpholino, a translation-blocking morpholino targeting the ATG initiation codon, was designed. Moreover, as control, a five mismatch-control morpholino targeting the same sequence and a five-base unrelated mismatch-control morpholino were used. To confirm the specificity of the *Gba1*MO, RT-PCR experiment were performed, revealing that aberrant splicing events in 2 dpf morphants occurred. Moreover, sequencing of the *Gba1* misspliced transcript confirmed the skipping of exon 2 (see chromatograms in fig.16). The skipping of the exon induced alteration in the protein formation and western blots analysis using a cross-reacting antibody showed almost a 5-fold decrease of total *Gba1* protein levels in 2 dpf morphants extracts when compared tp the control samples (fig.16). Morphants fish, despite a slight curvature of the trunk, did not exhibit a global particular phenotypes in respect to the control fish probably because only a partial depletion of the *Gba1* protein was induced by the morpholino.



**Figure 16:** (A) Representative chromatograms showing the exon 2 skipping produced by morpholino injection. The arrowhead indicate the nucleotide level at which the exon-skipping is produced. (B) Comparison between representative control larva (mismatch) and a morpholino injected (*Gba1* MO), at 3 dpf, showing the lack of apparent phenotypic differences. Only a mild curvature of the trunk is detectable. (C) RT-PCR on cDNAs from 48hpf larvae microinjected with 1.5 mg/ml (1), 1.75 mg/ml (2), 2 mg/ml (5) *Gba1* MO and 1.75 mg/ml (3), 2 mg/ml (4) control morpholino.  $\beta$ -Actin was used as internal control. Arrowhead indicates the shorter fragment

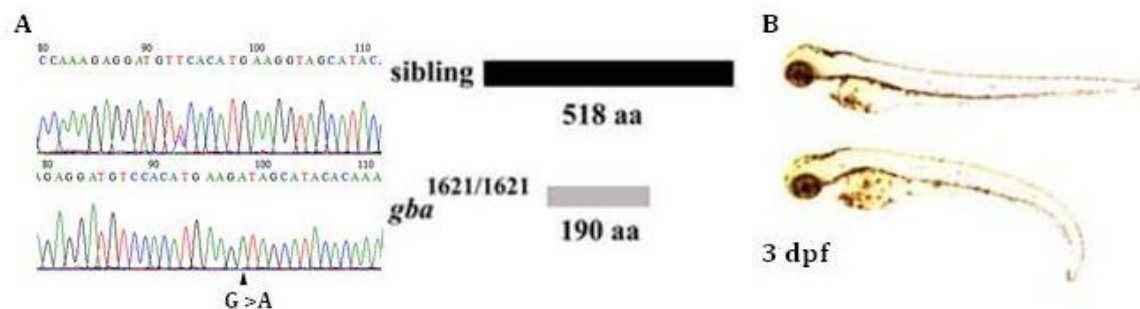


produced by antisense morpholino-mediated knockdown. **(D)** Representative western blot, showing the marked decrease of Gba1 protein levels after morpholino-mediated knockdown. Protein extracts are from 100 2 dpf mismatch-control and morphant microinjected larvae. Protein extract from the human Hek-293 cell line was used as control for protein band detection.  $\beta$ -Actin was used as loading control.

### 3.2.2 Characterization of a zebrafish stable mutant line for Gba1.

Since in 2001 the Sanger institute started the Zebrafish Genome Project, different mutant lines for a variety of alleles were produced in the context of the Zebrafish Mutation Project (ZMP). This project consists in a reverse genetic approach known as TILLING to identify mutations in specific genes by sequencing polymerase chain reaction (PCR)-amplified exons from thousands of N-ethyl-N-nitrosourea (ENU) mutagenized individuals.

To further investigate the role of the Gba1 enzyme in embryonic development, a stable genetic mutant line retrieved from the ZPM forward genetic screening (*gba1*<sup>sa1621/sa1621</sup> ENSDARG00000076058) was used. In these fish, a single G>A substitution in the splicing donor site of exon4, produces an aberrant Gba1 transcript introducing a premature stop codon. The translated Gba1 mutant protein is made of 190 amino acids, instead of the 518 amino acids of the wild-type Gba1 protein (fig.17). The phenotype of these mutant fish is very similar to that of morphants, characterized by a significantly shortened body axis beginning from 7 dpf, and a marked trunk curvature, when compared with age-matched control siblings (fig. 17 and Data not shown).



**Figure 17: (A)** Representative chromatograms of wild-type siblings and *gba1*<sup>sa1621/sa1621</sup> fish, showing the G to A substitution detectable in mutants. The produced truncated protein is shown in grey. **(B)** Representative 3 dpf wild-type sibling and *gba1*<sup>sa1621/sa1621</sup> fish are shown. Note the marked curvature of the trunk in the mutant.

### 3.3 GBA1 LOSS OF FUNCTION AFFECT MULTIPLE CELL LINEAGES IN FISH

#### 3.3.1 Hematological defects are observed in *Gba1* morphants and mutants

The Gaucher patients manifest multiple defects in different tissues. A main common symptom to all clinical subtypes of GD patients is the presence of hematological complication like anemia and thrombocytopenia .

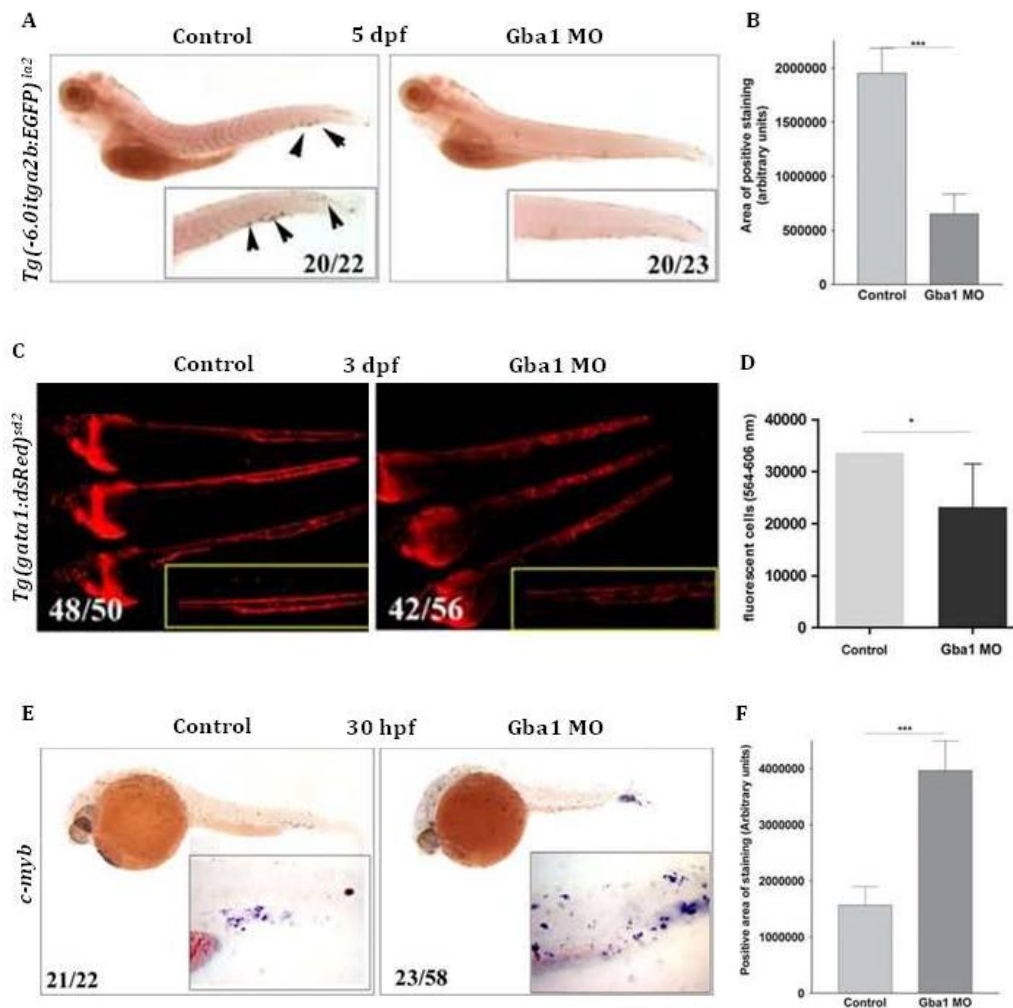
To address if this zebrafish *Gba1* morphants could resemble the GD phenotype, thrombocyte and erythrocyte populations were analyzed to understand if were affected by *Gba1* knockdown.

The *Gba1* morpholino was injected in *Tg(-6.0itga2b:EGFP)<sup>ia2</sup>* fish, in which thrombocyte precursor and mature thrombocytes are labeled. A strong reduction of transgene expression in morphant fish at 5dpf was detected, supporting a marked thrombocytopenia (fig.18).

To address if also erythrocyte were affected by *Gba1* loss of function, qualitatively and quantitatively evaluation by fluorescence microscope, confocal scanning and FACS analysis of the number of erythrocytes in *Tg(gata1:dsRed)<sup>sd2</sup>* microinjected with *Gba1* and mismatch-control morpholinos were conducted. By fluorescent microscope acquisition and FACS analysis, a significantly reduction number of erythrocytes in morphants at 3 dpf was found (fig.18).

Since erythrocyte were depleted in morphants and Gaucher patients usually exhibit increased macrophage activation, analysis of *c-myb* was carried out, which is a marker of definitive hematopoiesis and is important for the initial stage of myelopoiesis (Valledor et al. 1998). Ectopic expression of *c-myb* observed in *Gba1* morphants suggest an early hematopoietic defects triggered by *Gba1* dysfunction. To support the results of hematopoietic defects obtained by injection of *Gba1* morpholino, the heterozygous fish (*gba1<sup>sa1621/+</sup>*) was incross with the transgenic line *Tg(gata1:dsRed)<sup>sd2</sup>*. A reduction in the number of erythrocyte was observed also in the offspring obtained from the incross at 3 dpf that were similar to the data collected in the morphants fish (data not shown).

These results demonstrate that both morphants and mutant zebrafish models display a reduction in the erythrocyte population resembling the anemia aspects of the GD patients.



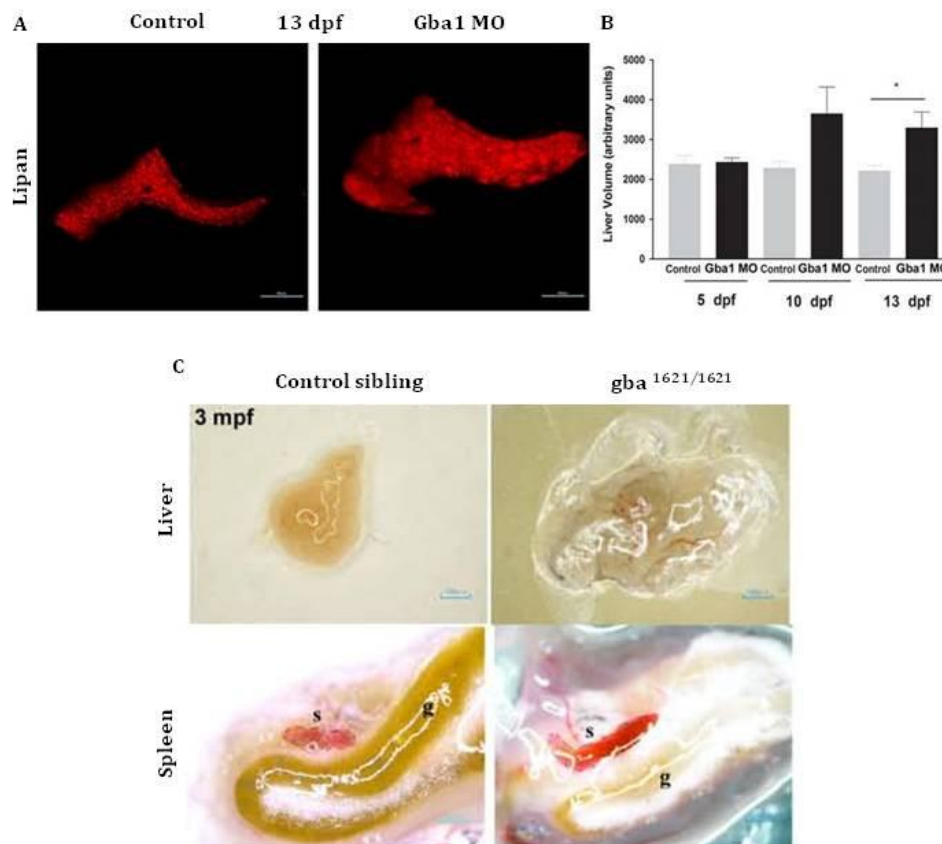
**Figure 18:** (A) Gba1 functional knockdown affects thrombocyte formation and differentiation. Gba1 MO-injected larvae show evident decrease of transgene expression in *Tg(-6.0itga2b:EGFP)<sup>la2</sup>* fish at 5 dpf detected by *in situ* hybridization. The number below each panel represent the fraction of fish with the observed phenotype. The inset depicts a magnification of the trunk area. Black arrowheads indicate positive stained cells. (B) Bar graph showing the quantitative decrease of EGFP measured by ImageJ analysis of acquired images from *in situ* hybridizations. Numbers on the Y-axis are related to the positively stained area in arbitrary units, assessed in 20 fish for each group ( $***P < 0.0005$ ; t-test). (C) Gba1 loss of function reduces erythroid precursors and mature erythrocytes. Representative *Tg(gata1:dsRed)<sup>sd2</sup>* fish showing reduced transgene expression after Gba1 knockdown. In the small inset, a magnification of the trunk area is shown. The number below each panel represent the fraction of fish with the observed phenotype. (D) Bar graph showing the significant reduction of *gata1*-positive cells assessed by FACS analysis in Gba1 morphants fish at 3 dpf. FACS analysis was carried out on cells sorted from 35 dissociated larvae in each experiment. The bar graph depicts the mean  $\pm$ SEM of four independent experiments ( $10^6$  recorded events) ( $*P < 0.05$ ; t-test). (E) Gba1 impairment increases the number of ectopic cMyb (+)-hematopoietic precursors. In the small inset, a magnified caudal view of the trunk is depicted. Numbers represent the fraction of fish with the observed phenotype. (F) Bar graph showing the quantitative increase of *c-Myb* expression measured by ImageJ analysis of acquired images from *in situ* hybridizations. Numbers on the Y-axis are related to the positively stained areas in arbitrary units, assessed in 20 fish for each group ( $**P < 0.005$ ; t-test).

## Results

### 3.3.2 Liver and spleen size are compromised in both morphant and mutant

Another debilitating symptom that affect the GD patients is the increase of the spleen and liver size. Hypersplenomegaly causes thrombocytopenia which in turn may lead to severe bleeding with anemia. Splenectomy is the available treatment to relieve the patients pain but can lead to further liver enlargements.

To address if even morphant fish display a liver enlargement, microinjection of the morpholino in the *gz15Tg* transgenic line (named also *Lipan*), which is a double transgenic line [*Tg(ela3l:EGFP)/Tg(fabp10a:DsRed)*] labeling the exocrine pancreas in green and the liver in red under epifluorescence, was carried out. As shown in figure 19A, a progressive and significant hepatomegaly in morphants after 13 dpf, reminiscent of the visceral phenotype in GD was observed. To address whether the same hepatomegaly was present in fish mutants, heterozygous fish (*gba1<sup>sa1621/+</sup>*) in the *Lipan* transgenic background were incrossed and a significant increase of liver size already at 10 dpf was found (data not shown). Moreover, observation on sacrificed 3 month old homozygous mutants revealed increase of the liver and spleen size also in adult stages (fig.19C).



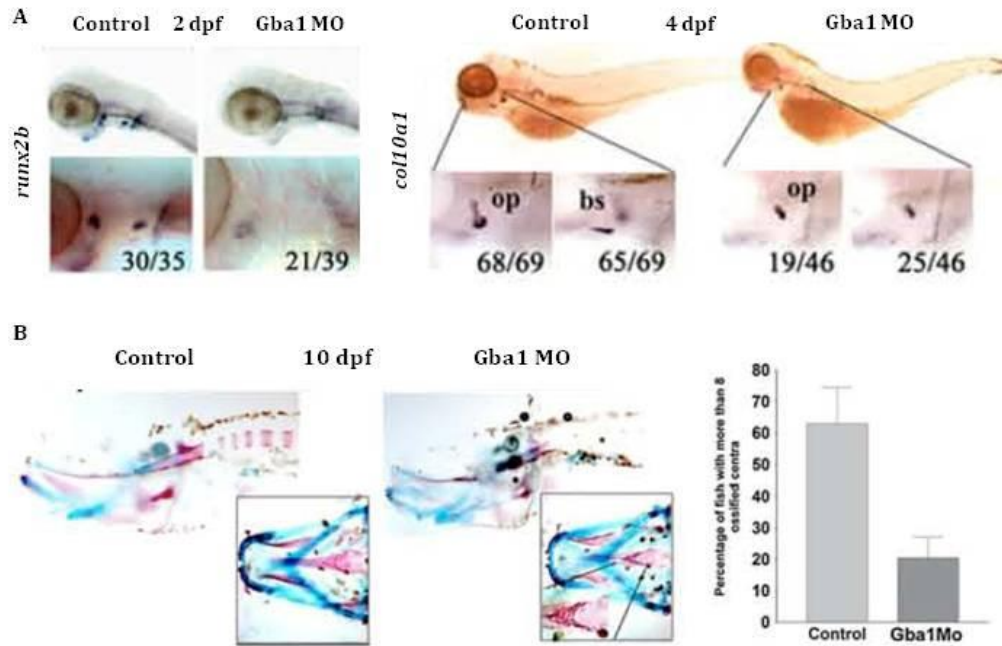
**Fig. 6: (A)** *Gba1* morphants display enlarged liver at 13 dpf. In the upper panel, a representative confocal Z-stack projection of the liver from *Lipan* control and morphant fish at 13 dpf. **(B)** Quantitative measurements of the liver area calculated by ImageJ on acquired images of the *Lipan* transgenic fish microinjected with control and

Gba1 morpholino at different life stages (5 dpf N<sub>control</sub>:14, N<sub>Gba1 MO</sub>: 20; 10 dpf N<sub>control</sub>:12, N<sub>Gba1 MO</sub>: 12; 13 dpf N<sub>control</sub>:18, N<sub>Gba1 MO</sub>: 10). Data are expressed as mean ±SEM of three independent experiments (\*P<0.05; t-test). **(C)** Representative liver and spleen from 3-month-old control sibling and *gba1<sup>sa1621/sa1621</sup>* fish, showing the enlarged liver and spleen size in the homozygous mutant (g:gut; s:spleen).

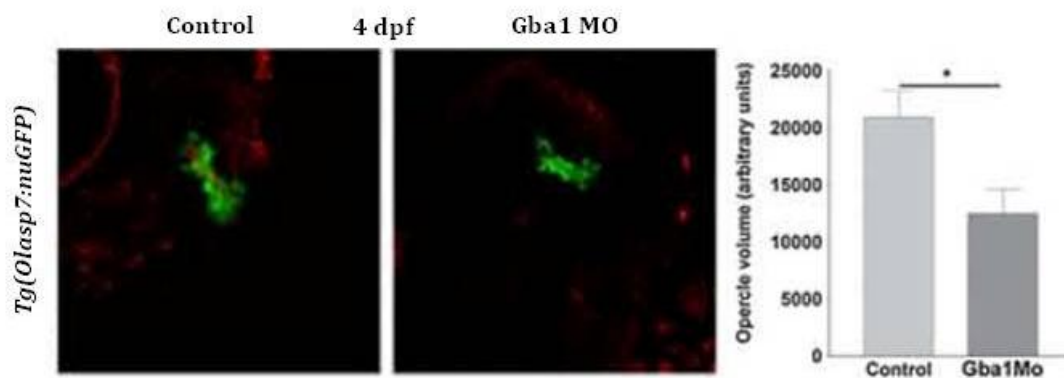
### 3.3.3 Gba1 morphants and mutants display severe bone abnormalities

To investigate if morphants fish exhibits bone development and mineralization defects, the expression of two early osteoblasts differentiation markers were analyzed by *in situ* hybridizations. The early osteoblast-specific *runx2b* and hypertrophic chondrocyte *col10a1* markers which label distinct populations involved in endochondral and intramembranous ossification processes during skeletal development were analyzed in Gba1 morphant and mismatch control at 2 dpf and 4 dpf. A significantly reduction in the expression of both markers in Gba1 morphants was detected (fig.20). Moreover, microinjection of the splicing morpholino in *Tg(Ola.Sp7:NLS-GFP)zfl32* transgenic fish, wich label *osterix (sp7)*-expressing cells was carried out and confocal analysis at 4dpf demonstrated a significant reduction of osterix-transgene expression, thus confirming an early disfunction of the osteoblast population (fig.21) Despite these defects in osteoblast cell lineage, no evident alterations of the cartilage tissue were observed. Evaluation of Gba1 morphants cartilage by Alcian blue staining that label mucopolysaccharides (fig.20B) and confocal analysis of *Tg(Col2a1aBAC:mCherry)<sup>hu5900</sup>* didn't showed alteration in this tissue. Indeed, multiple Alizarins staining on 10 dpf larvae showed a marked decrease in bone mineralization occurring in morphants at both the cephalic regions and vertebrae centra levels. (fig.20)

## Results



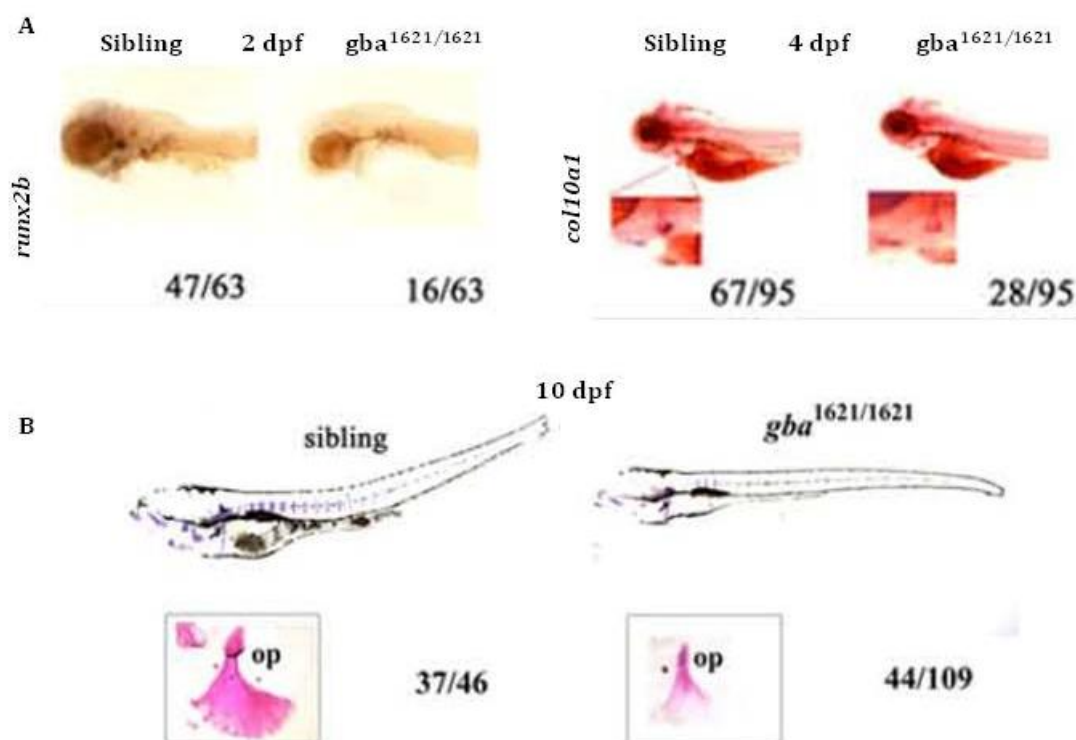
**Figure 20:** (A) (left) Reduced *runx2b* levels in 2 dpf Gba1 morphants. A representative larva is shown for each group (control and morphants). In the bottom panel, a magnification of the *runx2b*-stained area is shown. (right) Reduced *col10a1* mRNA levels in 4 dpf Gba1 morphants. A representative larva is shown for each group (control and morphants). In the bottom panel, a magnification of *col10a1*-stained opercle (op) and brachioistegal (bs) bone is shown. (B) Alcian blue and Alizarin red staining in a representative mismatch-control larva and Gba1 morphant at 10 dpf, showing lack of vertebrae centra ossification in Gba1 morphants. In the small inset a magnification of the cephalic area, showing the spongy aspect of parasphenoid bone in morphants. On the right, a graphical representation of the statistically significant difference in the percentage of larvae with more than eight ossified centra between control (N=70) and morphants (N=108).



**Figure 21:** Reduced transgene expression in *Tg(Olasp7:nuGFP)* fish after Gba1 knockdown. On the left a representative confocal Z-stack projection is shown: on the right ImageJ-based analysis of the opercle volume in control (N=5) and morphants (N=5).

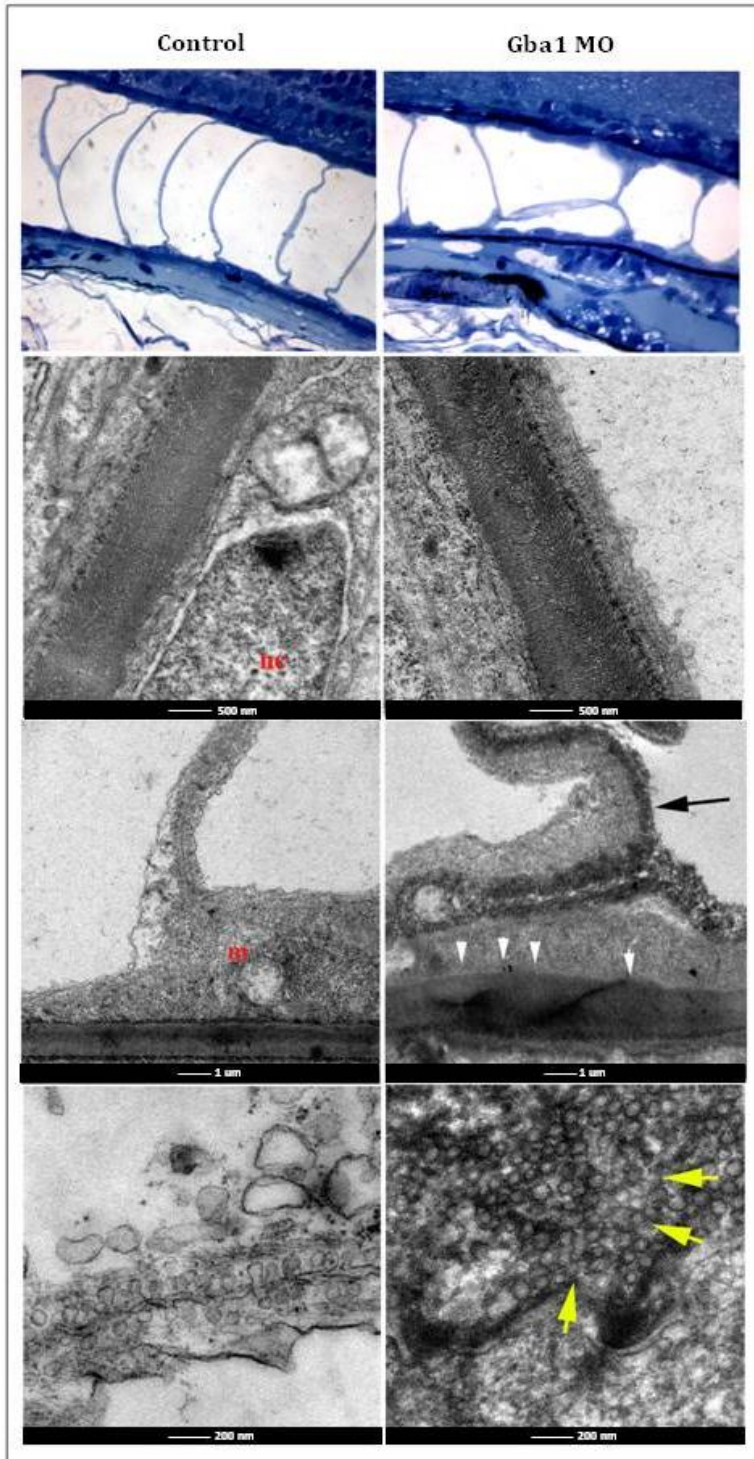


To confirmed the bone alteration observed in Gba1 morphants fish and to support the finding of a primary defect in the differentiation of early bone-forming cells, *in situ* hybridizations of fixed larvae derived from incrosses between Gba mutant carriers ( $gba^{sa1621/+}$ ) demonstrated an evident decrease of *runx2b* and *col10a1* expression in almost 25% of fish at 2 and 4 dpf, respectively (fig.22). Moreover, analysis of bone mineralization at 10 dpf by Alizarin red staining revealed a strong decrease of calcium deposition in mutant larvae at both rostral regions (opercle, inset of fig.22) and vertebrae centra.



**Fig. 22: (A)** Reduced *runx2b* (left) and *col10a1* (right)mRNA levels in  $gba^{sa1621/sa1621}$  detected by *in situ* hybridizations with antisense riboprobe. **(B)** Decreased bone mineralization in  $gba^{sa1621/sa1621}$  fish detected by alizarin red staining. A small inset highlighting the reduced opercle size in mutant fish is shown. The numbers below each panel indicate the fraction of fish with the observed phenotype. In all panels, fish are represented with anterior to the left. Data are expressed as mean  $\pm$  SEM of three independent experiments (\* $P < 0.05$ ; t-test).

To better characterize the type of vertebral abnormalities, thin and ultrathin sections of larvae at earlier stages (6 dpf) was performed. In Gba1 morphants, morphological alterations in the notochord was detected, ranging from outstretched notochord cells to a collapsed notochord in fish with the most severe phenotype. On TEM analysis, distinct ultrastructural phenotypes were observed, which included alterations of the medial notochord sheath, deteriorated mitochondria and notochord cell-shape, and a very limited accumulation of intracellular vesicles (fig.23).

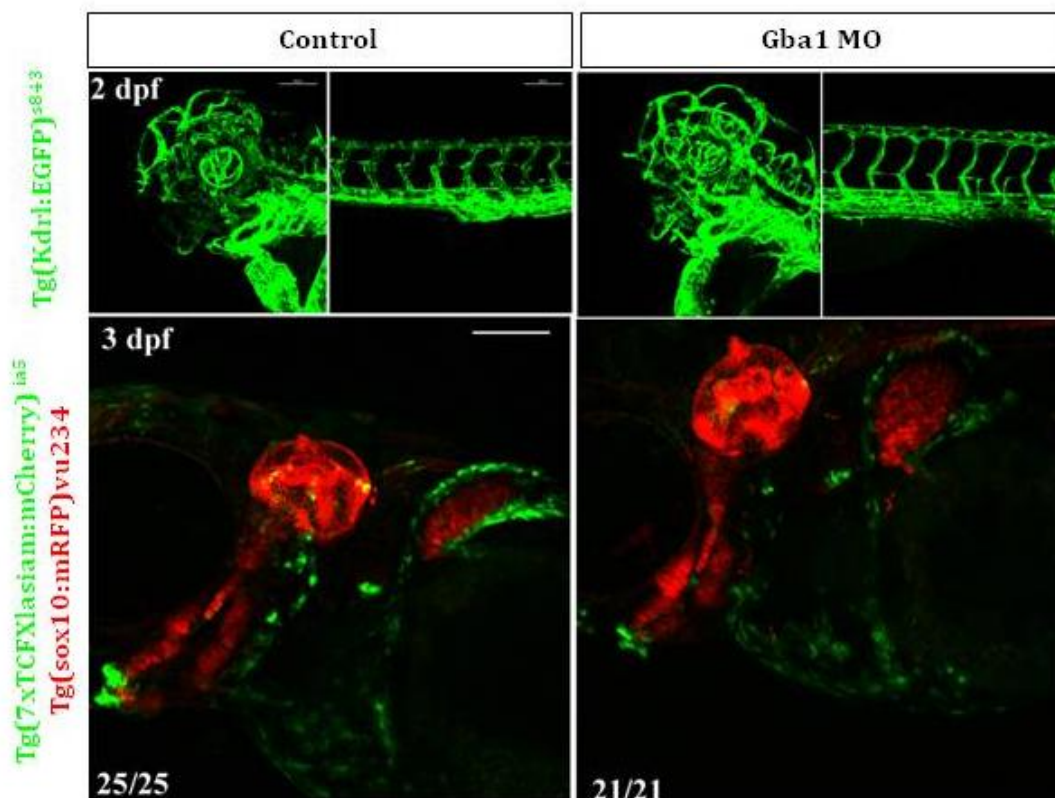


**Figure 23:** *gba1* morphants exhibit a misshapen notochord with ultrastructural defects at 6 dpf. (On the top) Light micrographs from Toluidine blue-stained semi-thin longitudinal section of representative control and morphant fish. (on the bottom) Longitudinal sections EM microphotographs of the notochord from the same fish. Note the misshapen medial sheath (white arrowheads) and notochord cell shape. An increased accumulation of intracellular vesicles is shown by yellow arrows. N: notochord; nc: notochord cell; m: mitochondrion. (N<sub>Gba1MO</sub>=3 ; N<sub>Control</sub>=3).



A very important step in bone formation is the blood vessels invasion of the hypertrophic cartilage. To understand if reduced osteoblast differentiation and bone mineralization defects observed in *Gba1* morphants were due to alteration in blood supply, microinjection *Gba1* morpholino in *Tg(kdrl:EGFP)<sup>s843</sup>* was carried out, but no alteration in the blood vessel architecture and microarchitecture of *Gba1* morphants were detected (fig.24).

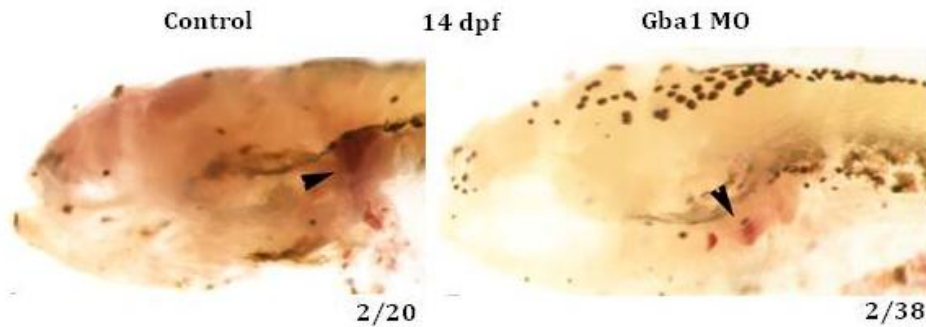
To ruled out a possible defect in the differentiation of neural crest cells, that contribute to bone formations, analysis of transgene expression of 3 dpf *Gba1* morphant in *Tg(sox10:mRFP)<sup>vu234</sup>* background were performed. As shown in figure 24, no modified transgene expression were detected in *Gba1* morphants respect the mismatch control larvae (fig.24).



**Figure 24:** Lack of vascular and neural-crest derived defects in *gba1* morphants. (top) Representative confocal Z-stack projection from a representative 2 dpf control and morphant *Tg(kdrl:EGFP)<sup>s843</sup>* fish, showing the absence of vascular defects at both cephalic (left) and trunk domains (right). (bottom) Representative confocal Z-stack projection of a 3 dpf *Tg(7xTCFXla.siam;EGFP)<sup>ia5</sup>/Tg(sox10:mRFP)<sup>vu234</sup>* control and morphant larva, demonstrating no apparent neural-crest derived abnormality. Numbers on the bottom of each panel describe the fraction of analyzed fish.

## Results

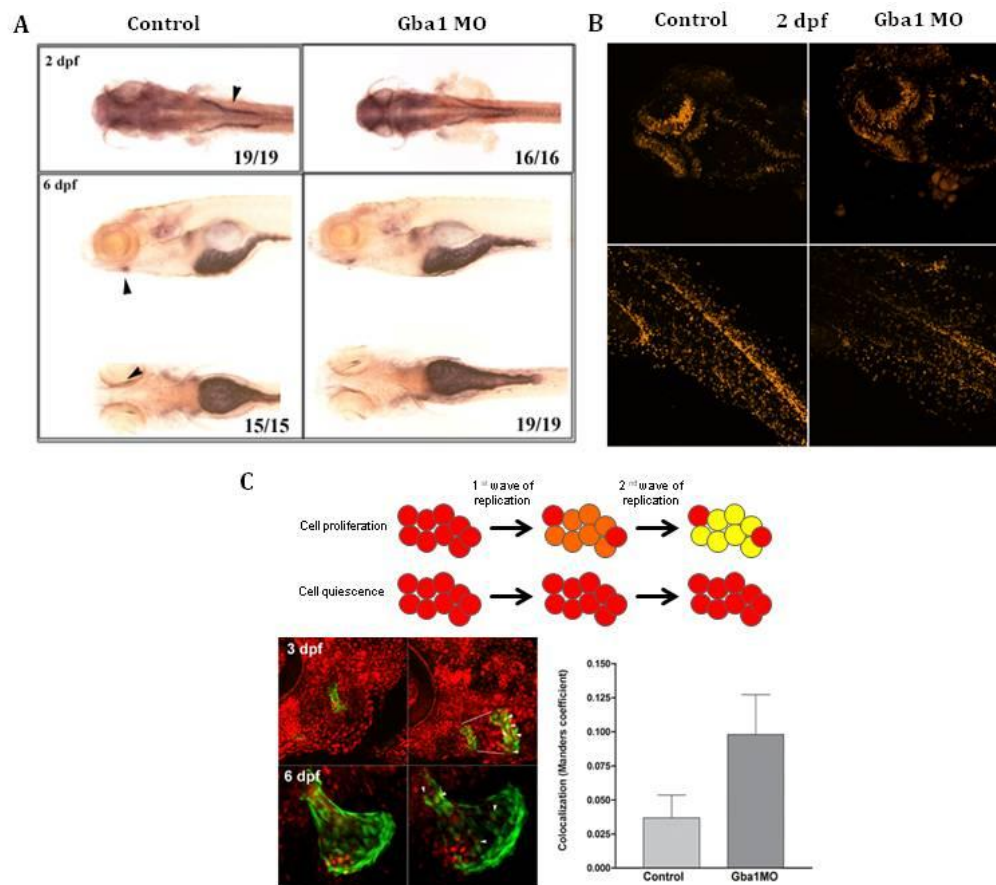
In the maintenance of bone homeostasis also the osteoclasts cell plays important role. In fact, over activation of these cell can lead to alteration of bone mineralization (Helfrich et al. 2007). Analysis of bone resorption by tartrate-resistant acid phosphatase (TRAP) staining in *Gba1* morphants at 14 dpf revealed no apparent increased levels of osteoclast activity (fig.25), suggesting that bone defects observed in *Gba1* morphants are not due to increased bone resorption.



**Figure 25:** Bone resorption is not active in the earliest life stages of *gba1* morphant fish. TRAP staining in 14 dpf control and morphants larvae, showing no significantly increased TRAP-positive areas in *gba1* morphants. Numbers on the bottom of each panel describe the fraction of fish with TRAP positive areas.

### 3.4 GLOBAL CELLULAR AND MOLECULAR DEFECTS DUE TO GLUCOCEREBROSIDASE DEFICIENCY ARE TRIGGERED DURING EARLY STAGES OF DEVELOPMENT

Since anemia, thrombocytopenia and a reduced number of *runx2b*-expressing osteoblasts could be due to overinduced apoptosis or decreased cell proliferation, *in vivo* proliferation and apoptosis assays at 2-6 dpf were performed, in both morphants and controls. No global evident differences in the rate of cell apoptosis in *Gba1* morphants were observed using cleaved caspase 3 immunohistochemistry (fig.26A) and *in vivo* TUNEL labeling (data not shown). Moreover, by means of EdU labeling (fig.26B) and *in vivo* phosphohistone tracking (fig.26B) the level of proliferation in *Gba1* morphants were analyzed. The rate of positive proliferating cells was not altered in *Gba1* morphants except for a slight, but not significant, decrease in the proliferation of *osterix*-expressing cells



**Figure 26:** GBA1 loss of function does not affect cell apoptosis and proliferation. **(A)** Immunohistochemistry for cleaved caspase 3 in 2 dpf and 6 dpf control and morphant larvae. Arrowheads indicate positive stained areas. In 2 dpf fish only a ventral view is shown, while in 6 dpf larvae both lateral and ventral view, with anterior to the left are shown. Numbers on the bottom of each panel indicate the fraction of positively stained fish. **(B)** EdU labeling of 48 hpf Gba1 larvae and control did not reveal alteration of cell proliferation **(C)** (top) A model depicting the gradual dilution of the fluorescent red signal after rounds of cell division in heat-shocked *Tg(h2b:RFP)* larvae, while in non-proliferating cells the signal maintains a high intensity. (bottom) Representative confocal Z-stack projection showing the partially but not significantly reduced proliferation in 3 dpf and 6 dpf *Tg(h2b:RFP)/Tg(Ola.Sp7:NLS-GFP)<sup>zfl32</sup>* fish. A graphic diagram is shown on the right side (six animals for each group were analyzed).

To better understand early molecular defects underlying the global cellular alterations, genome-wide microarray profiling of compared control and morphants gene expression patterns at 2 dpf was performed. Eight different RNA extracts were collected, each extracted from 150 larvae microinjected with Gba1 morpholino or control morpholino. In each individual microinjection experiment, control and Gba1 morpholino were injected in embryos derived from the same offspring to rule out potential intra-experiments variability. Therefore, a total of four distinct biological replicates for each condition was collected. The microarray results, showed that 131 genes were significantly upregulated (of which 62 were >1.5 fold) and 63 genes were

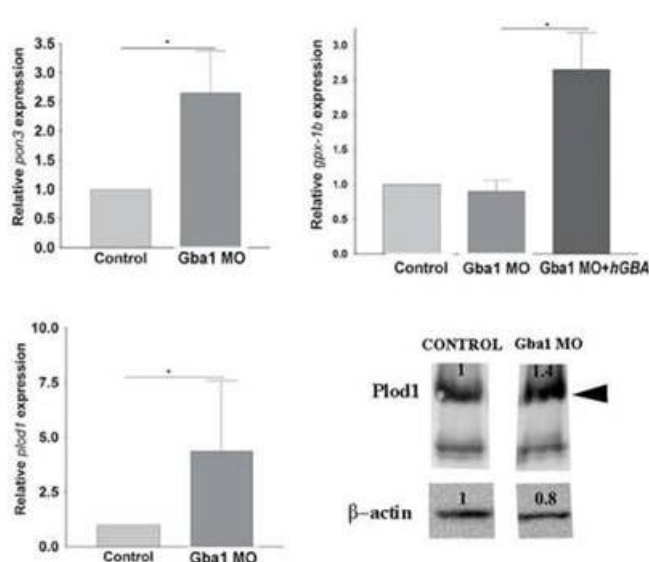
## Results

downregulated in Gba1 morphants (fig.28). Noteworthy, both the most up- and downregulated genes were associated with an oxidative stress-response. A >3-folds upregulation of the genes *plod1* (*procollagenelysine, 2-oxoglutarate 5-dioxygenase 1*) and *pon3* (*paraoxonase 3*) was found, while *gpx1b* (*glutathione peroxidase 1b*) expression levels were significantly decreased of ~1.5-fold. Interestingly, analyzing the microarray results many genes involved in intracellular vesicle trafficking, mitochondrial activity and transcriptional activity were differentially expressed in Gba1 morphants respect the control [Gene Expression Omnibus, accession no. GSE54754].

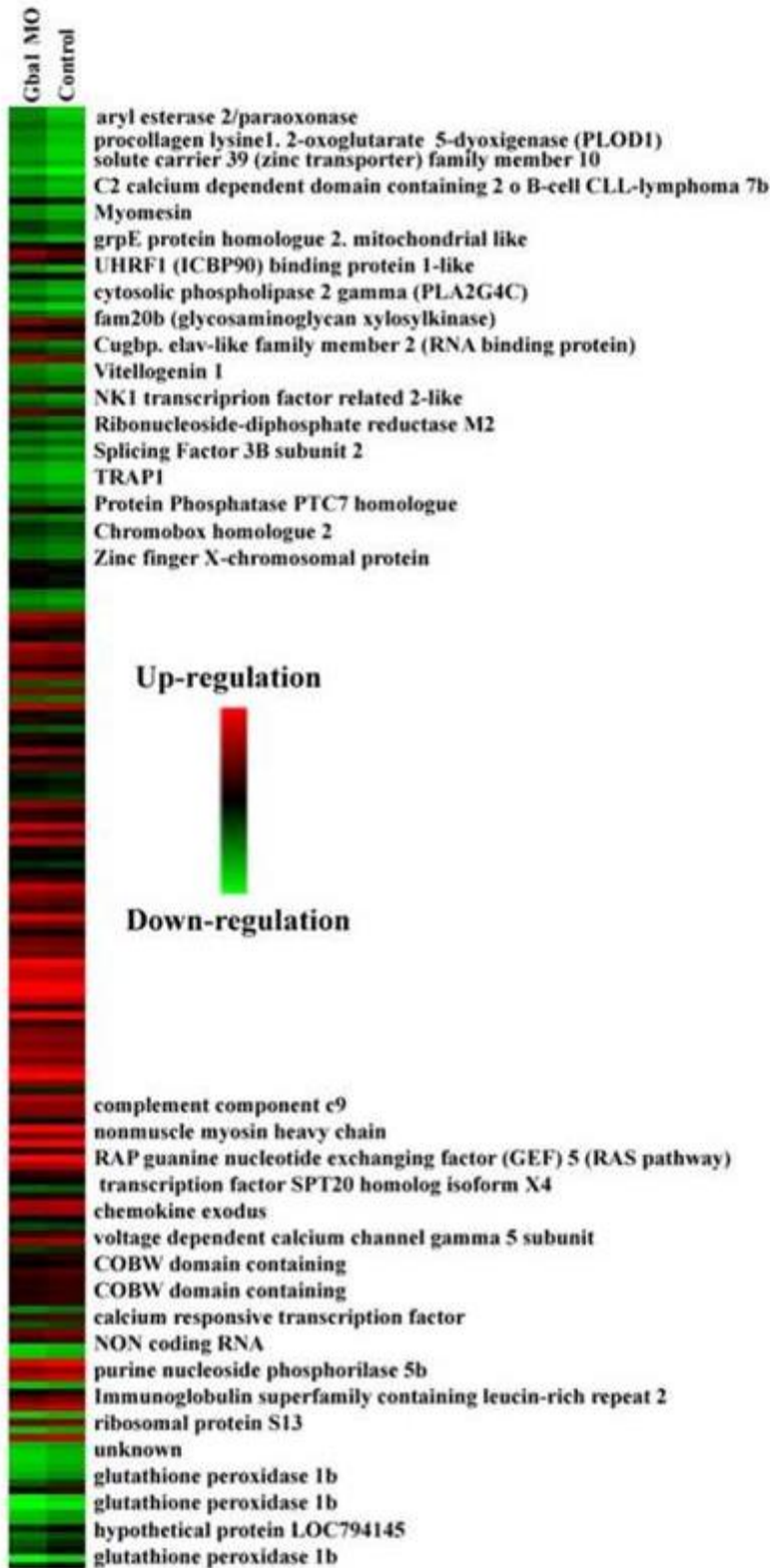
To confirm some of the data retrieved by microarray analysis, quantitative real-time PCR (q-PCRs) analysis on the same pooled RNA extracts used in microarray experiments from the 2 dpf control and morphant microinjected larvae was carried out. As shown in figure 28, the same degree of differential gene expression for *plod1* and *pon3* was detected, thus confirming the output of microarray analysis.

Moreover, western blot analysis using a cross-reacting PLOD1 antibody on 2 dpf pooled morphant and control protein lysates from 150 microinjected larvae, confirmed the q-PCRs obtained results at a proteomic level.

As shown in figure 27, an increase of Plod1 protein levels was detected in morphants when compared with matched control fish lysates. This results is in line with microarray profile for the *plod1* target gene.



**Figure 27:** Quantitative polymerase chain reaction (qPCR) analysis for *pon3*, *plod1* and *gpx1b*, highlighting significantly increased transcripts levels for *pon3* and *plod1*, while *gpx1b* mRNA levels decreased in morphants and significantly augmented in rescued larvae. RQ-PCRs were performed on the RNA extracts from the four biological replicates used in microarray analysis. Each pooled RNA was extracted from 150 microinjected larvae. Data are expressed as mean  $\pm$ SEM of five independent experiments (\* $P < 0.05$ ; t-test). On the bottom right, a representative western blot analysis demonstrates the correspondent increase between mRNA and protein levels in Gba1MO. Protein lysates were obtained from 150 microinjected larvae. Numbers on the top



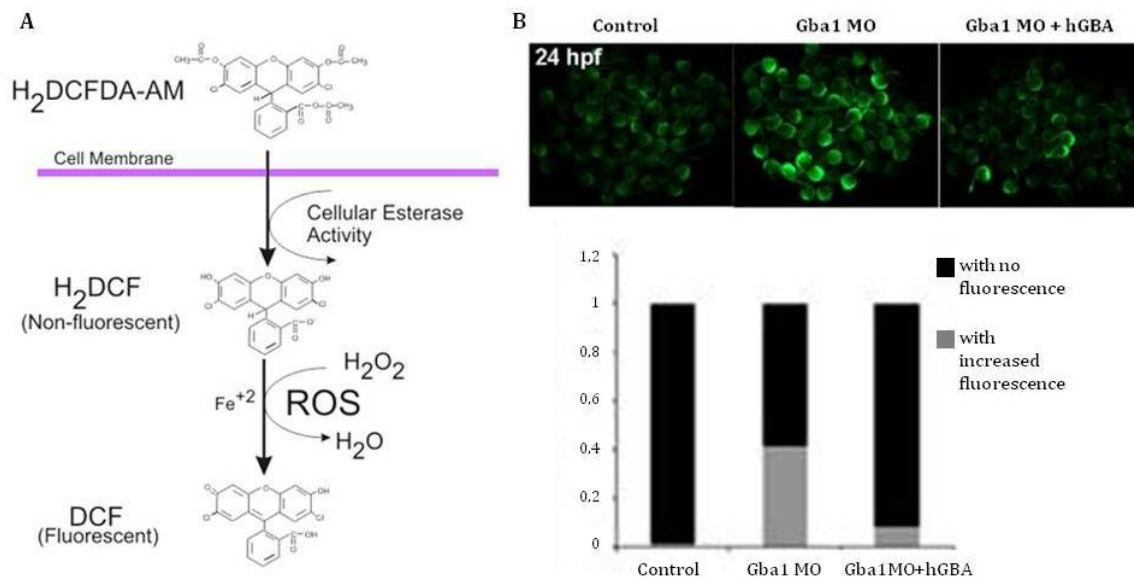
**Figure 28:** Heat map showing the differential expression of transcripts in Gba1 morphants versus control fish. A partial list of differentially expressed genes (>2-fold increased expression for upregulated genes and <1.5-fold expression for downregulated genes) is reported.



## Results

Since the upregulation of *plod1* and the downregulation of *gpx1b* could account for an early oxidative stress response, an additional *in vivo* analysis were perform. To address the issue, *in vivo* staining of 24 hpf (fig.29B) and 48 hpf morphant and control larvae with DCFDA (dichlorofluorescein, DCF, diacetate), which is a probe for reactive oxygen species (ROS), was carried out.

The DCFDA is cleaved intracellularly by non-specific esterase to form DCFH, which is further oxidized by ROS to form the fluorescent compound DCF. (fig. 29A) As shown in figure 29B, a significant increase of fluorescence in morphant fish microinjected with the DCFDA compound at 24 hpf was observed, when compared with controls. The direct effect of ROS-mediated increase of flourscence was specific, as the co-injection of a human GBA1 mRNA was able to strongly reduce ROS release.



**Figure 29:** (A) Schematic representation of the formation of fluorescent compound DCF by ROS. (B) (top) Oxidative stress increase detected by fluorescent DCFDA staining in Gba1 morphants. Representative whole fluorescent imaging of control, morphants and rescued morphant fish at 24 hpf. (bottom) Quantitative bar graph showing the percentage of fish with DCFDA-positive staining from three independent experiments.

### 3.5 CANONICAL WNT PATHWAY ACTIVITY IS SPECIFICALLY HAMPERED BY GLUCOCEREBROSIDASE IMPAIRMENT

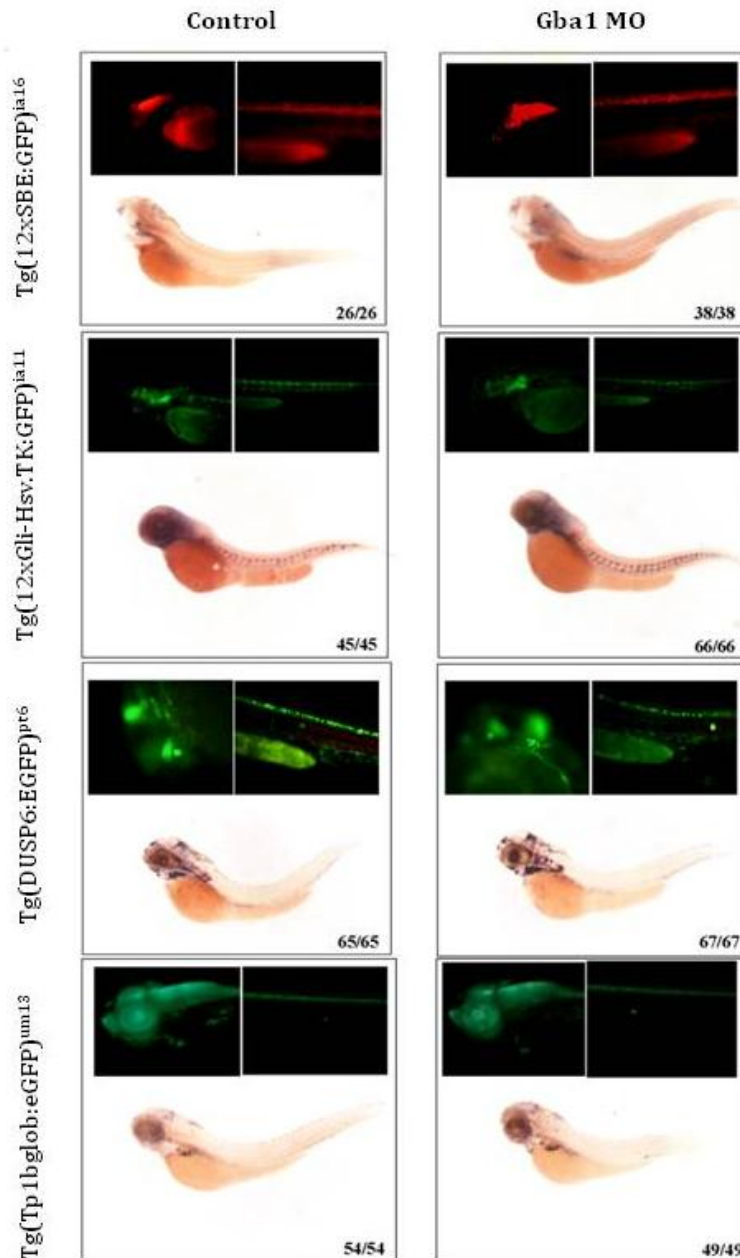
Since early apoptotic events or cell proliferation defects were ruled out, we focused our attention to potential cellular pathways involved in cell differentiation process. To screen for a candidate affected cell signaling, the Gba1 morpholino were tested on different generated signaling pathway reporter lines, in which a reporter gene (EGFP or mCherry) is driven by cell signaling responsive elements (fig.30) (Moro et al. 2013).

By both fluorescent microscopy imaging and *in situ* hybridization analysis, was detected a specific drop of reporter gene expression for the responsive line *Tg(7xTCFX.lasiam:EGFP)<sup>ia4</sup>*, in which domains of active canonical Wnt signaling are labelled (fig.30) (Moro et al. 2012).

To address whether the Wnt signaling defect was specific and reproducible in stable Gba1 mutants, the *gba1<sup>sa1621/+</sup>* carriers was crossed with the transgenic line and the offspring obtained from incrossed heterozygote *gba1<sup>sa1621/+</sup>* in the Wnt reporter background were analyzed. As shown in figure 30, in homozygous fish mutant (*gba1<sup>sa1621/sa1621</sup>*) a strong decrease of reporter expression was detected, which remained consistently low even later than 7 dpf (fig.30).

With RQ-PCRs experiments the decrease of Wnt reporter activity in transgenic fish microinjected with the Gba1 morpholino and control morpholino were quantitatively measured. To performe this task, for each condition (control and morphants) 100 larvae at 2 dpf were collected for a total amount of five biological independent replicates.

## Results



**Figure 30:** Representative 2 dpf (fluorescence) and 3 dpf (bright field) reporter fish after control and morpholino injection (Gba1 MO). Brightfield images have been taken after *in situ* hybridization using an antisense riboprobe against the reporter coding region. From upper panel, reporter for: TGF- $\beta$ , Shh, Notch and Fgf signaling pathways. Numbers below each panel describe the fraction of fish observed. All views are anterior to the left.

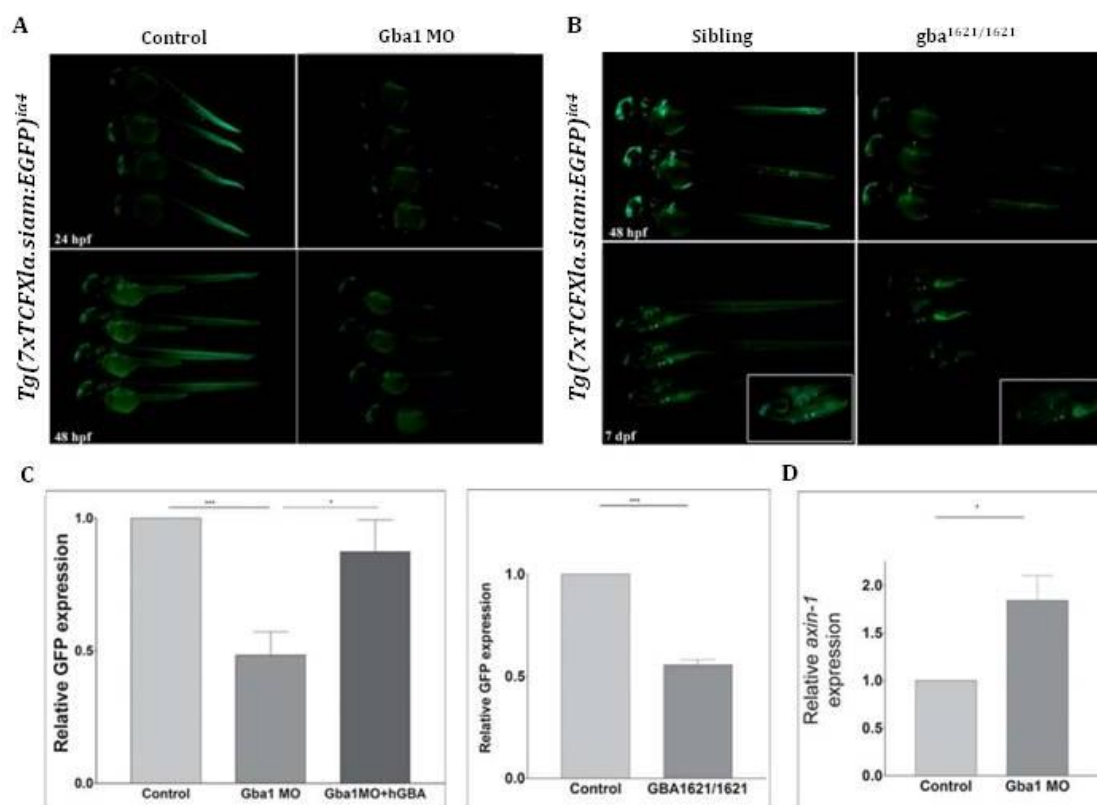
About a two-fold decrease of total GFP mRNA levels (fig. 31C) in morphant fish when compared to age-matched mismatch-control larvae was measured, thus supporting the direct effect of GBA1 loss of function on the transcriptional activity of the Wnt reporter. Noteworthy, the Wnt pathway deregulation was significantly reverted upon human *GBA1* mRNA overexpression in morphants (fig. 31C), thus supporting a direct link between Wnt signaling defects and Gba1 loss of function. To further confirm the canonical Wnt signaling involvement in Gba1 functional impairment, single genotyped homozygous mutant larvae were collected and several RQ-PCRs on RNAs from pooled 2 dpf homozygous mutants and wild-type siblings (N=3 for each condition) was performed. As shown in figure 31C, a significant decrease of Wnt



reporter transgene expression in mutant fish when compared to age-matched control siblings was detected. Notably, the decrease of reporter expression was similar to that assessed in morphant RNA extracts when compared with mismatch controls. Microinjection of hGBA mRNAs was partially able to rescue the decrease of reporter expression in mutant larvae (data not shown).

The activity of Wnt signaling pathway is generally modulated by the sequestration of  $\beta$ -catenin by the multiprotein complex comprised of Axin1 and GSK-3. To address if the reduction of the Wnt reporter activity observed both in morphants and mutant zebrafish larvae was due to increased expression level of these multiprotein complex, analysis of the *axin1* mRNAs by RQ-PCR on morphants and mismatch control extracts from the previously isolated pools were performed.

As shown in figure 31D, a significantly increased of *axin1* mRNA levels in 2 dpf morphants when compared with mismatch control larvae was measured. The same degree of *axin1* upregulation was not, however, detected in *gba1* mutants extracts (data not shown).



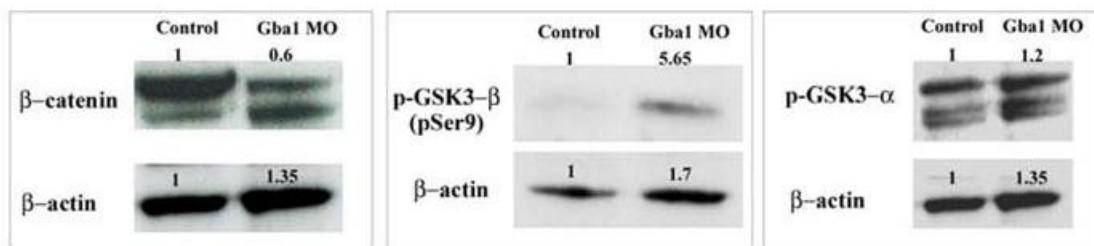
**Figure 31:** Canonical Wnt signaling is disturbed in *Gba1* morphants and *gba1*<sup>sa1621/sa1621</sup> fish. **(A)** Representative 24 hpf (top) and 48 hpf (bottom) Wnt reporter fish microinjected with control morpholino and *Gba1* morpholino, showing the marked decrease of reporter activity. **(B)** Representative 48 hpf (top) and 7 dpf (bottom) *gba1*<sup>sa1621/sa1621</sup> fish in the Wnt reporter background, showing the strong decrease of reporter activity. The small inset shows a magnified view of the cephalic region of the *gba1*<sup>sa1621/sa1621</sup> fish at 7 dpf. **(C)**(left) RQ-PCR analysis of GFP showing the significant decrease of reporter expression in Wnt reporter transgenics after *Gba1* morpholino-mediated knockdown. Note that the GFP mRNA levels were significantly restored when fish were co-injected with the human *Gba1* mRNA. RNA extracts were obtained from 100 pooled microinjected

## Results

control, morphant and rescued morphant fish in five independent experiments. (right) RQ-PCR analysis of GFP showing the significant decrease of reporter expression in *gba1*<sup>sa1621/sa1621</sup> fish in the Wnt reporter background. RQ-PCRs were carried out on RNAs from pooled 2 dpf homozygous mutants and wild-type siblings (N=3 for each condition). Data are expressed as mean  $\pm$  S.E.M of four independent experiments (\*P<0.05; t-test).

**(D)** Quantitative polymerase chain reaction (qPCR) analysis for *axin1*, showing the significant upregulation of *axin1* in Gba1 morphant fish. RNA extracts were obtained from 100 microinjected control, morphant fish in five independent experiments. Results are expressed as mean  $\pm$  SEM of five independent experiments (\*P < 0.05; \*\*\*P < 0.0005; t-test).

Immunoblot analysis of  $\beta$ -catenin in morphants and control protein lysate, obtained by protein extraction from 150 larvae for each condition was carried out, and a 2-fold decrease of total  $\beta$ -catenin protein levels in morphants was detected (fig.32). Moreover, by immunoblot the levels of Gsk3- $\beta$  were tested and found a 3-fold increase of Gsk3- $\beta$  protein levels in the previously obtained morphant lysates (fig.32). Indeed, levels of Glycogen synthase 3  $\alpha$  (Gsk3  $\alpha$ ), another  $\beta$ -catenin regulator (Doble et al. 2007) were not affected by Gba1 loss of function, as assessed by western blot on the same morphant and control protein extracts.

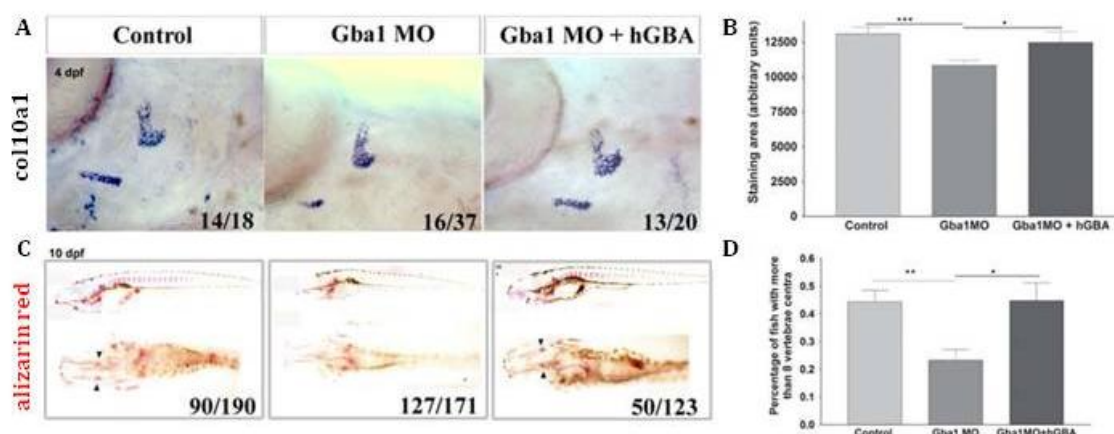


**Figure 32:** Representative Western blot analysis of total lysates from 100 pooled control and morphant fish at 2 dpf for  $\beta$ -catenin (left), p-Gsk3 $\beta$  (pSer9) (middle) and Gsk3 $\alpha$  (right).  $\beta$ -catenin and p-Gsk3 $\beta$  protein level decrease and increase are shown in the left and right image, respectively. Numbers on the top of each band represent quantitative measurements by Image-J analysis.

### 3.6 BONE DEFECTS ARE REVERSIBLY CORRECTED WHEN A HUMAN GBA1 IS OVEREXPRESSED IN MORPHANTS

Osteopenia has been shown to develop during early life stages in humans, thus justifying bone improvements when ERT is started in young patients (Mistry et al. 2011). To address if bone defects observed in this zebrafish model was due to direct effect of Gba1 depletion and if restore expression of this enzyme improved the osteopenic phenotype, a human *GBA1* mRNA were co-injected with the morpholino in wild type zebrafish embryos.

As shown in figure 33A and B, a significant recovery in the expression of the *col10a1* marker was observed, which was previously showed to be affected by Gba1 loss of function. Moreover, also bone mineralization can be restored to normal levels after hGBA overexpression in Gba1 morphants. Indeed, both cephalic bones and vertebrae centra mineralization were consistently recovered (fig.33C and D).



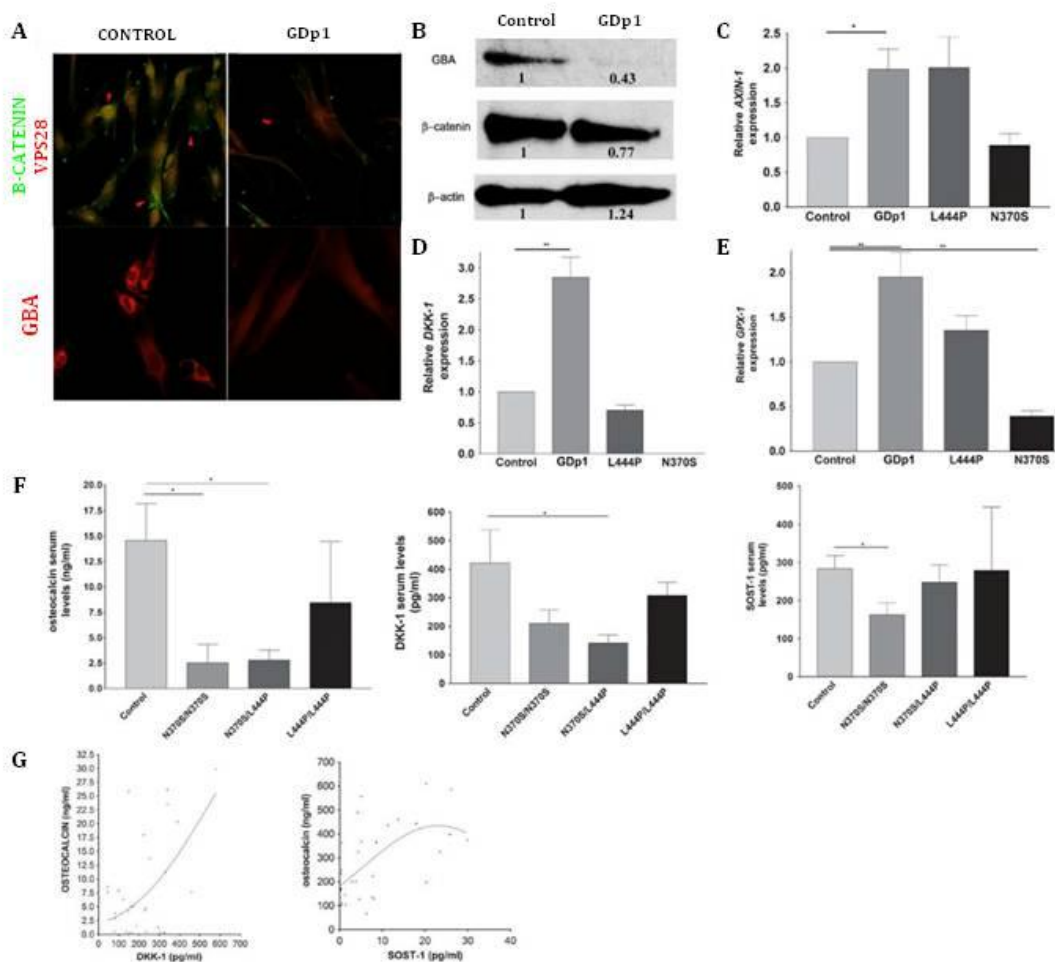
**Figure 33:** *Col10a1* decreased expression and bone mineralization are rescued upon human *GBA1* overexpression **(A)** Representative *in situ* hybridization for *col10a1* in 4 dpf control, Gba1MO and rescued fish. Number below each panel represents the fraction of fish with the observed phenotype. **(B)** Graphical diagram showing an Image-J based volume analysis of the *col10a1*-stained opercles in the different conditions. **(C)** Lateral (top) and ventral (bottom) views of 10 dpf alizarin-stained larvae, showing the recovery of bone mineralization after human *GBA1* forced expression. In the bottom mineralization of the ceratohyal cartilage is highlighted by arrowheads. **(D)** Graphic representation of the quantitative measurements of vertebrae centra in different conditions. Results are expressed as mean  $\pm$  SEM of five independent experiments ( \*P < 0.05, \*\*P < 0.005, \*\*\*P<0.000; t-test)

### 3.7 CANONICAL WNT SIGNALING ACTIVITY IS SIGNIFICANTLY IMPAIRED IN TYPE 1 GAUCHER DISEASE PATIENTS

The canonical Wnt signaling plays a pivotal role in bone remodeling (Regard et al. 2012) and to address whether Wnt signaling defects could also be detected in type 1 GD patients different assays were performed. Immunofluorescence analysis of  $\beta$ -catenin and glucocerebrosidase levels on fibroblasts from a healthy volunteer and type 1 GD patient that was compound heterozygous for [R170P]+[c.1225(-11delC)-(14T>A)] (Filocamo et al. 2000) showed a strong reduction in  $\beta$ -catenin protein levels and almost no immunoreactivity for glucocerebrosidase in the patient. Western blot analysis on total protein lysates from the same patient's fibroblasts confirmed a quantitative decrease of total  $\beta$ -catenin (more than 1.5-fold) and glucocerebrosidase (nearly 3-fold) levels (fig. 34B). To evaluate the mRNA levels of the intracellular, *Axin1*, and the extracellular, *DICKKOPF-1 (DKK1)*, negative regulators of the Wnt pathway, RQ-PCRs experiments was carried out in RNA extracts from cultured fibroblasts of (i) the same type 1 GD patient, compound heterozygous for [R170P]+[c.1225(-11delC)-(14T>A)](Filocamo et al. 2000), (ii) a N370S homozygous type 1 patient, and (iii) a L444P homozygous type 3 GD patient. As shown in figure 34C and D, a significant increase of both *Axin1* and *DKK-1* mRNAs in the compound heterozygote for the [R170P]+[c.1225(-11delC)-(14T>A)] alleles was observed, while *DKK-1* mRNA levels were almost undetectable in the N370S homozygote. Moreover, also a significantly reduced levels for the human *GPX1* mRNA in the N370S homozygote was detected.

The identification of bone turnover markers in relation to GD manifestations has been matter of debate (van Dussen et al. 2011; Drugan et al. 2002; Ciana et al. 2003). To investigate if Wnt-related modulators could be used as traceable blood serum markers, several analysis in a cohort of thirty patients affected by type 1 and 3 GD with a known genotype (Table 2) was carried out.

As shown in figure 34F, only type 1 GD patients homozygous for [N370S]+[N370S] and compound heterozygous for [N370S]+[L444P] displayed significantly decreased osteocalcin levels. When measuring blood serum levels for DKK-1 and sclerostin (SOST-1), another known extracellular Wnt pathway modulator, was detected that DKK-1 serum levels were significantly reduced in compound heterozygotes [N370S]+[L444P], while SOST-1 levels were significantly diminished in homozygotes [N370S]+[N370S]. Furthermore, significant evidence that osteocalcin levels positively correlate with both DKK-1 and SOST-1 levels in type 1 GD patients, regardless of a specific genotype (fig. 34G), point out a potential correlation between osteocalcin and the Wnt modulators DKK-1 and SOST-1.



**Figure 34:** Canonical Wnt signaling is impaired in type 1 GD patients. **(A)** Representative immunostaining for  $\beta$ -catenin/VPS28 (top) and GBA1 (bottom) in control fibroblasts and in fibroblasts from a type 1 Gaucher patient [R170P]+[c.1225(-11delC)-(14T>A)] (abbreviated to GDp1). Red arrowheads indicate spikes and the nuclear  $\beta$ -catenin staining in control cells. Cells from the Gaucher patient display a marked decrease of  $\beta$ -catenin and GBA staining. **(B)** Western Blot analysis of total cell lysates with GBA1 and  $\beta$ -catenin antibodies, showing decreased levels of  $\beta$ -catenin in GDp1 patient fibroblasts. Numbers on the top of each band represent quantitative measurements by Image-J analysis. **(C, D)** Increased levels of *Axin1* and *DKK1* mRNAs in GDp1 fibroblasts, as detected by qPCR analysis. Results are expressed as mean  $\pm$  SEM of three independent experiments (with \* $P < 0.05$ , \*\* $P < 0.005$ ; t-test). **(E)** Differential expression of *GPX-1* in type 1 GD fibroblasts from patients with different genotypes. Fibroblasts from a homozygous [N370S]+[N370S] patient display a significant reduction of *GPX-1* mRNA levels, while those from the patient with the rare genotype [R170P]+[c.1225(-11delC)-(14T>A)] were associated with significantly increased *GPX-1* mRNA levels. **(F)** Blood serum levels of OSTEOCALCIN, DICKKOPF-1 (DKK-1) and SCLEROSTIN (SOST-1) measured by ELISA show significant decrease of OSTEOCALCIN in homozygous [N370S]+[N370S] and compound heterozygous [N370S]+[L444P] (left bar-graph), significantly decreased DKK-1 levels in compound heterozygous [N370S]+[L444P] (middle bar-graph) and significantly decreased SOST-1 levels in homozygous [N370S]+[N370S] patients (right bar-graph). **(G)** (left) Correlation of DICKKOPF-1 (DKK-1) and OSTEOCALCIN serum levels. X-axis indicates DKK-1 serum level; y-axis indicates OSTEOCALCIN level in Gaucher patients.  $r=0.46$  ( $p<0.001$ ). (right) Correlation of SCLEROSTIN-1 (SOST-1) and OSTEOCALCIN serum levels. X-axis indicates SCLEROSTIN serum levels; y-axis indicates OSTEOCALCIN level in Gaucher patients.  $r=0.56$  ( $p<0.001$ ).

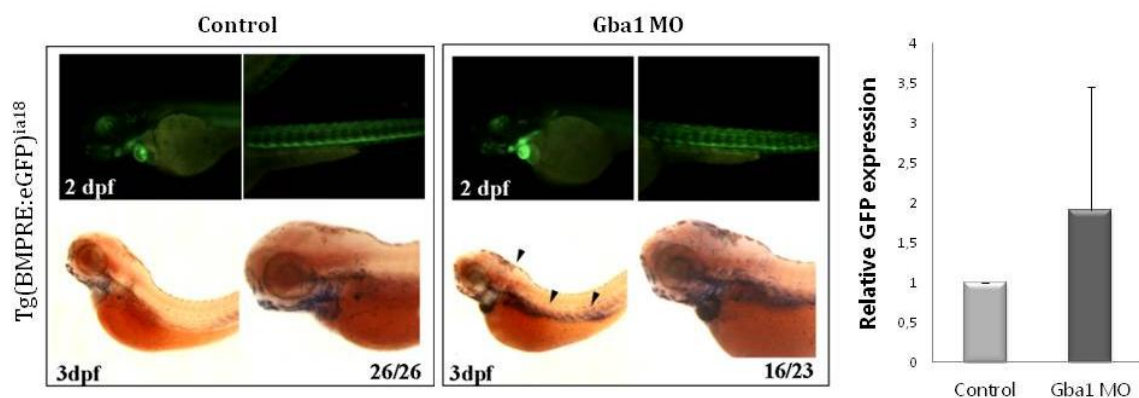
## Results

Subjects	Gender	Status (type of Gaucher disease)	Genotype <sup>§</sup>	Subjects	Gender	Status (type of Gaucher disease)	Genotype <sup>§</sup>
1	F	1	[L444P]+[W312S]	21	F	3	[N370S]+[L444P]
2	M	3	[L444P]+[L444P]	22	F	1	[N370S]+[V214X]
3	M	1	[N370S]+[L444P]	23	F	1	[D409H]+[?]
4	F	1	[N370S]+[L444P]	24	F	3	[N370S]+[L444P]
5	M	1	[N370S]+[N370S]	25	M	1	[N370S]+[total gene del]
6	M	1	Na	26	F	1	[N370S]+[total gene del]
7	F	1	Na	27	F	1	[N370S]+[IVS2G>A]
8	F	1	[N370S]+[RecNciI]	28	F	1	[N370S]+[IVS2G>A]
9	F	3	[L444P]+[L444P]	29	M	1	[N370S]+[L444P]
10	F	1	[N370S]+[N370S]	30	M	1	[N370S]+[RecNciI]
11	F	1	[N370S]+[N370S]	31	M	NOT AFFECTED	
12	F	1	[N370S]+[E388K]	32	F	NOT AFFECTED	
13	F	1	[N370S]+[E388K]	33	F	NOT AFFECTED	
14	M	3	[T231R]+[?]	34	F	NOT AFFECTED	
15	F	1	[L444P;E326K]+[L444P;E326K]	35	F	NOT AFFECTED	
16	M	3	[N370S]+[N370S]	36	M	NOT AFFECTED	
17	M	1	[N370S]+[RecNciI]	37	M	NOT AFFECTED	
18	M	1	[N370S]+[L444P]	38	M	NOT AFFECTED	
19	M	1	[N370S]+[?]	39	M	NOT AFFECTED	
20	F	1	[L444P]+[L444P]	40	M	NOT AFFECTED	

**Table 2:** Characteristics of affected and not-affected individuals recruited for blood serum analysis. Na: not available, genotyped elsewhere; ?: still unknown allele; <sup>§</sup> Reference cDNA sequence: GenBank accession no. M16328.1. Mutations at the protein level are described following the traditional nomenclature within the Gaucher field, which considers aminoacid 1 the first amino acid after the signal peptide. According to current manipulation nomenclature guidelines (<http://www.hgvs.org/mutnomen>), ascribing the A of the first ATG translational initiation codon as nucleotide +1, 39 amino acids should be added.

### 3.8 GBA1 DEFICIENCY INDUCED ALTERATIONS ALSO IN THE BMP SIGNALING PATHWAY

Together with Wnt signaling, another pathway that plays important roles in bone formations and homeostasis is the BMP signaling. To preliminary address if the lack of Gba1 enzymatic activity also affected this pathway, injection of the Gba1 morpholino in *Tg(BMPRE:GFP)* one-cell stage embryos was carried out. Increased GFP fluorescence in morphant when compared to the age-matched control larvae was detected already at 2 dpf. This results was also confirmed by *in situ* hybridization analysis of GFP mRNA levels on 3 dpf PFA-fixed larvae (fig.35).



**Figure 35: (Left)** Bmp pathway is affected by Gba1 loss of function. Representative 2 dpf (fluorescence) and 3 dpf (bright field) reporter fish after control and morpholino injection. The brightfield images were taken after *in situ* hybridization using an antisense riboprobe against reporter codon region. A Bmp upregulation (black arrowheads) is clearly evident in *gba1* morphants. Numbers below each panel describe the fraction of fish with observed phenotype. All views are anterior to the left. **(Right)** RQ-PCR analysis of GFP showing the significant increase of reporter expression in BMP reporter transgenics after Gba1 morpholino-mediated knockdown. RNA extracts were obtained from 100 pooled microinjected control and morphant fish in two independent experiments

Preliminary RQ-PCRs experiments to quantitatively measure the BMP reporter activity were performed in transgenic fish microinjected with the Gba1 morpholino and control morpholino. One hundred larvae at 2 dpf have been collected for each condition (control and morphants) for a total amount of two biological independent replicates.

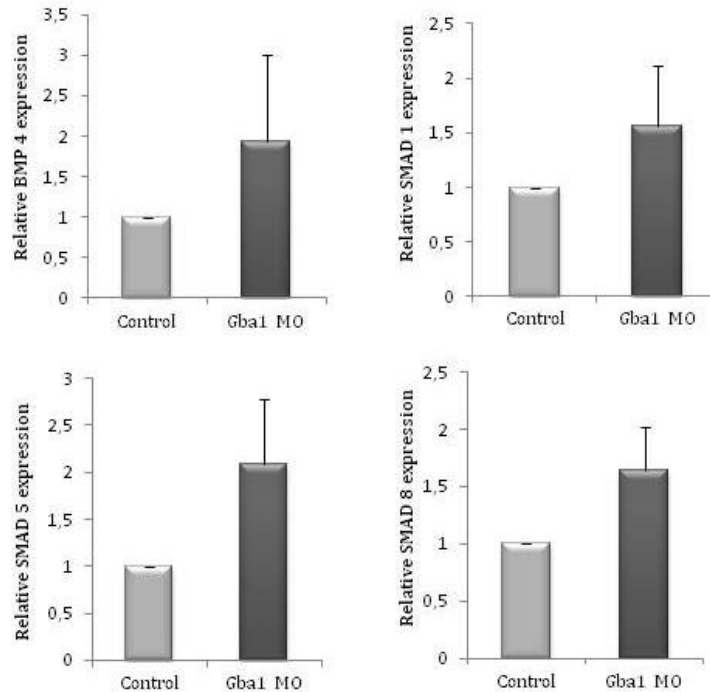
A consistent two-fold increase of total GFP mRNA levels (fig. 35) in morphant fish when compared to age-matched mismatch-control larvae was found.

The BMPs signaling cascade in osteocytes and chondrocytes, typically activates BMPs type I receptors (BMPR-I) and Smad 1, 5 and 8 proteins. This activation is generally performed by the binding of BMP 4 to the BMPR-I. To address if the upregulation of the pathway observed in the Gba1 morphant was due to an activation of these signaling transducers, the levels of *Smad1*, *Smad5*, *Smad8* and



## Results

*BMP4* mRNAs have been analyzed by RQ-PCR on morphants and mismatch control RNA extracts from the previously isolated pools. As shown in figure 36, increased mRNA levels of these BMPs transducers in 2 dpf morphants when compared with mismatched control larvae confirmed the alteration of this pathway.



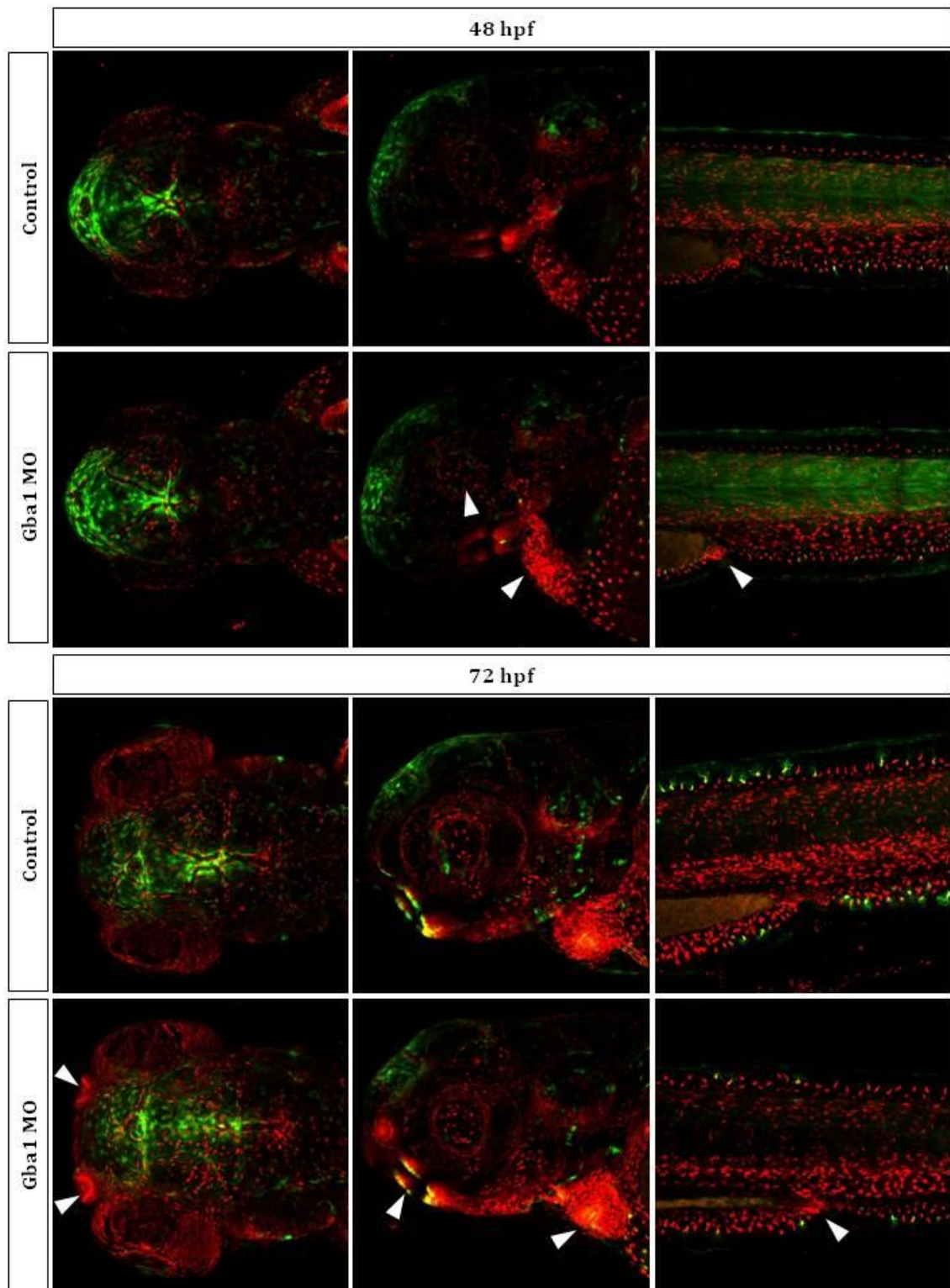
**Figure 36:** RQ-PCR analysis of *BMP4*, *Smad1*, *Smad5* and *Smad8* showing the significant increase level of mRNA in morphants respect the mismatch control larvae. RQ-PCRs were carried out on RNAs from pooled 2 dpf morphants and control fish in three independent experiments .

To address if the alteration of the of Wnt and BMP signaling activity due to *Gba1* dysfunction was detectable in distinct tissues or organs, injection of the splicing morpholino in double Wnt (in green) and BMP (in red) reporter fish, (*Tg(7xTCFXla.siam;EGFP)<sup>ia4</sup>/Tg(BMPRE:nlsmCherry)<sup>ia17</sup>*) was performed.

Confocal analysis of 48 hpf morphant and aged matched control larvae revealed an upregulation of BMP levels in heart, in the eyes, in the olfactory pit, in the rhombencephalon, in the jaw, mouth and yolk extension of *Gba1* morphant larvae (fig. 37). Further investigation on 72 hpf *Gba1* morphant larvae confirmed the BMP upregulation in the same tissue and revealed also a strong reduction in the Wnt signaling reporter activity in the cleithrum and eyes of morphants. Intriguingly, a reduction in the number of fin mesenchymal Wnt-positive cells in the trunk of morphant larvae was noticeable at this stage. (fig. 37)

These preliminary results, showed a concomitant alteration of BMP and Wnt signaling in different tissues of *Gba1* morphants.





**Figure 37:** Confocal imaging of double *Tg(7xTCFXla.siam;EGFP)<sup>ia4</sup>/Tg(BMPRE:nlsCherry)<sup>ia17</sup>* Gba1 morphant and mismatch control at 48 hpf and 72 hpf. Increased level of BMP reporter activity were detected (arrowhead).



#### 4. DISCUSSION

Lysosomal storage disorders are rare inherited disorders in which alterations of lysosomal enzymes function lead to accumulation of undigested material in the lysosome.

Among these metabolic disorders, Gaucher disease is the most frequent in the worldwide population and it is due to mutations in the gene encoding for the lysosomal enzyme  $\beta$ -glucocerebrosidase. Patients affected by GD display the presence of enlarged macrophages called “Gaucher cells” in different tissues already in childhood and manifest several different phenotypes ranging from hepatosplenomegaly to severe neurological defects. Moreover, GD-associated skeletal alterations contribute to the morbidity and disability of affected patients (Guggenbuhl et al. 2008).

Despite enzyme replacement therapy (ERT) is able to ameliorate the hematological symptoms and the hepatosplenomegaly, skeletal and neurological complications of the disease are poorly recovered even after a long-term therapy (Mistry et al. 2011). Although the pathophysiology of the skeletal involvement has not been elucidated yet, the broad spectrum of bone complications has been mostly associated with the infiltration of Gaucher cells in the bone marrow compartment. However, Gaucher cells build-up in the bone marrow can explain only part of the bone alterations.

Throughout the past decades, the generation of animal models that mimic the complete spectrum of GD phenotypes has represented an important tool to unravel the pathogenic mechanism behind the clinical symptoms. In 2010, Mistry and colleagues conditionally deleted the GBA1 gene in cells of the hematopoietic and mesenchymal lineages, obtaining a non-neuronopathic GD1 mouse model displaying hepatosplenomegaly, hematological defects and skeletal complications, such as osteonecrosis and osteopenia, similar to the human GD1. In their work, they demonstrated that osteopenia in the conditional knockout mouse model was due to defects in osteoblastogenesis and it was not characterized by increased bone resorption due to the activation of the osteoclast population (Mistry et al. 2010). This work shed a new light on the possible pathogenic mechanism behind the skeletal defects of GD.

Despite the availability of all mice models mimicking different Gaucher disease phenotypes, a completely reliable animal model does not exist and the pathogenic alterations occurring during early life stages can not be explored and elucidated yet.

## Discussion

The aim of my PhD project was to investigate the bone pathogenetic mechanisms of Gaucher disease using a new animal model. To address this purpose, I've used the zebrafish model which has become a powerful organism to study biological processes and vertebrate developmental biology since 1970s. The rapidity of organogenesis of the zebrafish embryo and the conserved anatomy and physiology of several organs when compared to higher vertebrates, have made this little vertebrate a good model in different field of biomedical research.

Analysis of the zebrafish Gba1 revealed a high level of aminoacidic identity and similarity when compared with the human and mouse orthologues, highlighting a potentially conserved enzymatic role. Moreover, the spatio-temporal characterization of *gba1* mRNA expression pattern performed on wild type embryos and larvae, showed early expression beginning already from the one-cell stage. At later stages, the expression of *gba1* was ubiquitous in the whole organism and a high expression levels were particularly detected in some specific tissues like the central nervous system, gut, liver, bones and heart. All this data, suggest that this enzyme may have a role since early life stages of development and showed for the first time the *gba1* expression pattern in a vertebrate model.

The zebrafish model allow to follow the embryonic development step-by-step leading to the evaluation of protein loss of function effects since early life stages. To address this point in this project, a morpholino against the *gba1* mRNA was designed and a stable genetic mutant line retrieved from the ZPM forward genetic screening (*gba1*<sup>sa1621/sa1621</sup> ENSDARG00000076058) was used to analyze the effects of Gba1 loss-of-function since early embryonic development. Both these zebrafish models do not globally display gross abnormalities, except for a body trunk curvature and a reduced body size. However, deeper analysis enable to show that both models display an increased liver and spleen size. Morphants fish obtained by the microinjection of the Gba1MO in the *Lipan* transgenic line and the offspring generated by incrossed heterozygous fish (*gba1*<sup>sa1621/+</sup>) in the same transgenic background showed a progressive and significant hepatomegaly and increased spleen size also in adult stages, reminiscent of the visceral phenotype displayed by GD patients. Further characterization by means of the transgenic line *Tg(-6.0itga2b:EGFP)<sup>ia2</sup>* in which thrombocyte precursors and mature thrombocytes are labeled, showed a reduction in the transgene expression in morphant fish at 5dpf. Moreover, together with defects in the thrombocyte lineage, also a reduction in the number of erythrocytes in morphant and mutant fish at 3 dpf in *Tg(gata1:dsRed)<sup>sd2</sup>* transgenic background was observed. Altogether, these results pointed out defects in thrombocyte and erythrocyte lineages cells, resembling the thrombocytopenia and anemia defects of Gaucher patients. Preliminary analysis of *c-myb* expression,

which is a marker of definitive hematopoiesis and is important for the initial stage of myelopoiesis, revealed increased ectopic expression of this marker in morphants fish. This observation suggested that reduction of thrombocyte and erythrocyte cells lineage triggered by Gba1 dysfunction are probably due to early defects of hematopoietic stem/progenitor cells and the activation of a pro-myeloid differentiation program.

The pathophysiology of skeletal abnormalities affecting Gaucher patients, has never been elucidated due to limited phenotypes displayed by available animal models. To address if these two novel Gba1 zebrafish model exhibited skeletal abnormalities, a staining of ossified structures in larvae was performed showing a marked decrease of bones mineralization.

The mechanism of bone formation is a finely regulated process, generally divided into three stages, in which mature osteoblasts derive from a mesenchymal stem cell precursor. Specific transcription factors are expressed during this maturation process. To evaluate if bone mineralization defects observed in both zebrafish models were due to alterations in the osteoblasts differentiation program, several markers were analyzed. Morphant and mutant larvae displayed a reduction in the expression of the hypertrophic chondrocyte *col10a1* and early osteoblast-specific *runx2b* markers, which label distinct populations involved in endochondral and intramembranous ossification processes during skeletal development. Moreover, reduction in osterix-transgene expression in the microinjected Gba1 MO *Tg(Ola.Sp7:NLS-GFP)<sup>zfl32</sup>* transgenic fish, but no evident alteration of cartilage labeled tissue in *Tg(Col2a1aBAC:mCherry)<sup>hu5900</sup>*, confirmed an early differentiation program defects in the osteoblast population.

Progressive-free radical damage has been considered a key component in the tissue damage and link between oxidative stress and reduction in osteoblastogenesis has been already described (Almeida 2012). Molecular analysis and in vivo labeling demonstrated the occurrence of an early increased oxidative stress in Gba1 morphants that is rescued when Gba1 forced expression is induced. These results suggest a link between correct Gba1 function and antioxidant response.

Therefore, the loss-of-Gba1 function, induced an alteration in the osteoblasts differentiation program and bone mineralization defects due to a reduced expression of key bone-related markers, such as *runx2b* and *col10a1*. RUNX2, a master transcription factor involved in osteoblast and chondrocyte differentiation has been shown to be regulated by several molecular pathways, such as FGF and Wnt signaling in the osteoblast lineage (Komori 2011) and positively regulates *Col10a1* expression in mice (Komori 2010). To address if this alteration in the osteoblasts differentiation program was due to dysfunction of one or more major

## Discussion

cell molecular pathway involved in osteoblastogenesis, microinjection of the Gba1MO in several signaling reporter transgenic lines was performed. A strong reduction in the canonical Wnt pathway activity was found and this data were confirmed even by analyzing the offspring from incrossed heterozygote *gba1<sup>sa1621/+</sup>* in the Wnt reporter background in which reporter expression remained low even later than 7 dpf. The Wnt signaling pathway is involved in many cellular processes and plays important roles in the osteoblast differentiation. The canonical Wnt signaling is propagated through its major transducer, the  $\beta$ -catenin, which accumulates in the cytoplasm and then translocates into the nucleus to activate the transcription of targeted genes. sWestern blot analysis in Gba1 morphants, revealed decreased  $\beta$ -catenin protein level and increased levels of GSK-3 $\beta$ , Axin and Dkk1, which are negative regulators of the Wnt signaling. Moreover, the forced expression of a human GBA1 mRNA in morphants was able to rescue Wnt reporter activity deregulation already at 2 dpf and recover the expression of the downstream *col10a1* target at 4 dpf.

Together with the reduction of the Wnt signaling pathway, preliminary data showed that Gba1 loss of function was associated with increased BMP signaling activity. Real-time PCR experiments confirmed up regulation of BMP signaling effectors Smad1/5/8 mRNA levels together with increased of BMP type I receptor ligand BMP4 in this zebrafish models.

In a recent review, the importance of endocytic vesicles in the transduction of several pathways such as Wnt, BMP and FGF signaling has been described (Dobrowolski & De Robertis 2011). The stabilization of  $\beta$ -catenin and the transcriptional activation of WNT target genes require persistent inhibition of GSK-3 $\beta$  for several hours, that is generally sequestered inside multivesicular bodies (MVBs) (Blitzer & Nusse 2006). A possible explanation of the alteration of the Wnt signaling observed in Gba1 loss of function zebrafish models could be that impairment of lysosomal activity may affect the correct Gsk-3 $\beta$  sequestration into MVBs, thus leading to Gsk-3 $\beta$  accumulation in the cytoplasm and the downstream  $\beta$ -catenin degradation. Wnt signaling perturbation occurs during early stages of embryonic development, thus affecting the cell differentiation program of several stem cell progenitors, such as hematopoietic and mesenchymal stem cells leading to later defects, such as osteopenia and anemia. Moreover, recent findings suggest that loss-of- BMP signaling function in osteoblasts via BMPRIA upregulates canonical Wnt signaling during embryonic and postnatal bone development, suggesting a negative regulation of Wnt signaling by BMP (Kamiya et al. 2010). This regulatory mechanism of BMP and Wnt signaling in bone formation seems to be at least in part mediated by Sost/sclerostin and Dkk1 that are both direct targets of BMP signaling

and negative regulators of Wnt signaling. Which is the tight regulatory mechanism linking these two signaling pathways in a context- and age-dependent manner *in vivo*, is still to be understood due to their differential role in tissue development and remodeling. Probably in the bone formation context, BMP signaling inhibits Wnt signaling by upregulating Sost/sclerostin expression.

The reduction of serum DKK-1 and SOST-1 levels observed in type 1 GD patients in this work, seems in apparent contrast with the notion that both proteins are Wnt pathway negative regulators. This finding can be explained by the fact that these effectors represent an indirect measurement of osteoblast and osteocyte populations, confirming a consistent reduction of bone-forming cells in affected patients.

In this work, by means of morpholino technology and a stable Gba1 mutant line, a new zebrafish animal model for Gaucher disease has been generated and characterized. Both models display hepatosplenomegaly, thrombocytopenia, anemia and defects in bone mineralization that resemble the human disease making them good tools to dissect the pathophysiology of Gaucher disease. Moreover, alterations of Wnt and BMP signaling pathways observed in these models, provide a new potential mechanistic link between bone defects in type I Gaucher disease and GBA1 loss of function, in which impairment in the glucocerebrosidase activity triggers early deregulation of these pathways, inducing defects in the osteoblasts differentiation program.





## 5. REFERENCES

- Akiyama, H. et al., 2002. The transcription factor Sox9 has essential roles in successive steps of the chondrocyte differentiation pathway and is required for expression of Sox5 and Sox6. *Genes and Development*, 16(21), pp.2813–2828.
- Almeida, M., 2012. Aging mechanisms in bone. *BoneKEy Reports*, 1(7), pp.1–7.
- Amato, D. et al., 2004. Gaucher disease: Variability in phenotype among siblings. *Journal of Inherited Metabolic Disease*, 27(5), pp.659–669.
- Americo, J., Filho, F. & Shapiro, B.E., 2015. Tay-Sachs Disease. , 61, pp.1466–1468.
- Balch, W.E. et al., 2008. Adapting proteostasis for disease intervention. *Science (New York, N.Y.)*, 319(5865), pp.916–919.
- Bandyopadhyay, A. et al., 2006. Genetic analysis of the roles of BMP2, BMP4, and BMP7 in limb patterning and skeletogenesis. *PLoS Genetics*, 2(12), pp.2116–2130.
- Baron, R. & Kneissel, M., 2013. WNT signaling in bone homeostasis and disease: from human mutations to treatments. *Nature medicine*, 19(2), pp.179–92.
- Beis, D. et al., 2005. Genetic and cellular analyses of zebrafish atrioventricular cushion and valve development. *Development (Cambridge, England)*, 132(18), pp.4193–4204.
- Beutler E, Gelbart T, W.C., 1993. Identification of six new Gaucher disease Mutations. *Genomics*, 15(1), pp.203–5.
- Van Bezooijen, R.L. et al., 2004. Sclerostin is an osteocyte-expressed negative regulator of bone formation, but not a classical BMP antagonist. *The Journal of experimental medicine*, 199(6), pp.805–14.
- Blitzer, J.T. & Nusse, R., 2006. A critical role for endocytosis in Wnt signaling. *BMC cell biology*, 7, p.28.
- Calvi, L. et al., 2003. Osteoblastic cells regulate the haematopoietic stem cell niche. *Nature*, 425(6960), pp.841–846.
- Chalès, G. et al., 2004. Histiocytoses héréditaires et sporadiques. *EMC-Rhumatologie-Orthopedie*, 1(5), pp.406–422.
- Choi, J.H. et al., 2011. Aggregation of  $\alpha$ -synuclein in brain samples from subjects with glucocerebrosidase mutations. *Molecular Genetics and Metabolism*, 104, pp.185–188.
- Christiane Nusslein-Volhard, R.D., 2002. *Zebrafish: A Practical Approach*, 261

## References

- Ciana, G. et al., 2003. Bone marker alterations in patients with type 1 Gaucher disease. *Calcified tissue international*, 72(3), pp.185–9.
- Corey, D.R. & Abrams, J.M., 2001. Morpholino antisense oligonucleotides: tools for investigating vertebrate development. *Genome biology*, 2(5), p.REVIEWS1015.
- Covassin, L. et al., 2006. Global analysis of hematopoietic and vascular endothelial gene expression by tissue specific microarray profiling in zebrafish. *Developmental Biology*, 299(2), pp.551–562.
- Doble, B.W. et al., 2007. Functional redundancy of GSK-3alpha and GSK-3beta in Wnt/beta-catenin signaling shown by using an allelic series of embryonic stem cell lines. *Developmental Cell*, 12(6), pp.957–71.
- Dobrowolski, R. & De Robertis, E.M., 2011. Endocytic control of growth factor signalling: multivesicular bodies as signalling organelles. *Nature Reviews Molecular Cell Biology*, 13(1), pp.53–60.
- Doyon, Y. et al., 2008. Heritable targeted gene disruption in zebrafish using designed zinc-finger nucleases. *Nature biotechnology*, 26(6), pp.702–708.
- Driever, W. et al., 1996. A genetic screen for mutations affecting embryogenesis in zebrafish. *Development (Cambridge, England)*, 123, pp.37–46.
- Drugan, C. et al., 2002. Biochemical markers of bone turnover as tools in the evaluation of skeletal involvement in patients with type 1 Gaucher disease. *Blood cells, molecules & diseases*, 28(1), pp.13–20.
- Van Dussen, L. et al., 2011. Markers of bone turnover in Gaucher disease: modeling the evolution of bone disease. *The Journal of clinical endocrinology and metabolism*, 96(July 2011), pp.2194–2205.
- De Duve, C. et al., 1955. Tissue fractionation studies. 6. Intracellular distribution patterns of enzymes in rat-liver tissue. *The Biochemical journal*, 60(4), pp.604–617.
- Farfel-Becker, T., Vitner, E.B. & Futerman, a. H., 2011. Animal models for Gaucher disease research. *Disease Models & Mechanisms*, 4(6), pp.746–752.
- Fecht, H.J., 1992. Animal model of Gaucher's disease from targeted disruption of the mouse glucocerebrosidase gene. Nature Publishing Group. *Nature*, 356, pp.133–135.
- Feng, X.-H. & Derynck, R., 2005. Specificity and versatility in tgf-beta signaling through Smads. *Annual review of cell and developmental biology*, 21, pp.659–693.
- Ferron, M. et al., 2010. Insulin Signaling in Osteoblasts Integrates Bone Remodeling and Energy Metabolism. *Cell*, 142(2), pp.296–308.

- Filocamo, M. et al., 2000. Identification of a novel recombinant allele in three unrelated Italian Gaucher patients: implications for prognosis and genetic counseling. *Blood cells, molecules & diseases*, 26(4), pp.307–11.
- Fleming, H.E. et al., 2008. Wnt Signaling in the Niche Enforces Hematopoietic Stem Cell Quiescence and Is Necessary to Preserve Self-Renewal In Vivo. *Cell Stem Cell*, 2, pp.274–283.
- Fuller, M., Meikle, P.J. & Hopwood, J.J., 2006. Epidemiology of lysosomal storage diseases: an overview. In *Fabry Disease: Perspectives from 5 Years of FOS*. p. Chapter 2.
- Fulzele, K. et al., 2010. Insulin Receptor Signaling in Osteoblasts Regulates Postnatal Bone Acquisition and Body Composition. *Cell*, 142(2), pp.309–319.
- Glass, D.A. et al., 2005. Canonical Wnt signaling in differentiated osteoblasts controls osteoclast differentiation. *Developmental cell*, 8(5), pp.751–64.
- Gong, Y. et al., 2001. LDL receptor-related protein 5 (LRP5) affects bone accrual and eye development. *Cell*, 107(4), pp.513–523.
- Guggenbuhl, P., Grosbois, B. & Chalès, G., 2008. Gaucher disease. *Joint Bone Spine*, 75(2), pp.116–124.
- Haffter, P. et al., 1996. The identification of genes with unique and essential functions in the development of the zebrafish, *Danio rerio*. *Development (Cambridge, England)*, 123, pp.1–36.
- Hammond, C.L. & Schulte-Merker, S., 2009. Two populations of endochondral osteoblasts with differential sensitivity to Hedgehog signalling. *Development (Cambridge, England)*, 136(23), pp.3991–4000.
- Hartung, A. et al., 2006. Different routes of bone morphogenic protein (BMP) receptor endocytosis influence BMP signaling. *Molecular and cellular biology*, 26(20), pp.7791–7805.
- Hayes, S., Chawla, A. & Corvera, S., 2002. TGF $\beta$  receptor internalization into EEA1-enriched early endosomes: Role in signaling to Smad2. *Journal of Cell Biology*, 158(7), pp.1239–1249.
- Heining, E. et al., 2011. Spatial segregation of BMP/smud signaling affects osteoblast differentiation in C2C12 cells. *PLoS ONE*, 6(10).
- Helfrich, M.H. et al., 2007. The pathogenesis of osteoclast diseases: Some knowns, but still many unknowns. *BoneKEy-Osteovision*, 4(2), pp.61–77.
- Holleran, W.M. et al., 1994. Ultrastructure and Permeability Barrier Alterations in Gaucher Disease. *The Journal of clinical investigation*, 93, pp.1756–1764.

## References

- Howe, K. et al., 2013. The zebrafish reference genome sequence and its relationship to the human genome. *Nature*, 496(7446), pp.498–503.
- Hruska, K.S. et al., 2008. Gaucher disease: Mutation and polymorphism spectrum in the glucocerebrosidase gene (GBA). *Human Mutation*, 29(5), pp.567–583.
- Huang, P. et al., 2012. Reverse Genetic Approaches in Zebrafish. *Journal of Genetics and Genomics*, 39(9), pp.421–433.
- Huelsken, J. & Birchmeier, W., 2001. New aspects of Wnt signaling pathways in higher vertebrates. *Current Opinion in Genetics & Development*, 11(5), pp.547–553.
- Hwang, W.Y. et al., 2013. Efficient genome editing in zebrafish using a CRISPR-Cas system. *Nature biotechnology*, 31(3), pp.227–9.
- Itoh, N. & Ornitz, D.M., 2008. Functional evolutionary history of the mouse Fgf gene family. *Developmental Dynamics*, 237(1), pp.18–27.
- Jacob, A.L. et al., 2006. Fibroblast growth factor receptor 1 signaling in the osteochondrogenic cell lineage regulates sequential steps of osteoblast maturation. *Developmental Biology*, 296, pp.315–328.
- Kamiya, N. et al., 2010. Wnt inhibitors Dkk1 and Sost are downstream targets of BMP signaling through the type IA receptor (BMPRIA) in osteoblasts. *Journal of bone and mineral research : the official journal of the American Society for Bone and Mineral Research*, 25(2), pp.200–210.
- Kanferl, J. et al., 1975. The Gaucher mouse. 67(1).
- Kaplan, A. et al., 1977. Phosphohexosyl recognition is a general characteristic of pinocytosis of lysosomal glycosidases by human fibroblasts. *The Journal of clinical investigation*, 60(5), pp.1088–93.
- Kirby, B.B. et al., 2006. In vivo time-lapse imaging shows dynamic oligodendrocyte progenitor behavior during zebrafish development. *Nature neuroscience*, 9(12), pp.1506–1511.
- Klein, A., 2013. Lysosomal Storage Disorders : old diseases , present and future challenges. *Pediatric Endocrinology Reviews (PER)*. Volume 11 Supplement 1.
- Komori, T., 2010. Regulation of bone development and extracellular matrix protein genes by RUNX2. *Cell and Tissue Research*, 339(1), pp.189–195.
- Komori, T., 2011. Signaling networks in RUNX2-dependent bone development. *Journal of Cellular Biochemistry*, 112(3), pp.750–755.
- Korz, S. et al., 2008. Requirement of vasculogenesis and blood circulation in late stages of liver growth in zebrafish. *BMC developmental biology*, 8, p.84.

- Kramer, I. et al., 2010. Osteocyte Wnt/beta-catenin signaling is required for normal bone homeostasis. *Molecular and cellular biology*, 30(12), pp.3071–85.
- Krause, C. et al., 2010. Distinct modes of inhibition by sclerostin on bone morphogenetic protein and Wnt signaling pathways. *The Journal of biological chemistry*, 285(53), pp.41614–26.
- Kronenberg, H.M., 2003. Developmental regulation of the growth plate. *Nature*, 423(6937), pp.332–336.
- Lachmann, R.H. et al., 2004. Twin pairs showing discordance of phenotype in adult Gaucher's disease. *QJM - Monthly Journal of the Association of Physicians*, 97(4), pp.199–204.
- Lawson, N.D. & Weinstein, B.M., 2002. In vivo imaging of embryonic vascular development using transgenic zebrafish. *Developmental biology*, 248(2), pp.307–318.
- Li, N. et al., 2009. Tracking gene expression during zebrafish osteoblast differentiation. *Developmental Dynamics*, 238(2), pp.459–466.
- Lin, H.F. et al., 2005. Analysis of thrombocyte development in CD41-GFP transgenic zebrafish. *Blood*, 106(12), pp.3803–3810.
- Little, R.D. et al., 2002. A mutation in the LDL receptor-related protein 5 gene results in the autosomal dominant high-bone-mass trait. *American journal of human genetics*, 70(1), pp.11–19.
- Liu, Z. et al., 2007. FGF18 is required for early chondrocyte proliferation, hypertrophy and vascular invasion of the growth plate. *Developmental Biology*, 302(1), pp.80–91.
- Lloyd-Evans, E. et al., 2008. Niemann-Pick disease type C1 is a sphingosine storage disease that causes deregulation of lysosomal calcium. *Nature medicine*, 14(11), pp.1247–55.
- Long, F., 2011. Building strong bones: molecular regulation of the osteoblast lineage. *Nature Reviews Molecular Cell Biology*, 13(1), pp.27–38.
- Long, F. et al., 2004. Ihh signaling is directly required for the osteoblast lineage in the endochondral skeleton. *Development (Cambridge, England)*, 131(6), pp.1309–1318.
- Loots, G.G. et al., 2005. Genomic deletion of a long-range bone enhancer misregulates sclerostin in Van Buchem disease. *Genome Research*, 15(7), pp.928–935.
- Mikosch, P., 2011. Gaucher disease and bone. *Best Practice and Research: Clinical Rheumatology*, 25(5), pp.665–681.

## References

- Mishina, Y. et al., 2004. Bone morphogenetic protein type IA receptor signaling regulates postnatal osteoblast function and bone remodeling. *Journal of Biological Chemistry*, 279(26), pp.27560–27566.
- Mistry, P.K. et al., 2010. Glucocerebrosidase gene-deficient mouse recapitulates Gaucher disease displaying cellular and molecular dysregulation beyond the macrophage. *Proceedings of the National Academy of Sciences of the United States of America*, 107(45), pp.19473–19478.
- Mistry, P.K. et al., 2011. Osteopenia in Gaucher disease develops early in life: Response to imiglucerase enzyme therapy in children, adolescents and adults. *Blood Cells, Molecules, and Diseases*, 46(1), pp.66–72.
- Mitchell, R.E. et al., 2013. New tools for studying osteoarthritis genetics in zebrafish. *Osteoarthritis and Cartilage*, 21(2), pp.269–278.
- Molina, G. a, Watkins, S.C. & Tsang, M., 2007. Generation of FGF reporter transgenic zebrafish and their utility in chemical screens. *BMC developmental biology*, 7, p.62.
- Montero, A. et al., 2000. Disruption of the fibroblast growth factor-2 gene results in decreased bone mass and bone formation. *The Journal of clinical investigation*, 105(8), pp.1085–93.
- Moro, E. et al., 2013. Generation and application of signaling pathway reporter lines in zebrafish. *Molecular Genetics and Genomics*, 288(5-6), pp.231–242.
- Moro, E. et al., 2012. In vivo Wnt signaling tracing through a transgenic biosensor fish reveals novel activity domains. *Developmental Biology*, 366(2), pp.327–340.
- Nakashima, K. et al., 2002. The novel zinc finger-containing transcription factor Osterix is required for osteoblast differentiation and bone formation. *Cell*, 108(1), pp.17–29.
- Olsen, B.R., Reginato, A.M. & Wang, W., 2000. Bone development. *Annu Rev Cell Dev Biol*, 16, pp.191–220.
- Parsons, M.J. et al., 2002. Zebrafish mutants identify an essential role for laminins in notochord formation. *Development (Cambridge, England)*, 129(13), pp.3137–3146.
- Platt, F.M. & Jeyakumar, M., 2008. Substrate reduction therapy. *Acta Paediatrica, International Journal of Paediatrics*, 97(SUPPL. 457), pp.88–93.
- Poole, K.E.S. et al., 2005. Sclerostin is a delayed secreted product of osteocytes that inhibits bone formation. *The FASEB journal : official publication of the Federation of American Societies for Experimental Biology*, 19(13), pp.1842–1844.

- Regard, J.B. et al., 2012. Wnt signaling in bone development and disease: Making stronger bone with Wnts. *Cold Spring Harbor Perspectives in Biology*, 4(12), pp.1–18.
- Rentzsch, F. et al., 2006. Crossveinless 2 is an essential positive feedback regulator of Bmp signaling during zebrafish gastrulation. *Development (Cambridge, England)*, 133(5), pp.801–811.
- Sazani, P. et al., 2001. Nuclear antisense effects of neutral, anionic and cationic oligonucleotide analogs. *Nucleic acids research*, 29(19), pp.3965–3974.
- Schaniel, C. et al., 2011. Wnt-inhibitory factor 1 dysregulation of the bone marrow niche exhausts hematopoietic stem cells. *Blood*, 118(9), pp.2420–2429.
- Shemesh, E. et al., 2013. Enzyme replacement and substrate reduction therapy for Gaucher disease. *Cochrane Database of Systematic Reviews*, (1).
- Shore, E.M. & Kaplan, F.S., 2010. Inherited human diseases of heterotopic bone formation. *Nature reviews. Rheumatology*, 6(9), pp.518–27.
- Sidransky, E., 2004. Gaucher disease: Complexity in a “simple” disorder. *Molecular Genetics and Metabolism*, 83(1-2), pp.6–15.
- Sidransky, E., 2012. Gaucher disease: insights from a rare Mendelian disorder. *Discovery medicine*, 14(77), pp.273–81.
- Sidransky, E. et al., 1992. Gaucher patients with oculomotor abnormalities do not have a unique genotype. *Clinical genetics*, 41(1), pp.1–5.
- Sidransky, E. & Lopez, G., 2012. The link between the GBA gene and parkinsonism. *The Lancet Neurology*, 11(11), pp.986–998.
- Simpson, M. a et al., 2011. Mutations in NOTCH2 cause Hajdu-Cheney syndrome, a disorder of severe and progressive bone loss. *Nature genetics*, 43(4), pp.303–305.
- Solnica-Krezel, L., Schier, a. F. & Driever, W., 1994. Efficient recovery of ENU-induced mutations from the zebrafish germline. *Genetics*, 136(4), pp.1401–1420.
- Spoorendonk, K.M. et al., 2008. Retinoic acid and Cyp26b1 are critical regulators of osteogenesis in the axial skeleton. *Development (Cambridge, England)*, 135(22), pp.3765–3774.
- Streisinger, G. et al., 1981. Production of clones of homozygous diploid zebra fish (*Brachydanio rerio*). *Nature*, 291(5813), pp.293–296.
- Traver, D. et al., 2003. Transplantation and in vivo imaging of multilineage engraftment in zebrafish bloodless mutants. *Nature immunology*, 4(12), pp.1238–1246.

## References

- Tu, X. et al., 2012. Indian hedgehog requires additional effectors besides Runx2 to induce osteoblast differentiation. *Developmental biology*, 362(1), pp.76–82.
- Valledor, a F. et al., 1998. Transcription factors that regulate monocyte/macrophage differentiation. *Journal of leukocyte biology*, 63(4), pp.405–417.
- Veeman, M.T., Axelrod, J.D. & Moon, R.T., 2003. A second canon: Functions and mechanisms of  $\beta$ -catenin-independent Wnt signaling. *Developmental Cell*, 5(3), pp.367–377.
- Volff, J.-N., 2005. Genome evolution and biodiversity in teleost fish. *Heredity*, 94(3), pp.280–294.
- Walker, M.B. & Kimmel, C.B., 2007. A two-color acid-free cartilage and bone stain for zebrafish larvae. *Biotechnic & histochemistry : official publication of the Biological Stain Commission*, 82(1), pp.23–28.
- Wennekes, T. et al., 2009. Glycosphingolipids - Nature, function, and pharmacological modulation. *Angewandte Chemie - International Edition*, 48(47), pp.8848–8869.



## **APPENDIX**

